

4D Printing with Bio-based Polymers for Adaptive Wearable Devices

YEJUN FU

4D Printing with Bio-based Polymers for Adaptive Wearable Devices

A ninety-point research portfolio submitted in fulfilment of the requirements for the degree of Master of Design Innovation.

YEJUN FU

Victoria University of Wellington
School of Design 2019

Supervised by Tim Miller and Simon Fraser

Abstract

Compared to conventional manufacturing processes, 3D printing has proved its capability of building various structures with high accuracy and material economy. 4D printing adds the fourth dimension, time, to 3D printing technology. Changing through time is a key property of products built by 4D printing. This research focused on bio-based responsive materials, as a means of initiating change and transforming 3D printing to 4D printing.

A number of studies have been done to develop the performance of responsive materials or to explore geometric structures for these materials in order to configure products that can benefit from this transformation. Precedents in medical field show great potential for combining bio-based materials with 4D printing in manufacturing highly customised products that adapt to the shape, movement and physiological requirements of a human body.

This research project was initiated by the development of printable and responsive bio-based polymers through the National Science Challenge (NSC) Portfolio 5 Spearhead Project “*Additive manufacturing and 3D or 4D printing of bio-composites*”. The research is inspired by the adaptability and biocompatibility of the medical precedents and explores the possibility of engaging 4D

printing in building wearable devices; exemplified by an adaptive wrist splint for progressive rehabilitation. This included researching wound healing processes and related rehabilitation methods to determine the required functionality of the splint and exploring relevant biological structures as inspiration for the design geometry.

Working alongside materials scientists, the design was developed along two paths. Firstly, using the new experimental polymers and testing their responsiveness to configure a printable shape-shifting layer of the splint that adapts to changes in the wrist during the healing process. Secondly, integrating these experiments into 3D models for an adaptive splint, comprised of three layers, that responds to the requirements of progressive rehabilitation.

The research challenges the properties of the new materials and the associated printing processes, and more research will need to be done to improve both printability and responsive performance. However, the design of the splint provides a case study for potential applications in the broader field of wearable devices that incorporate multiple layers of responsive materials and different geometries that can adapt to the needs of a human body.

Acknowledgments

I would like to thank my supervisors Tim Miller and Simon Fraser for their invaluable advice and guidance throughout my project. Thanks also for the opportunities they provided for me to learn knowledge and experience from the external professionals.

The prototypes in the project would not be completed without the funding support of National Science Challenge. All the biopolymers used in this project were developed by the National Science Challenge development team for cellulose and bio-based polyester composite formulations, including John McDonald-Wharry, Kim Pickering, Marie Joo Le Guen, Maxime Barbier, Yejun Fu, Maryam Namini Mianji.

I am grateful to Dr John McDonald-Wharry for the knowledge of material science and the continuing support on paste-printing.

Thanks to Kim Pickering for the opportunity of doing internship for my project in the University of Waikato.

Thanks to Brian Robinson, Viv Butcher, Karen Porter, Melissa Brazier, Denise Douglas for their professional opinions and advice from clinical experience.

Thanks to Kirsten Reid for offering me advice on English writing and encouraging me all through my studies.

Thanks to my colleagues and the design staff at VUW. Thanks especially to Phil and Mark for their technical assistance.

To my friends, thanks for supporting me and being blunt when I asked for opinions.

Contents

ABSTRACT	_____ III	3	EXPLORATION OF THE NEW MATERIALS AND DETERMINATION OF THE MATERIAL SPECIFICATIONS FOR THE PROJECT	_____ 26	4	EXPLORATION OF DESIGN	_____ 42	5.3	Final prototypes for the functions determined by geometric structures incorporating the multi-flexibility of the materials determined by geometric structures	_____ 78
ACKNOWLEDGMENTS	_____ V				4.1	The scenario and concept design	_____ 44			
INTRODUCTION	_____ 2	3.1	Properties and performances of the available materials	_____ 30	4.2	Design development with the new materials for the responsive performance	_____ 48			
TERMINOLOGY	_____ 3	3.1.1	Printability	_____ 30	4.2.1	Design of the geometric structures	_____ 48	5.4	Reflection	_____ 81
1 METHODOLOGY	_____ 6	3.1.2	Responsiveness	_____ 32	4.2.2	Design of the printing paths	_____ 54	6	DISCUSSION	_____ 84
2 BACKGROUND RESEARCH	_____ 12	3.1.3	Shrinkage, collapse, blistering caused by water and cracks	_____ 35	4.3	Design development for full functions based on the scenario	_____ 64	7	CONCLUSION	_____ 88
2.1 4D Printing and precedents	_____ 14	3.2	Determination of the material specifications for the project	_____ 38	5	RESULTS AND REFLECTION	_____ 72		LIST OF FIGURES	_____ 91
2.2 Requirements of rehabilitation and potential application of 4D printing	_____ 16	3.2.1	Request on the specifications of materials	_____ 38	5.1	Final prototypes printed with the new materials for responsive performance	_____ 74		REFERENCES	_____ 93
2.3 Biomimicry	_____ 18	3.2.2	Feedback from the material scientist	_____ 39	5.2	Experiments for responsive performance on the final prototypes printed with the new materials	_____ 76		APPENDIX	_____ 95
2.4 Biological structures as inspirations for my project	_____ 22	3.2.3	Discussion and reflection	_____ 40						

Introducton

4D printing has increased the value of 3D printing by embedding predictable changes into products. Momeni, M.Mehdi Hassani. N, Liu, and Ni (2017) described these changes as “a targeted evolution of the 3D printed structure, in terms of shape, property, and functionality” (p. 43).

The basis of 4D printing is the responsive property of the printing materials. In 4D printing, responsive materials not only function as construction material, but also as the agent of change. The “actuation, sensing and programmability” involved in the predictable changes do not rely on any electronic or mechanical components to work, because each fiber of a responsive material can work as a tiny integrated functional unit (Tibbits, McKnelly, Olguin, Dikovsky, & Hirsch, 2014, p. 540).

The materials science team of the NSC Portfolio 5 Project developed a group of bio-based responsive polymers. These responsive polymers were the basis of my research which studied these new materials and explored their design potential. Working alongside the material scientists, I gained knowledge of the available materials, collected first-hand experience in

designing, printing and testing these materials, developed a new printing approach for paste printing, and improved the quality of prototypes printed with new materials.

In addition to the research focused on 4D printing and responsive materials, the project also included research on biomimicry and progressive rehabilitation. The similarity in the performance of a triggered responsive material and a living organism encouraged me to study the relationship between biological structures and their performances. The result of my research on the various soft tissue and skeleton structures of animals provided me with the inspiration for the geometric design aspect of my project.

The research on the precedents of a self-assembly stent for use inside the human body made by 4D printing motivated me to explore the possibility of using responsive material to build a wearable splint which could adapt to the physiological change that occurs during the healing process. My intent was that by 3D printing this adaptive wearable device we could precisely control the material distribution and 4D performance for specific needs. To conduct a comprehensive study, I selected an injured wrist as

the body part to design for because of its medium size and its complex structure. This structure consists of multiple bones and joints and consequently its healing process requires devices for rehabilitation to fulfil more complicated tasks.

The most obvious finding to emerge from this study was the possibility of incorporating multi-layered responsive materials and different geometries for adaption to a human body with changing requirements of immobilisation and movement. This dynamic aspect was also defined by the notion of incorporating a progressive physiotherapy treatment by reducing the stiffness of the splint according to the prescription of a therapist. The second major finding was that the printability of paste printing could be improved considerably by incorporating direct G-code strategies resulting in a more precise control of printing paths using a CAD programme in combination with the slicing software.

Terminology

3D printing:

A manufacturing process, which builds physical three-dimensional objects according to digital three-dimensional models by layering up strands of material extruded from the nozzle of a printer.

4D printing:

3D printing with responsive materials. This technology integrates predictable changes into 3D printed structures.

ABS:

Acrylonitrile butadiene styrene, a thermoplastic polymer.

ADLs:

Activities of daily living

Agilus:

The name of a flexible material used in J750 printing.

Biomimicry:

A way of learning from nature, in terms of form, material, construction, process, and function, which is a tool used in design.

CAD:

Computer aided design

FDM:

Fused deposition modeling

Flexural modulus:

A mechanical property indicating the ability of a material in resisting bending.

G-Code:

A numerical control programming language used to control automated machine tools, for example a 3D printer.

Grasshopper:

A visual programming language used in Rhinoceros 3D modeling CAD programme.

Hydro swelling:

The expansion of material caused by immersing it in water.

Hyrel 3D:

The brand of the syringe-printer used in my project.

IADLs:

Instrumental activities of daily living

J750:

A 3D printer manufactured by Stratasys, which has the capacity to print multiple materials of different flexibility with 0.014mm nozzle.

MADE:

Multi-property additive-manufacturing design experiments. The name of a research stream at the design school at Victoria University of Wellington.

Paste-printing:

A 3D printing process, in which the printing materials keep the status of paste before and after printing.

PE:

Polyethylene, a common plastic.

Phase transition:

The change of a material’s status between distinct forms, such as gas, liquid and solid.

PLA:

Polylactic acid, a thermoplastic polymer.

Printing paths:

The paths along which materials are deposited in 3D printing.

Print head collision:

The situation when a nozzle crashes into the printed model.

PROM:

Passive range of motion

PTFE:

Polytetrafluoroethylene, a synthetic polymer

Rapid movement:

The travelling of a nozzle without the deposition of material.

Rhino:

The abbreviation of Rhinoceros, the name of a 3D modeling CAD programme.

RhinoSlic3r:

A plugin provided by Slic3r for Rhino. It enables Rhino to convert geometric shapes to printing paths in the format of G-Codes and to convert G-Codes to the geometric shape composed of printing paths.

Skirt:

A period of printing path before printing the target model. It is typically used to stabilise the extrusion of paste in paste-printing.

SMPs:

Shape Memory Polymers

SME:

Shape memory effect. The effect that an SMP can return to a stored permanent shape after it is deformed to a temporary shape.

Slic3r:

The name of a programme, which slices digital 3D models into printing paths in the format of G-Code.

Spiral vase mode:

A mode provided by Slic3r, which attempts to convert the perimeter of a 3D CAD model to a continuous printing path.

Stl:

A file format of 3D CAD models, which is widely accepted by 3D printers as a typical format of inputted data.

Syringe-printer:

A 3D printer, which uses a syringe as the container of materials. Typically used in paste-printing.

Traveling paths:

The paths which the nozzle of a printer moves along in 3D printing.

Vero:

The name of a rigid material used in J750 printing.

Young’s modulus:

A mechanical property indicating the stiffness of a solid material.

1 Methodology

My research explores the design opportunities of 4D printing with bio-based polymers for manufacturing adaptive wearable devices. The project was initiated by the development of printable responsive bio-based polymers. The controllable responsive performances of these new materials are the basis of the design. To make my design more grounded, I discussed the potentials of using 4D printing in building wearable devices with a wrist splint as an exemplar. Biomimicry was used as a tool to inspire the design of the geometric structures.

I employed two methodologies in response to the research question, which are: *research for design* and *research through design* (Frankel & Racine, 2010). Research for design (RFD) provided me with information in relevant fields and enabled me to find design opportunities and inspirations before I started to design. Research through design (RTD) allowed me to produce valuable ideas and principles from practice, which can be used to guide my future practice in pursuit of similar research questions. RTD has been applied in the design of the splint, as well as in exploring and suggesting the properties of new materials. The whole process is shown in the following diagram (Figure 1).

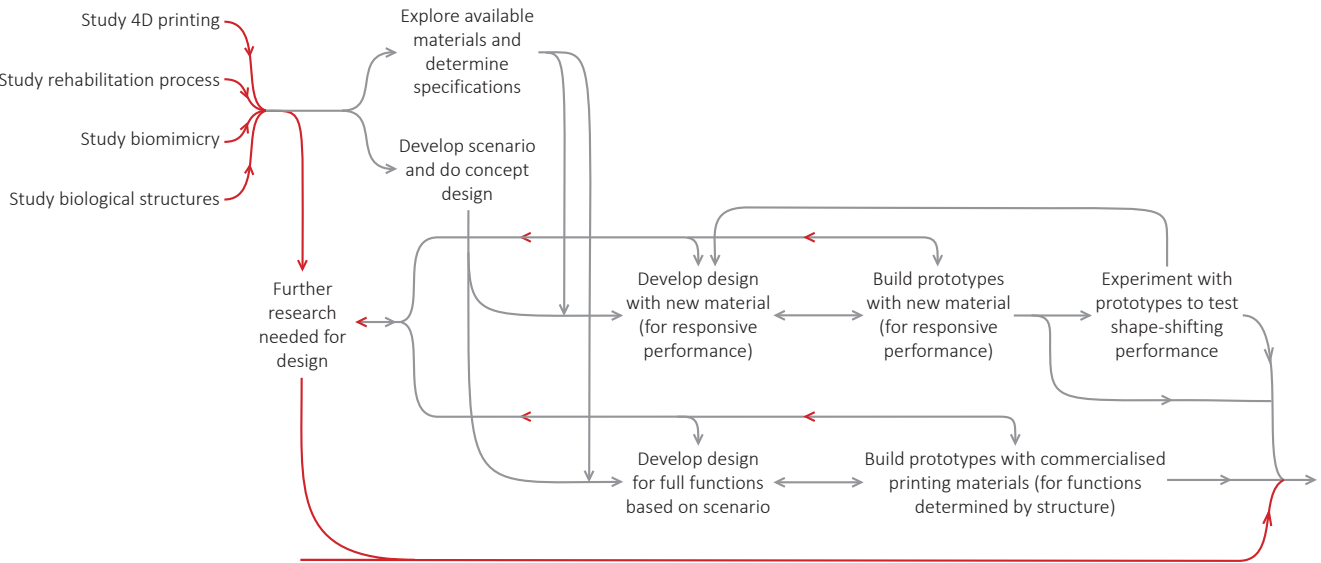


Figure 1. Author, Research process

Red: The initial RFD and further RFD required by ongoing design practice

Grey: The RTD initiated by RFD and the RTD informed by ongoing design practice

Aim 1: To explore literature and precedents for a 3D printed self-actuating wearable device, exemplified by a wrist splint

In this phase, I focused on RFD to frame the research problem. I conducted qualitative studies of literature and precedents (Creswell, 2013, Hanington & Martin, 2012) to develop a necessary comprehension of the existing knowledge and techniques, which might inform my project.

I established four objectives to achieve Aim 1:

1a) Study relevant research and precedents of 4D printing;

1b) Study the rehabilitation process of an injury and research the requirements for the different stages;

1c) Study literature about and precedents of biomimicry;

1d) Study relevant biological structures.

By studying 4D printing and its existing design exemplars, I developed an understanding of this new technology, formed an overview about the capabilities of 4D printing in terms of material, and discovered the potential to benefit wearable designs. Research

on rehabilitation processes of injuries enabled me to understand the requirements for designing a rehabilitation supporting device, and discover potential design opportunities for 4D printing. Studies on literature about and precedents of biomimicry provided me with an in-depth comprehension of biomimicry as a design tool. Research on relevant biological structures inspired my geometric design. Knowledge obtained in this phase was used to inform my design, and vice versa, the development of design informed the direction of further research necessary for a better design.

Aim 2: To design and build an adaptive splint, and discuss the potential capability of 4D printing in building a wearable device

In this phase, I mainly used RTD in my research. I established five objectives to achieve Aim 2:

2a) Explore the properties of the available bio-based polymers and determine the design specifications for materials to be used, with the support of material science researchers in the NSC project;

2b) Develop a scenario and produce a concept design;

2c) Develop the design with the available new material, and in parallel develop the design for full target functions based on the

scenario to fulfil the requirements of rehabilitation;

2d) Build prototypes with the new material, and in parallel build prototypes for target functions based on the scenario;

2e) Experiment on the prototypes built with the new material;

2f) Reflect on the design and the capability of 4D printing and the range of potential wearable applications.

To explore the properties of available materials and determine my design specifications for the target materials, I continually designed and 3D printed informative structures with the new bio-based polymers in development. These structures were designed either to test the properties (printability, curability, responsiveness, etc.) of the materials to inform the following round of material development, or to find possible features that can realise target performances. Through the design process, this research is iterative in cooperation with the ongoing development of the bio-based polymers.

As a method of design, developing a scenario is a way for a designer to improve the understanding of the target users' requirements to make the design ideas more clear and precise

(Hanington & Martin, 2012). I constructed the scenario of using the splint according to the research on the rehabilitation process of an injury, in combination with the capability of 4D printing.

The following design processes were conducted by applying RTD and had a feature of parallel-pathed development. The strategy of parallel development was naturally formed during real practice because of the advantages and limits brought by the new materials. On the one hand, the new materials had customisable responsive properties and potentially better qualities in bio-compatibility and sustainability than the majority of the materials that commercial 3D printers could use. On the other hand, the new experimental materials under ongoing development had lower printability than most commercial materials. Besides, during curing of the new materials contraction issues can cause shrinkage, distortion cracks. These problems meant it was not feasible to build a product with the new materials that could realise all the functions before my project was done. So I started to develop my design along two paths in parallel for different needs: Along one path, I designed 3D CAD models, converted them into codes of printing paths and edited the codes for printing with the new materials to realise the responsive shape-shifting of the splint. I sent the data to the University of Waikato (UoW) for printing (where I found the only available paste-printer to print with the

new materials). Along the other path, I designed 3D CAD models for the full target functions based on my scenario. To observe and test the functions determined by the geometric structures, such as the multi-flexibility and the zip for putting on the splint, I printed the prototypes on a J750 3D printer, which could print multiple materials with high accuracy.

I conducted experiments on the prototypes built with the new materials to test the responsive performances of the designs. Observations of the prototypes and reflection on the results of experiments were collected to inform the next round of design development. This was an iterative procedure, in which “visual form” (as manifested in the sketches, CAD models and prototypes) was considered to be “a valid form of knowledge” (Swann, 2002, p. 52). The procedure continued until the final prototypes were achieved. The final prototypes and the result of the experiment on the responsive performance show the potential capability of an adaptive splint, as well as the possibility of combining multiple layers of responsive bio-polymers and different geometric structures to build wearable devices to adapt to needs of a human body.

2 Background Research

2.1 4D Printing and precedents

I developed a growing interest in 3D printing technology in 2017 when I began to study industrial design. 3D printing is a manufacturing process that closely connects computer-aided design with products. To me, this process provides high-accuracy results faithful to design and, more importantly, redefines realisable designs. In the same year, I was offered the scholarship by National Science Challenge, to explore the design scope of 4D printing. Momeni, M.Mehdi Hassani.N, Liu, and Ni (2017) described a 4D printing process as “a targeted evolution of the 3D printed structure” over time triggered by stimuli, “in terms of shape, property, and functionality” (p. 43). From my research and practice, I gained an insight about the way of designing for 4D printing.

Firstly, designing for 4D printing requires more thoughts on the selection of materials. Usually in designing for 3D printing, materials are an available resource to realise target aesthetic qualities or functions, but materials play a more important role in 4D printing. The “sophisticated multiphysics constitutive behavior” (Mao et al., 2016, p. 2) of responsive materials is the basis to realise the target change in a 4D printing process. For this reason,

it is essential to study the responsive property of materials before making an initial choice of materials. The selection of materials should be guided by the required dynamic performances of the design, with consideration of available stimuli in its working environment, according to a number of design explorations in the medical field (Zarek, Mansour, Shapira, & Cohn, 2017; Miao et al., 2017; Hendrikson et al., 2017). In these precedents, the response of materials enables the devices to complete shape-shifting after reaching target positions or adapt their changes to the physiological growth of a human body.

Among all responsive polymers used in 4D printing, hydrogels and shape memory polymers (SMPs) are usually regarded as two main types of polymers in terms of realising the switch “between multiple configurations” (Ding et al., 2017, p. 1). Ding et al. (2017) described the mechanism behind a hydrogel-based shape-shifting as “mismatch strains between the two materials” (p. 1). They explained that by integrating a hydrogel, which swells when it is immersed in a solvent, with a non-swelling polymer in a structure, mismatch strains can be created when the structure is immersed in the solvent. Miao et al. (2017) described the mechanism behind the shape-shifting behaviour of heat-stimulated SMPs (a widely applied type of SMPs) as a recover to a memorised shape triggered by heat. They explained that at the first stage a structure

made of an SMP can be set to a permanent shape by building chemical or physical crosslinks while a transition temperature. At the next stage, it can be deformed and fixed to a temporary shape as is heated above and then cooled down below the transition temperature. At the final stage, the structure can return to its permanent shape when it is again heated over transition temperature. In addition to these two main types of polymers, there are other responsive materials that can be triggered by other stimuli including light (Kuksenok & Balazs, 2015) through other mechanisms including dissolution (Kokkinis, Schaffner, & Studart, 2015).

Secondly, designing for 4D printing requires more thoughts about the physical distribution of materials. To be more specific, during the design process, it is vital to take the properties of selected materials as a factual basis to define the distribution of materials to prescribe local performances of a smallest unit (e.g. a component of a hinge) and the global performances of a whole object. The selection of responsive materials will inform the designer of possible structures. For example, by placing hydrogels strategically, designers can control a 3D printed structure to do complex shape-shifting. Precedents include a linear structure that self-assembled into a group of letters (Tibbits, 2014), a flat grid that deformed into a double-curvature surface (Raviv et al.,

2014), flowers that curled up in controlled ways (Sydney Gladman, Matsumoto, Nuzzo, Mahadevan, & Lewis, 2016). The first two precedents made use of the different degree of expansion between a hydrogel and a non-expansion rigid material.

The researchers programmed the direction and the degree of bending for each joint by controlling geometry design. The third precedent was based on the same principle, but on a micro scale. The researchers embedded stiff cellulose fibrils in a soft hydrogel, and they achieved “anisotropic swelling behaviour” (Sydney Gladman, Matsumoto, Nuzzo, Mahadevan, & Lewis, 2016, p. 412) of the hydrogel composite by controlling the alignment of the fibrils.

2.2 Requirements of rehabilitation and potential application of 4D printing

4D printing has revealed its capability of producing products that adapt to the physiological growth of the human body. This capability enables 4D printing to benefit the users from inside the human body, as is shown in the medical precedents mentioned in the previous section. Considering the applications in other fields such as healthcare and sports, I found the adaption of the products provided by 4D printing could also benefit from outside the human body, for example as a wearable device for rehabilitation.

Rehabilitation is a complex process for two reasons. The first reason is that various healing tissues change their status over different lengths of time. Pitts, Willoughby, and Morgan (2013) divided the healing of a wound into three stages: inflammatory, proliferation and mature. They provided the healing rates of different types of connective tissues: loose ones and dense ones. Loose connective tissues such as skin, blood vessels and muscle have shorter healing timelines: 1 to 3 days at inflammatory the stage, 3 to 10 days at the proliferation stage, and 11 to 21 days at

the mature stage. Dense connective tissues such as bone, ligament and tendon have longer healing timelines: 1 to 4 weeks at the inflammatory stage, 4 to 8 weeks at the proliferation stage, and 8 to 12 weeks at the mature stage. The status of injured tissues changes throughout the whole process.

The second and more important reason is that different rehabilitation techniques and methods are required at different stages because different changes happen in the tissues. Generally, we know that immobilisation is necessary for the rehabilitation of an injury, but immobilisation alone is far from sufficient. According to the research carried out by Cyr and Ross (1998), immobilisation without any controlled motion can be harmful. LaStayo, Winters, and Hardy (2003) studied the healing process and the management of a fracture. They stated that in the later period of an inflammatory stage “controlled mobilization” or “protected mobilization” is needed (p. 90), and in the following phases of the rehabilitation splint and passive range of motion (PROM) are needed for repairing and remodeling the fractured bone. The grades of mobilisation in therapy can usually be divided into five levels (Rasavong, MPT, COMT, & MBA, 2015; Manske & Rohrborg, 2016). According to their description, the amplitude, speed and oscillation of the mobilisation varied from grade to grade, and the amount of the resistance applied onto the healing tissues during

mobilisation increased from Grade I to Grade V.

Pitts, Willoughby, and Morgan (2013) listed the main tasks in different phases of a wound-healing process and summarised the appropriate techniques and methods for rehabilitation. For example, they provided an overview that:

- In the first phase, the main tasks include controlling edema, protecting healing tissues, and reducing pain reflex. Devices are used to allow the mobilisation of Grade I and II for patients to regain the ability to do Activities of Daily Living (ADL).

- In the second phase, the main task is to strengthen the healing tissues. Devices are used to increase and control the load on the tissues during the mobilisation of Grade III to prepare the patients for Instrumental Activities of Daily Living (IADL) tasks.

- In the last phase, the main task is to further strengthen the healing tissues. Devices are used to further increase the variety and difficulty of mobilisation to prepare the patients for their essential job tasks.

The complex requirements of rehabilitation have inspired me to consider building adaptive wearable devices by 4D printing. From

Pitts, Willoughby, and Morgan’s (2013) summary (Figure 2), we can tell that the devices to be used to apply these techniques and methods need to perform a variety of functions, including immobilisation, protection, and allowing controlled motions. A cast or splint for an injured wrist, for example, will usually need to fulfill the following needs at different stages:

- To appropriately immobilise a swollen wrist at an early stage;
- To accommodate the normal size of the wrist when the swelling decreases;
- Finally to provide certain flexibility in certain areas to allow prescribed exercises for consolidation.

Currently, these needs are fulfilled by frequently changing devices. These devices cost an amount of time and material to build, and frequent change of devices results in repeated visits, which brings inconvenience to both the patients and the therapists. Thus this research explores the responsive property of bio-based materials and the design opportunities of the production of a 4D printed splint to improve the above situation. Furthermore, 4D printing opens up a new opportunity to build a customised adaptive splint that can continuously fulfil various needs at different stages to largely improve the experience of patients during rehabilitation.

Level of Woud Healing	Functions of Devices	Goals
<i>Level I</i>	Inflammatory/ healing wound care, edema control, scar management, protective orthoses, rehabilitation for initial stage	Independence with self-care tasks
<i>Level II</i>	Maturation/ load rehabilitation, scapular stabilisation, corrective orthoses	Independence IADL tasks
<i>Level III</i>	Maturation rehabilitation	Independence in essential job tasks

Figure 2. Functions and goals of devices for various phases of the wound-healing process

2.3 Biomimicry

My project is a design exploration for adaptive wearable devices based on new materials and the requirements of rehabilitation. Doing this project is very exciting to me because I can improve the capability of design and provide functions that benefit the experience of users. I am also as fascinated by nature, in terms of the subtle performances enabled by biological structures and materials, as I am by design. So when I did my project, I took biological structures as the inspiration for my design.

People have developed metaphors to compare the manufacturing industry with nature. Tavsan and Sonmez (2015, p.2285) described nature as “a big factory, where the faults are kept at a minimum, choosing the most suitable material of all for the purpose, recycling them, and even changing every ingredient as conditions impose.” Kennedy (2017) compared evolution in nature with practice in design. She argued that because nature preserves only the most adaptive organisms, the practice of nature is far more advanced in selecting good designs. These opinions might explain the reason why humans wish to learn from how nature builds its products to inform the design of our products.

One of the most common concepts about learning from nature is biomimicry. Kellert, Heerwagen, and Mador (2011, p. 28) stated that the term biomimicry means to borrow “designs and strategies” from nature. Long before humans could analyse nature in a systematic way, we had already started biomimicry. Kennedy (2017, p. 51) provided several examples in her paper: Leonardo da Vinci (1452–1519) designed flying machines based on the structure of birds and bats; Sir Marc Brunel (1769–1849) invented an underwater construction based on his observation of the naval shipworm, and George de Mestral (1907–1990) invented the widely used Velcro based on the structure of a burr, which accidentally stuck to his jacket.

Not only does biomimicry have a deep history, but it is also predicted to have long-term impacts. In her paper, Kennedy (2017) exemplified the impacts with a 2013 Fermanian Business & Economic Institute Report commissioned by the San Diego Zoo. The report estimated that by 2030, biomimicry could account for \$425 billion in US GDP and \$1.6 trillion in global GDP, and it could generate \$50 billion savings associated with reduced resource depletion and lower carbon dioxide pollution.

Despite the long history of biomimicry and the prediction of its promising future, it is hard to say whether learning from nature

is always a good option in a real project. On the one hand, the context and the bio-target of an organic process in nature are usually different from the context and the task of human design. McNichol (2002) quoted Robert Full’s argument in a presentation that the target of evolution was building products which were “just good enough” rather than perfect, so what to borrow from nature needed to be considered according to the specific task in a real project.

On the other hand, even if we have found a strategy in nature that is appropriate to be employed to fulfil our design task, the result of the project can still vary. This is because the approach of learning from nature includes the creativity of humans, which can largely influence the results. In architecture field, the term biophilic design is used to describe a way to learn from nature, which emphasises the importance of cooperating built environment with nature (Kellert & Heerwagen, 2011). But Kellert (2011) continued to state that the values of biophilic design can greatly vary and be affected by human knowledge, experience, choice. We need methods to guide the process of learning from nature to achieve better outcomes.

Researchers have developed several methods for designers to find their paths to learn from nature. Benyus (1997) divided biomimicry

into three levels, from reductive to holistic biomimicry, which are:

- mimicking of natural form;
- mimicking of natural process;
- mimicking of natural systems.

Based on Benyus’ theory, Volstad and Boks (2012) summarised the ideas of reductive biomimicry and holistic biomimicry: Reductive biomimicry means to borrow “biological technologies” from nature without aiming to obtain sustainability (p. 191); in contrast, holistic biomimicry considers sustainability as a key target in learning from nature. Furthermore, Volstad and Boks (2012) categorised the application of reductive biomimicry, into three approaches:

- Approach 1 focuses on materials;
- Approach 2 focuses on structure and mechanics/dynamics;
- Approach 3 focuses on shape.

Likewise, Zari (2007) also divided biomimicry into three levels in her research on the biomimetic approaches to architectural

design. They are organism level, behaviour level and ecosystem level. She explained that the approach at the organism level is to mimic a specific organism; the approach at the behaviour level is to mimic how an organism behaves or relates to its context; the approach at the ecosystem level is to mimic an ecosystem.

Zari’s way of division is similar to Benyus’. However, I believe Zari’s strategy is more coherent and informative for two reasons. Firstly, the two strategies are the same in the definition of the third level mimicry of an ecosystem. But between the first and second levels, Benyus separated form from process, while Zari separated a single unit from its interaction with its community. After that, Zari kept dividing the level of biomimicry according to the level of the object to be mimicked. By comparison, Benyus first divides the level of biomimicry according to the aspects of the object to be mimicked, and then moves on to the level of the object. Secondly, each level in Zari’s system includes five aspects (form, material, construction, process and function) of the object to be mimicked. This provides a wider range of choices and more specific instructions on the application of biomimicry at various levels.

I studied biomimicry precedents and categorised the approaches applied in these precedents according to Zari’s way of division, as is shown in Figure 3.


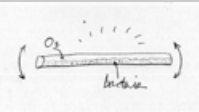
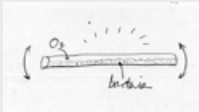









Level of Biomimicry	Approaches	Precedents	
Organism level	Form		Bone Armchair designed by Joris Laarman A project inspired by the shape of bones
	Material		
	Construction		
	Process		Ambio lamp designed by Teresa van Dongen A project using bioluminescent bacteria in a saltwater to grow
Behaviour level	Form		
	Material		Ambio lamp designed by Teresa van Dongen A project using bioluminescent bacteria in a saltwater to grow
	Construction		Carbon-fibre pavilion designed by the researchers and students from the University of Stuttgart A project woven by robots and drones, inspired by the silk hammocks spun by moth larvae
	Process		
Ecosystem level	Form		Dragonfly Metabolic Farm by Vincent Callebaut Architectures A project mimicking the metabolic process and the interaction between an organism and the natural environment
	Material		Algae Canopy designed by EcoLogicStudio A project using algae farm as a system to provide energy
	Construction		
	Process		Algae Canopy designed by EcoLogicStudio A project using algae farm as a system to provide energy
Ecosystem level	Form		Dragonfly Metabolic Farm by Vincent Callebaut Architectures A project mimicking the metabolic process and the interaction between an organism and the natural environment
	Material		
	Construction		
	Process		
Ecosystem level	Form		Dragonfly Metabolic Farm by Vincent Callebaut Architectures A project mimicking the metabolic process and the interaction between an organism and the natural environment
	Material		Algae Canopy designed by EcoLogicStudio A project using algae farm as a system to provide energy
	Construction		
	Process		Algae Canopy designed by EcoLogicStudio A project using algae farm as a system to provide energy
Ecosystem level	Form		Dragonfly Metabolic Farm by Vincent Callebaut Architectures A project mimicking the metabolic process and the interaction between an organism and the natural environment
	Material		
	Construction		
	Process		

Figure 3. Author, Biomimicry approaches applied in the precedents according to Zari’s way of division

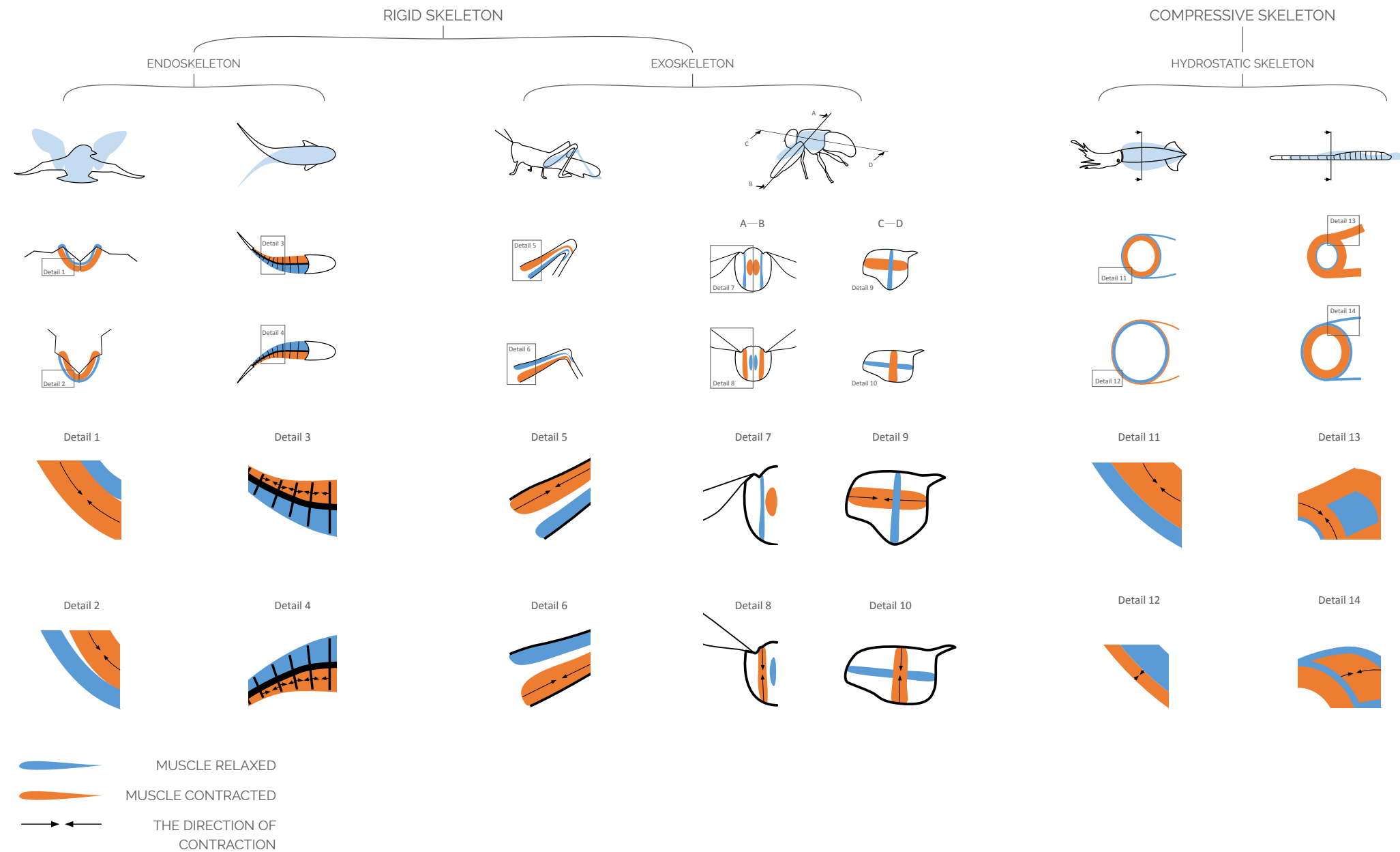


Figure 4. Author, Typical skeleton-muscle structures of animals and the mechanics behind movements

2.4 Biological structures as inspirations for my project

The project was designed based on analytical thinking about the properties of the available materials as the starting point and to fulfil the requirements of rehabilitation as the expected functions. Biomimicry was used as a tool to inspire the geometric design. Along with the continuing development of materials by the material scientists, I was continually updated with discovered properties of the new materials. Based on these properties, I studied various biological structures as the inspirations for the project to deliver the target performances.

At the early stage of material development, I was informed that there would be two types of bio-based polymer formulations available for my project: one type was rigid, and the other type was soft and flexible. At that time it had not been explored how they could work in a structure to deliver responsive performances, such as shape-shifting. However, the multiple rigidity of the available materials reminded me of mammals' skeleton-muscle structures and the functions which these structures enable. The relative motion between their hard skeletons and soft muscles

allows these animals to complete shape-shifting and movements. I studied the skeleton-muscle structures of various animal species and found a few typical structures. I then drew a diagram (Figure 4) to summarise the features of these structures and the mechanics behind movements.

As I examined these skeleton-muscle structures, I found that animals with rigid skeletons rely on the contraction of muscles to realise the shape-shifting of their body parts and the resulting movements. The role of rigid skeletons in these movements is to locate the muscles and transmit the force generated by the muscles. Considering the mechanics behind movements, insects' exoskeletons work similarly to the endoskeletons of mammals. I had the idea that I might be able to learn from these biological structures to realise the function for my project. For example, the shape-shifting function can be used to adapt the splint to an injured wrist at different stages. In the beginning, the structure can provide a large inner volume for the swollen wrist. Later when swelling decreases, the splint can shift to a shape with a smaller inner volume to provide appropriate immobilisation for the normal-sized wrist. If the new biopolymers with different levels of stiffness have different degrees of thermal expansion or hydro swelling, they can be combined in a structure and consequently the shape-shifting of the splint can be triggered by heat or

moisture.

Compared with the systems including rigid skeletons, I observed that the systems with hydrostatic skeletons worked differently. Kier (2012) stated that the physical basis of hydrostatic skeletons is the unchanging volume of muscles, other tissues and fluids. He explained that when the contraction of muscles results in the decrease of one dimension, the unchanging volume ensures the consequent increase of another dimension, which leads to the "deformations, movements and changes in stiffness" of these animals' bodies (p. 1247). How the contraction of muscles affects the change of dimension depends on the alignment of the muscle fibres. For example, if we consider the mantle of a squid to be a cylindrical elastic container with two layers of muscle walls, we can understand the mechanics behind a squid's change of shape are based on the activities of its different muscle fibers. The inner wall of the elastic container consists of muscle fibers aligned along the circumference of the cylinder (circular muscle fibers), and the outer wall consists of muscle fibers aligned along the radius (radial muscle fibers). As is shown in Detail 11 (Figure 4), the contraction of the circular muscle fibers and the relaxation of the radial muscle fibers in collaboration bring about the decrease of the circumference of the container as well as the inner volume, so the water inside the squid's body is squeezed out. Reversely, when the

squid needs to suck in water, the radial muscle fibers on the outer layer contract and the circular muscle fibers on the inner layer are relaxed, which results in the increase of the container’s thinner volume, as is shown in Detail 12 (Figure 4). The mechanics behind the shape-shifting performed by this type of skeleton-muscle structure reminded me that it was not only the combination of hard and soft materials that could enable shape-shifting. In a multi-layer structure, such as the mantle of a squid, according to the performances of different muscle fibers, we can see that by controlling the geometric design of the components that make up each layer, there is a chance to guarantee the deformation of the whole structure.

Later I printed with the new experimental materials at the UoW during my internship (which is reported in the following section) and acquired more first-hand information about the two new groups of experimental materials: the rigid cellulose-biopolyesters (CBs) and the soft cellulose-biopolyester foams (CBFs). I conducted more research on relevant biological structures to inspire my design based on the mechanical properties of these materials. I compared the Young’s modulus of the new materials, provided by Dr John McDonald-Wharry, with that of a few typical materials existing in organisms, as is shown in Figure 5.

Material	Young's Modulus (MPa)
Pregnant locust intersegmental membrane	0.2
The new experimental cellulose-biopolyester foams	~0.3 MPa to 10 MPa
Aorta, pig	0.5
Abductin (bivalve hinge ligament)	4
Cartilage	20
Tendon (mainly collagen)	1,500
The new experimental cellulose-biopolyesters	~1,800 MPa to 14,000 MPa
Horn, bovid (mainly keratin)	4,000
Wood, dry, with grain (typical)	10,000
Locust apodeme (mainly chitin)	12,000
Bone (large mammal)	18,000
Mollusk shell (nacre)	50,000

Figure 5. Author, Comparison between the new experimental materials and some typical natural materials

The data of the experimental materials are from Dr John McDonald-Wharry.
The data of other materials are from Vogel (2003)

Young’s modulus indicates the stiffness of a material (Vogel, 2003). According to the comparison, I found the stiffness of the most rigid material available for my project is similar to that of a locust apodeme, a part of a locust’s exoskeleton. They are both semi-stiff materials. This discovery triggered my interest in looking into the body of a locust, in which semi-stiff materials form the exoskeleton supporting the locust’s weight. Considering the design as a wearable device that is expected to be durable and relatively light, I especially looked into the structure of a locust’s wing, in which the veins hold the thin membrane as a whole in daily movements.

I found an inspiring paper about the structure of insects' wings by Dirks and Taylor (2012). According to this paper, the existence of veins increases the stiffness of the wing, but the “longitudinal veins” (LVs) and “cross veins” (CVs) (p. 2) of a locust wing have different forms: the LVs are continuous cylindrical tubes with a relatively constant diameter, while the CVs have diverse diameters. The different forms of the veins are shown in Figure 6.

Dirks and Taylor (2012) stated that the typical structure of these CVs increased the flexibility of the wing of a locust when the wing was bent. This structure inspired me to think about the geometric structure of the reinforcing parts in my wrist splint.

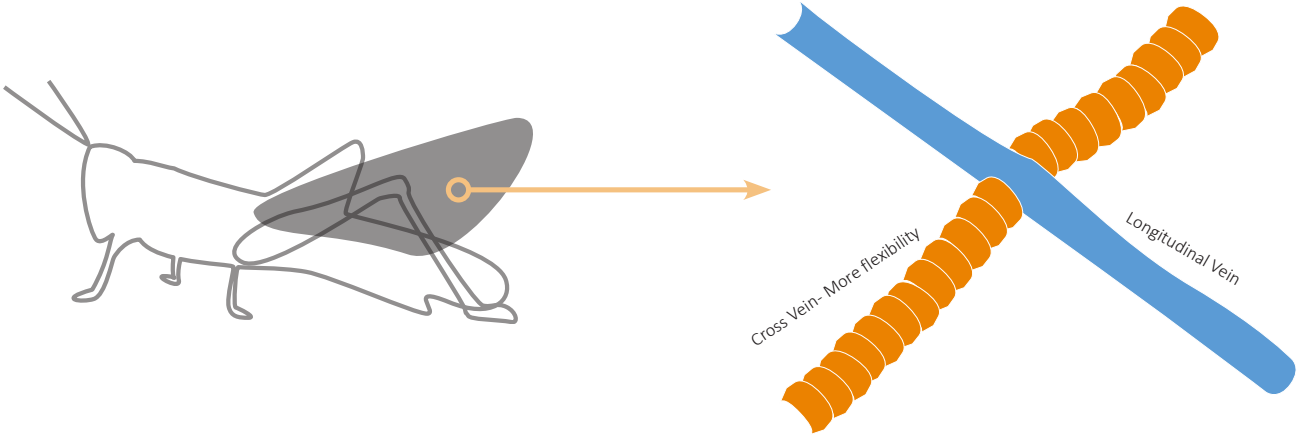


Figure 6. Author, Two types of vein forms on a locust wing

3 Exploration of the New Materials and Determination of the Material Specifications for the Project

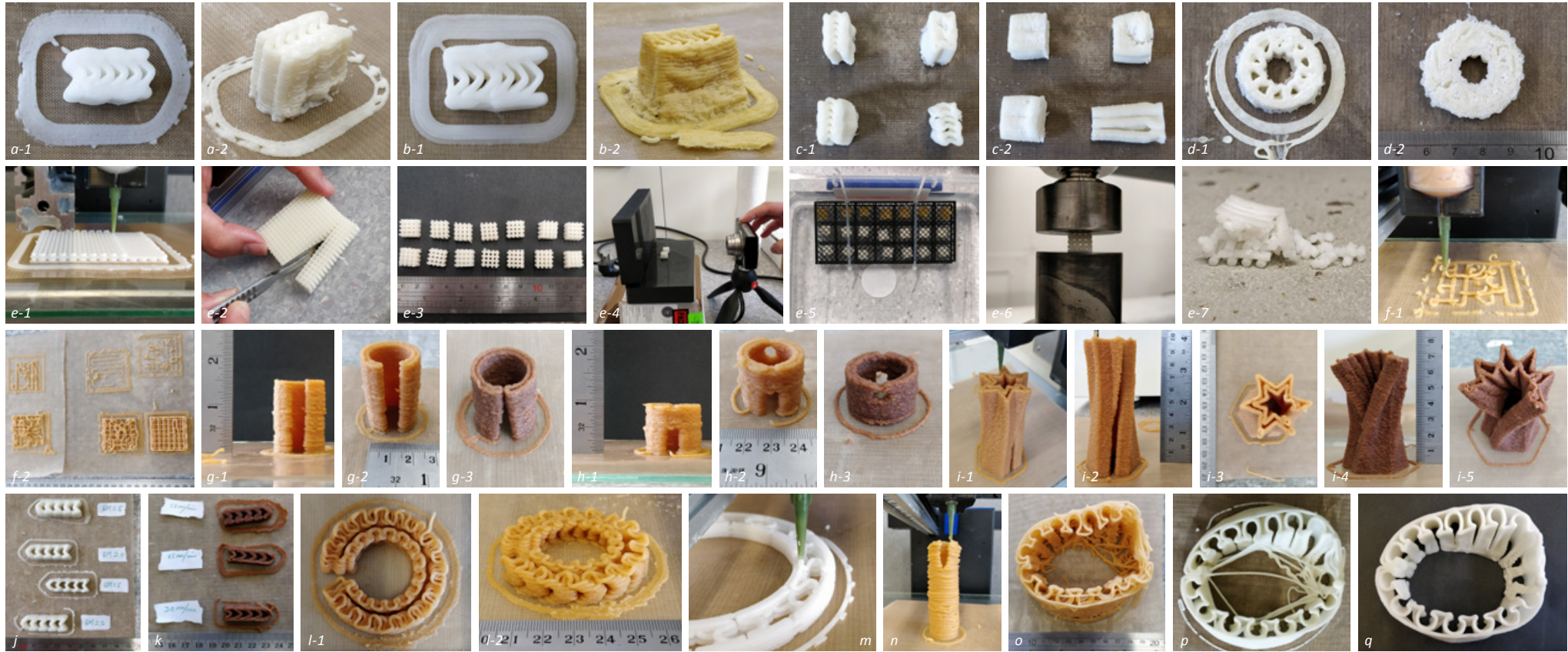


Figure 7. Author, Exploration of new experimental materials

Shrinkage, distortion, blistering caused by water occurred in the models printed with the new foam materials, as is shown in Figure 7(a-1) to 7(d-2). Systematic tests were done to study the mechanical properties of the foam materials printed in a lattice structure, as is shown in Figure 7(e-1) to 7(e-7). Initiating the printing of a new material required several rounds of test printing to optimise the extruding speed and the travelling speed of the nozzle, because of the unknown viscosity, as is shown in Figure 7(f-1) and 7(f-2). Figure 7(g-1) to (i-5) show the exploration of the vase mode in printing with the rigid material. The quality of prints largely depends on the extruding speed and the travelling speed of the nozzle, as is shown in Figure 7(j) and (k). Figure 7(l-1) to (o) show the printing test of more complex structures, including an early design of the splint, with different materials based on the previous printing. Figure 7(p) and (q) shows the best print and the expected model, which was achieved after unexpected extrusions inside the model were cut off.

In essence, printing can now become a Materials Science chamber where the designer is able to customize the deposition of materials, anisotropic behaviors and active sensing based on the surrounding environment.

(Tibbits, McKnelly, Olguin, Dikovsky, and Hirsch, 2014, p. 540)

4D printing and Material Science inspire each other. New responsive materials have brought fundamental challenges to the 4D printing processes to achieve high-quality prints, but they have also greatly enhanced the chance to realise unconventional functions.

The Science for Technological Innovation challenge, as one of New Zealand's National Science Challenges (NSCs), is hosted by Callaghan Innovation, and funded by the Ministry of Business, Innovation and Employment. The Challenge is divided into five portfolios. My work is a part of Portfolio 5 Spearhead projects, "Additive manufacturing and 3D and/or 4D printing of bio-composites". To fulfil the requirements of the project, the development team includes members from various organisations, including SCION, Auckland University of Technology, Massey University, Victoria University of Wellington, University of Auckland, AgResearch, UoW and GNS. These material scientists, engineers and designers are cooperating to develop new responsive bio-based materials and explore the design scope of

3D/4D printing with these materials.

At an early stage of my project, I did an internship at the UoW to collaborate directly with the material scientist, Dr John McDonald-Wharry, in a lab setting and learn knowledge about the available materials. More importantly, as a designer, working on the site enabled me to collect a large amount of first-hand experience in designing, printing and testing these materials. Based on the knowledge and experience I gained from the actual practice at the UoW, I returned to the design studio and developed my designs. As I gradually framed my design concepts, I was able to provide the material scientist with revised requirements and expectations of the properties for the new materials. I then spent a substantial amount of time improving the printability of the new materials and the quality of the prototypes, as which will be explained in this and the following chapters.

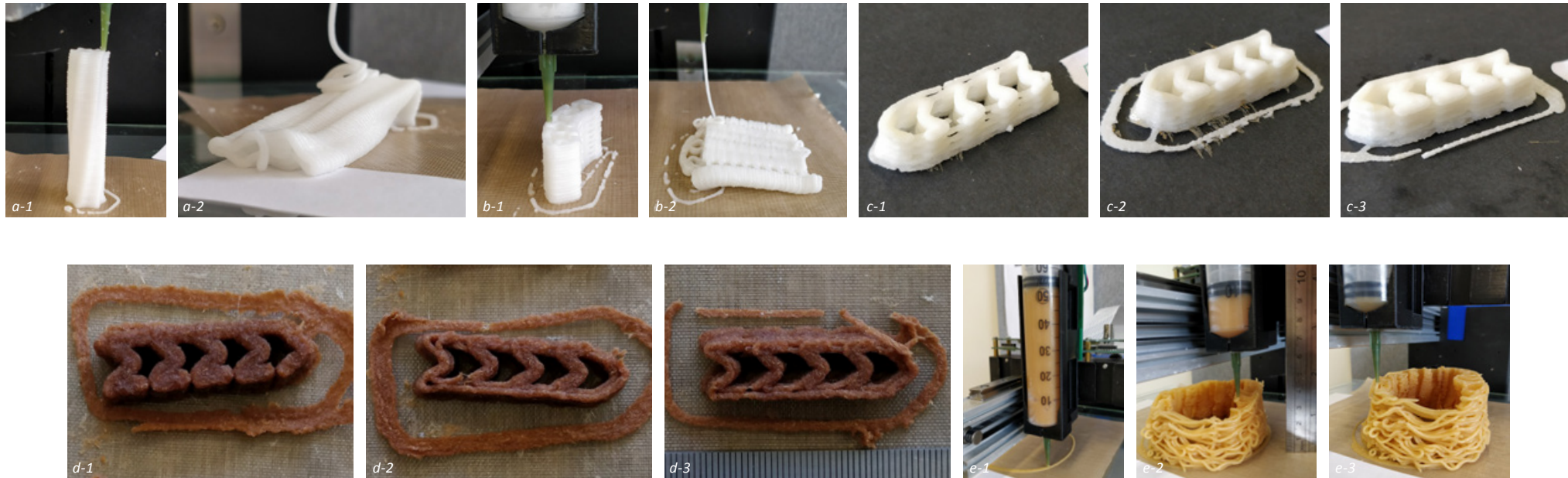


Figure 8. Author, Study on the printability of the new materials

Figure 8(a-1) to (b-2) show the collapse of prints during printing. Figure 8(c-1) to (c-3) show the different effects of printing resulted from different extruding speed. Figure 8(d-1) to (d-3) show the different effects of printing resulted from different travelling speed. Figure 8(e-1) to (e-3) show a model printed by a full syringe of material (about 55 ml).

3.1 The properties and performances of the available materials

3.1.1 Printability

Momeni, M.Mehdi Hassani.N, Liu, and Ni (2017) stated that there are two requirements for the materials used in 4D printing: intelligence and printability. If we consider responsiveness as a key factor that determines the functions of the final product, printability affects the outcome at a much earlier stage. As printing is a core process of 4D manufacture, the printability of a material determines whether and how well the material can be employed. The printing process that suits a material is decided by the properties of the material, such as the synthesis process and the phase transition of the material. The printing quality of a material is decided by how well the printing process suits the material and the compatibility of the material with current printing technology.

Most commercial printers, such as the fused deposition modeling (FDM) printer and the Connex printer, usually combine their printing processes with curing to achieve solidified prints after printing. Curing is a process applied to materials in order to change

their state or properties to reach a relatively stable status. This can be realised by changing their inner structures, for example, using chemical or physical crosslinks to set a permanent shape of heat-stimulated SMPs (Miao et al., 2017). Different from the printing process of the FDM printer and the Connex printer, the printing process used by the bio-based polymers in this project is paste-printing (Figure 7). The materials are deposited through a nozzle onto a platform, in a similar way to decorating a cake with whipped cream. Curing is carried out in an oven after printing. All the research on paste-printing in my project is based on this printing process and the paste printer at the UoW. That is to say, during printing, no external intervention, such as heat and light, is applied to solidify the extrusion material. In this case, the prints are soft. This largely influenced the design of the geometric structures of the models, because the deposited structures need to be stable enough to support themselves until they are sent for curing. This means the models cannot be too thin or too high (Figure 8), or have an excessive overhang, and often the movements of the build platform need to be slowed down to avoid collapse due to shaking.

Moreover, the new materials are shear thinning materials, such as whipped cream and ketchup. The materials are relatively thick when they are kept still. During printing, the shear created by the plunger of the syringe will make the materials thin and flowing.

The materials will regain thickness after being deposited. The complex behaviour of the materials increases the difficulty in controlling the start and stop of extrusion in an instant way during printing.

These problems we faced in printing were also encountered by other researchers working with other materials such as ceramics, clay and biomedical gels. Lewis, Smay, Stuecker, and Cesarano (2006) stated in their paper that during the deposition of ceramic materials, it was undesirable to interrupt the flow of the material. For this reason, they believed it was very useful to avoid start-stop occasions during the process.

To improve the printability of these new materials, I improved the design approach for paste-printing. I started from printing with stl models and ended by printing with G-Codes. Using G-Code for printing allows various extrusion rates and speeds of nozzle travelling throughout the printing of one model, and thus achieving a more accurate control of the amount of extrusion. More importantly, using G-Code allows reducing rapid movement to the minimum, thus enhancing the quality of printing.

Printing with stl models created with CAD programmes is a widely used approach. Usually when inputting an stl model, the software

used by the 3D printer will automatically slice the stl model to connected layers and convert these layers into a printing path. The printing path is then coded to guide the operation of the printer. In practice though, I found the automatic slicing was not satisfactory for our printing, because of the leaking of paste. As is mentioned, our new materials were thinner during the printing process than kept still. When the syringe stopped to create shear, the materials farthest from the plunger, that is to say, near the nozzle, were still at the thin and flowing status because of their inertia. So it was not possible to stop extrusion instantly. For the same reason, it was not possible to start extrusion instantly either. In conclusion, stopping and restarting printing would result in over extrusion and delayed extrusion.

Therefore, I explored and analysed different printing techniques to develop more suitable methods and techniques for paste-printing. The processes are shown in the following chapter.

Other situations to consider in designing with the new materials include the accuracy of printing, the capacity of the syringe, the influences of the extruding speed and the traveling speed (Figure 8).

The thickness of the extrusion used in this project is about 1.4mm,

which is mainly defined by the diameter of the nozzle. The reason why I selected this nozzle is that according to the experience provided by Dr John McDonald-Wharry, the material is more likely to block a thinner nozzle. The thickness of extrusion is also affected by the extruding speed and the traveling speed. The thickness can be reduced by decreasing the extruding speed or increasing the travelling speed.

Our printer uses a 60 ml syringe (Figure 8), a limited volume of print material, in comparison to an FDM printer that uses a roll of solid filament, which is heated above its melting point for extrusion and is cooled down to become solid. A standard 1kg roll of filament for FDM printing can support the printing of an 800ml model (PLA) or a 960ml model (ABS). In comparison, the maximum volume of a syringe that our printer can hold is about 55ml, slightly larger than half of an average sized apple. Theoretically, we can pause the printing to replace the used up syringe with a full one and continue the process, but printing with multiple syringes of material(s) requires some optimisation in printing process to acquire models with good quality. This optimised process for printing with two syringes of two different materials is shown in the following chapter.

3.1.2 Responsiveness

- Shape-memory triggered by heat

I tested the shape-memory performance of the circular corrugated segment printed with a rigid experimental, Formulation QX3. Figure 9 shows a dynamic process of shape-shifting. The image was produced by overlapping four shots from the video that recorded the shape-shifting process triggered by heat from a hair dryer.

The prototype was 3D printed and cured in an oven at 105 degrees centigrade for 48 hours as a permanent shape. Then it was heated up to over 80 degrees centigrade, deformed into a temporary shape and cooled down to lock the shape. During the experiment, the prototype was heated up to about a hundred degrees centigrade to fully return to its permanent shape.

This experiment shows that the shape-memory of the material can be used to realise shape-shifting and thus the change of inner volume for the splint to adapt to the decrease of swelling. The problem is the current working temperature of this material is too high for human skin.

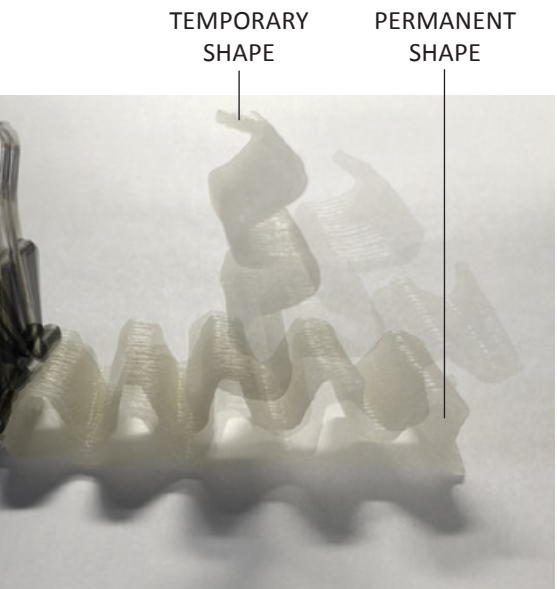


Figure 9. Author, Shape-shifting

- Decrease of anti-bending stiffness triggered by water

Our material development team tested the flexural modulus of a rigid experimental material, Formulation H. The result shows the material progressively loses the ability to resist bending with repeated water immersions over a time frame (Figure 10).

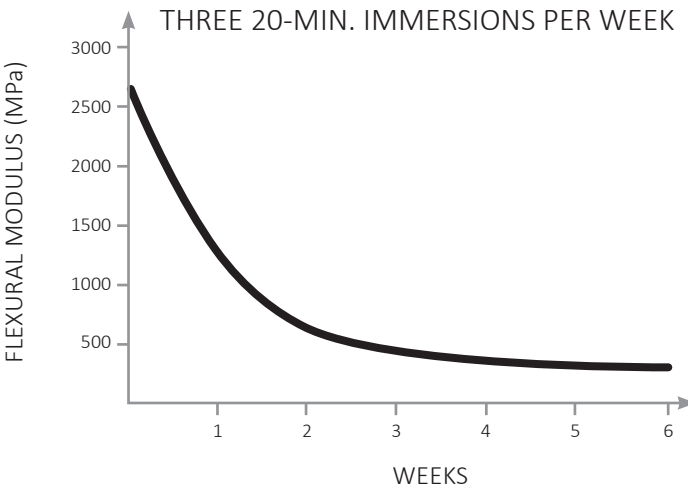


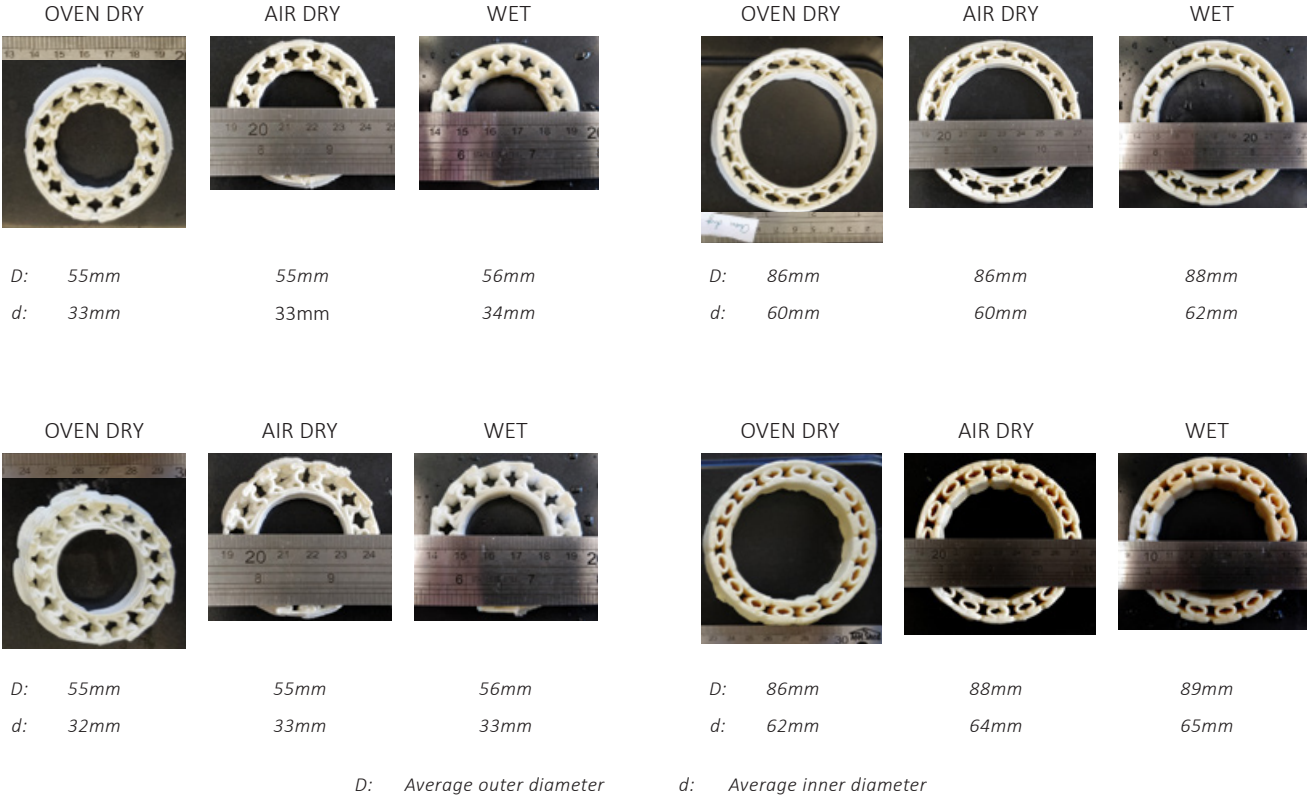
Figure 10. Author, Decrease of stiffness

- Hydro swelling

I printed a collection of linear segments and several circular segments to study the hydro swelling behaviour of two foam materials. More importantly, I expected to see whether the hydro swelling behaviour of the materials in cooperation with the multi-layered structure can provide a predictable change of inner volume for a circular model.

I compared the dimensions of the prototypes at three different statuses: oven dry, air dry and wet. In the first round of tests, the prototypes were immersed in water for about 15 minutes. Then I found the inner volume change of the circular segments was not obvious to observe (Figure 11), and the size change of the linear segments was even harder to see. Besides, I found the experimental foam material which was used to print the linear segments was relatively strong when both dry and wet, while the material used to print the circular segments could be easily damaged when wet. I redid the test on the linear segments to obtain more accurate data.

In the second round of tests, the linear segments were immersed in water for 24 hours to perform thorough hydro swelling. I documented the dimensions and calculated the average



OVEN DRY



AIR DRY



WET



D: 86mm

d: 60mm

OVEN DRY



AIR DRY



WET



D: 55mm

d: 32mm

OVEN DRY



AIR DRY



WET



D: 86mm

d: 62mm

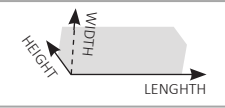





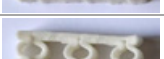

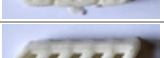




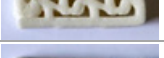
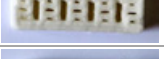



D: Average outer diameter

d: Average inner diameter

Figure 11. Author, First round of research on hydro swelling

Figure 12. Author, Second round of research on hydro swelling

proportion of hydro swelling, as is shown in Figure 12. In conclusion, the experimental foam materials have a certain level of hydro swelling, but currently the combination of the materials and the multi-layered structure cannot enable an obvious inner volume change for a circular model.

	Pattern Code	Picture	Length		Expansion of Length	Width		Expansion of Width	Thickness		Expansion of Thickness
			Oven Dried	Immersed in Water for 24 hr		Oven Dried	Immersed in Water for 24 hr		Oven Dried	Immersed in Water for 24 hr	
	A		36	39	8.3%	10	11	10.0%	7	8	14.3%
	B		37	39	5.4%	10	11	10.0%	7	8	14.3%
	C		37	39	5.4%	10	11	10.0%	7	8	14.3%
	D		38	40	5.3%	10.5	11.5	9.5%	7.5	8	6.7%
	E		38.5	40	3.9%	10	11.5	15.0%	7	8	14.3%
	F		37	38.5	4.1%	10	11	10.0%	6	7.5	25.0%
	G		37.5	39	4.0%	10	11	10.0%	7	8	14.3%
	H		36.5	39	6.8%	10	11	10.0%	7	7.5	7.1%
	I		39	41	5.1%	11	11.5	4.5%	7	8	14.3%
	J		38	39.5	3.9%	10.5	11	4.8%	7.5	8	6.7%
	K		38	39	2.6%	11	11.5	4.5%	7.5	8	6.7%
	L		38	40	5.3%	11	11.5	4.5%	8	8	0.0%
	M		38	40	5.3%	10.5	11	4.8%	7	7.5	7.1%
	N		38.5	40.5	5.2%	10	11	10.0%	7	7.5	7.1%
	O		38.5	41	6.5%	10	11.5	15.0%	7	7.5	7.1%
	P		38.5	40	3.9%	11	11	0.0%	7	7.5	7.1%
	Q		37.5	39.5	5.3%	10.5	11	4.8%	7	7.5	7.1%
Average Expansion Proportion			5.1%			8.1%			10.2%		

3.1.3 Shrinkage, collapse, blistering caused by water and cracks

In addition to the printability and the responsiveness, which are directly relevant to 4D printing technology, four important properties of the new materials need to be taken into consideration. These properties affect the models during curing.

For our materials, curing is an essential process after printing. The target of curing is to solidify the prints to complete the manufacture of a 3D structure. The phase of our materials changes during curing, because synthesis reactions happen in the ingredients. In these chemical reactions, the ingredients cross-link and produce water. The curing process for our materials is stimulated by heat. After printing, the models are kept in an oven at 105 degrees centigrade for 48 hours for the ingredients to fully cross-link with each other and for the water in the paste to be fully vapourised. Depending on the specific ingredients in a paste and the amount of paste is used, the curing processes could be further optimised.

- Shrinkage

Models shrink after curing (Figure 13a), mainly because when

water is vapourised and leaves the models, the volume of the material decreases. The shrinkage does not only affect the dimensions of a model. We observed anisotropic shrinkage. In other words, the degrees of shrinkage along different directions are different. Anisotropic shrinkage affects the shape of a model. The degrees of shrinkage along relevant directions should be considered in making a CAD model, so that after curing the model can precisely match the target design. But because the degree of shrinkage is largely determined by the amount of water that leaves during curing, the formulation of a material affects the degree of shrinkage. Because at the early stage of material development, the formulation was continuously changed to acquire better strength and better printability of the materials, more research was done to measure the degrees of shrinkage of the selected material along various directions at a later stage. The measurement was taken as the basis to rectify the CAD models and to optimise the process of building prototypes, as is shown in the following chapter.

- Collapse

Another property that affects the shape of the models is a tendency towards collapse. Collapse happened to some of my models in the first several hours after sent into the oven, possibly because the heat in the oven makes the paste more fluid

before the ingredients start to cross-link. Unlike shrinkage, the influence of which can possibly be rectified, the harm of collapse is unrectifiable. I observed that whether a model will collapse will happen largely depends on the shape of it. Firstly, a leaning wall is more easily to collapse than a vertical wall. Secondly, a higher model is more easily to collapse (Figure 13b). Thirdly, a model in which its weight is distributed unevenly is more easily to collapse. These must be taken into consideration in design to avoid the damage of a model.

- Blistering caused by water

Another tendency that will harm a model is blistering caused by water. As is mentioned, the water in a model will all be vapourised and leave the model in curing. The amount of water in the model depends on the formulation of the material, which could be reduced, but it was not possible to avoid water from generating based on the principle of the current applied cross-link reactions. In this case, if a model does not include enough voids as appropriate paths for the water steam inside the model to leave, the water steam will make its own way by breaking the model (Figure 13c). Generally, the larger a model is, the more voids it should include to avoid the damage from the blistering of water. Besides, closed voids will not be useful, because steam needs a

continuous way towards out of the model. This limits the variety of structures that can be built with these materials.

- Cracks

The occurrence of cracks in models is closely related to the formulation of the material. It might be the result of uneven shrinkage. It happened more frequently in larger models and on thin walls (Figure 13d).

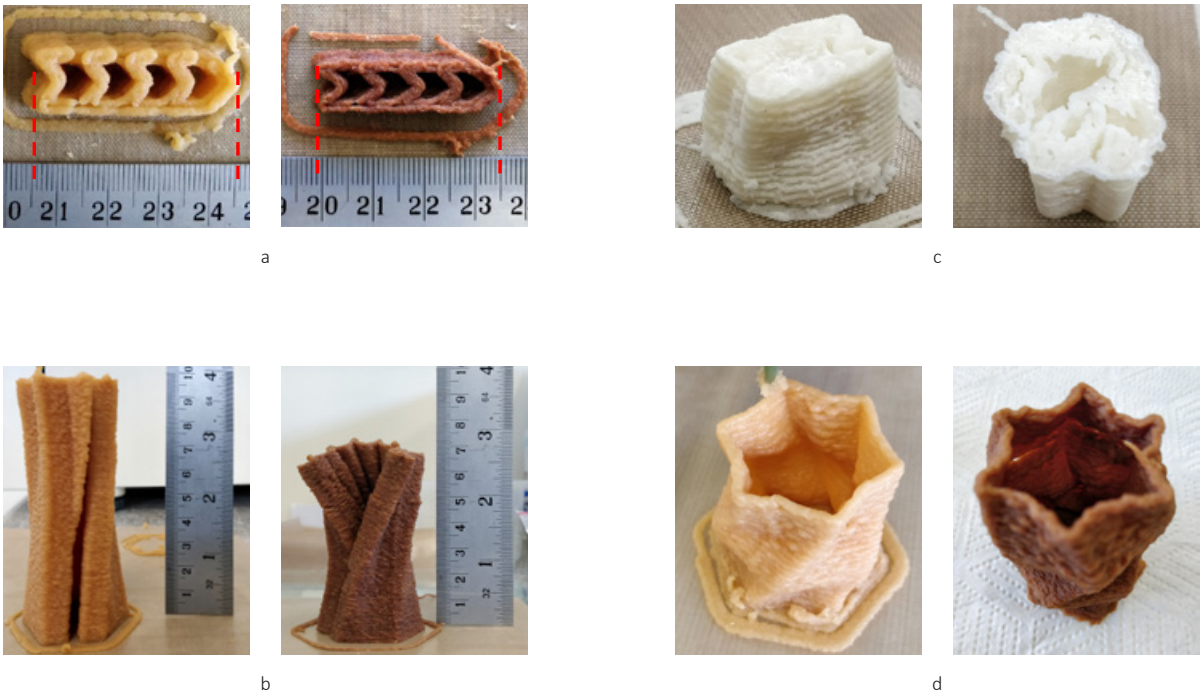


Figure 13. Author, Shrinkage, collapse, blistering caused by water and cracks

<i>Rehabilitation stage of a wrist</i>	Recover from swelling (Immobilisation)		Start to take exercises (Consolidation)			
<i>Function of the splint</i>	Contraction around wrist as swelling decreases		Increase flexibility in target areas (one-off)		Increase flexibility in target areas (for repeated use)	
<i>Stimulus</i>	Moisture ⁱ		Moisture		Heat or Moisture	
<i>Response of the material</i>	Resetable shape-shifting and mechanical force (swelling)		Irreversible damage or disintergration		Resetable shape-shifting and mechanical force (shape memory)	
<i>Design features and mechanism</i>	1) Multi-thickness 2) Multi-density 3) Multi-pattern		1) Multi-thickness 2) Multi-density		1) Multi-thickness 2) Multi-density	
<i>Available material</i>	Foam	Non-foam	Foam	Non-foam	Foam	Non-foam
<i>Current status</i>	Not strong enough for immobilisation or support	Need to test the degree of expansion in demonstrators	Not strong enough for immobilisation or support	Possible	Not strong enough for immobilisation or support	The change of stiffness is slower than expected
<i>Possibility to improve</i>	ⁱⁱ	Will design ⁱⁱⁱ demonstrators	ⁱⁱ	Will design ^{iv} demonstrators	ⁱⁱ	^{viii}

Figure 14. Author, Summary of design possibilities based on one material and request on the specifications of the material

<i>Rehabilitation stage of a wrist</i>	Recover from swelling (Immobilisation)		Start to take exercises (Consolidation)	
<i>Function of the splint</i>	Contraction around wrist as swelling decreases		Increase flexibility in target areas (one-off)	
<i>Stimulus</i>	Moisture ^v		Moisture	
<i>Responses of the materials</i>	M1: Resetable shape-shifting and mechanical force (swelling) M2: Not responsive ^{vi}		M1: Not responsive M2: Irreversible damage or disintergration	
<i>Design features and mechanism</i>	M1: 1) Multi-thickness; 2) Multi-density; 3) Multi-pattern M2: Reinforcing components		M1: 1) Multi-thickness; 2) Multi-density M2: Reinforcing components	
<i>Available materials</i>	M1: Foam M2: Non-foam		M1: Foam M2: Non-foam	
<i>Current status</i>	Need to test the degree of contraction in a bilayer demonstrator ^{vii}		M2: The change of stiffness is slower than expected	
<i>Possibility to improve</i>	Will design the demonstrators		^{iv}	

Figure 15. Author, Summary of design possibilities based on dual material and request on the specifications of the materials

M1: Material 1, M2: Material 2

3.2 Determination of the material specifications for the project

3.2.1 Request on the specifications of materials

Based on the acquired information about the properties of the new materials and the target functions of the splint, I looked into the possibilities of realising my design and listed them in Figure 14 and 15. In each table, I included the request on the specifications of the materials for each possibility. I sent the tables to Dr John McDonald-Wharry for him to estimate whether the new materials had the potential to fulfil the requirements.

Although at that stage the simultaneously ongoing progresses of both material development and design exploration resulted in significant uncertainty, these two tables helped me to summarise the possible directions for further design. The tables also provided a basis for Dr John McDonald-Wharry and me to have a clearer communication on the specification of materials and for him to offer me a comprehensive assessment on the requested performances of the materials.

3.2.2 Feedback from the material scientist

Based on the previous tables (Figure 14 and 15), I received Dr John McDonald-Wharry's feedback on each item. Based on his feedback:

- i) Can also use shape memory effect (SME)
- ii) Has a certain level of feasibility
- iii) Would need to work on the alignment of the strands
- iv) Has a relatively high feasibility
- v) Can also use moisture or heat to trigger SME
- vi) Shape memory non-foam has a relatively high feasibility
- vii) Several mechanisms can be tested
- viii) The speed of change can be further optimised according to needs

3.2.3 Discussion and reflection

After rounds of discussion with Dr John McDonald-Wharry based on the properties of the materials and the requirements of rehabilitation, I formed my decision on the specifications of the materials. I then selected two out of four performances provided by the available responsive materials for my project (Figure 16).

I decided to employ the SME of the rigid material in the middle layer to enable shape-shifting for the splint's change of inner volume. The effect of water plasticisation was selected to be employed in both the middle layer and the outer layer to provide the splint with the immobilisation and the extra reinforcement which both weaken through time.

Theoretically, we could use the same rigid material for both middle and outer layers as long as the material has both of these two effects: shape memory and water plasticisation. The shape memory effect can easily be turned off if the material is not deformed to a different temporary shape after it is cured into a permanent shape.

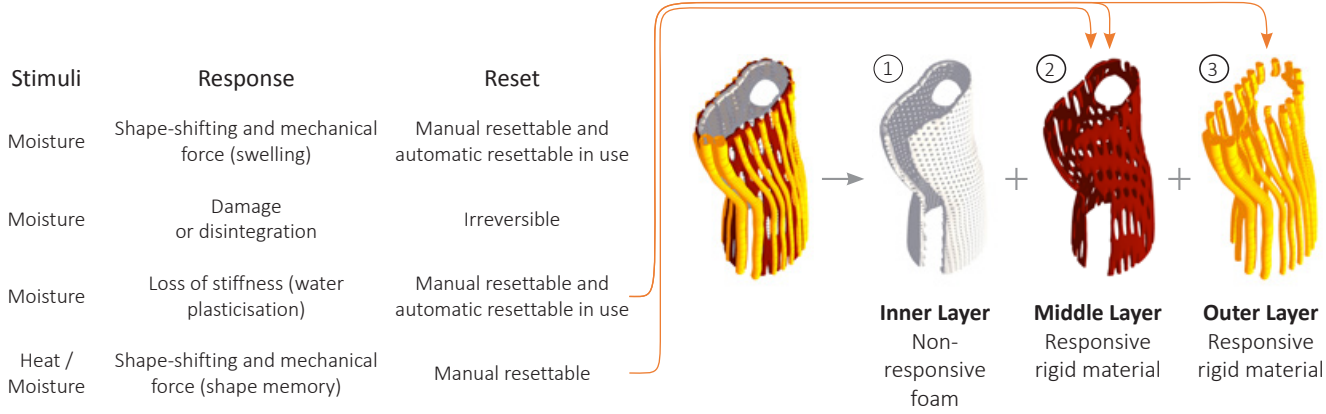


Figure 16. Author, Determined responsive performances of the new materials potentially available for the project and the specific application in the structure

4 Exploration of Design

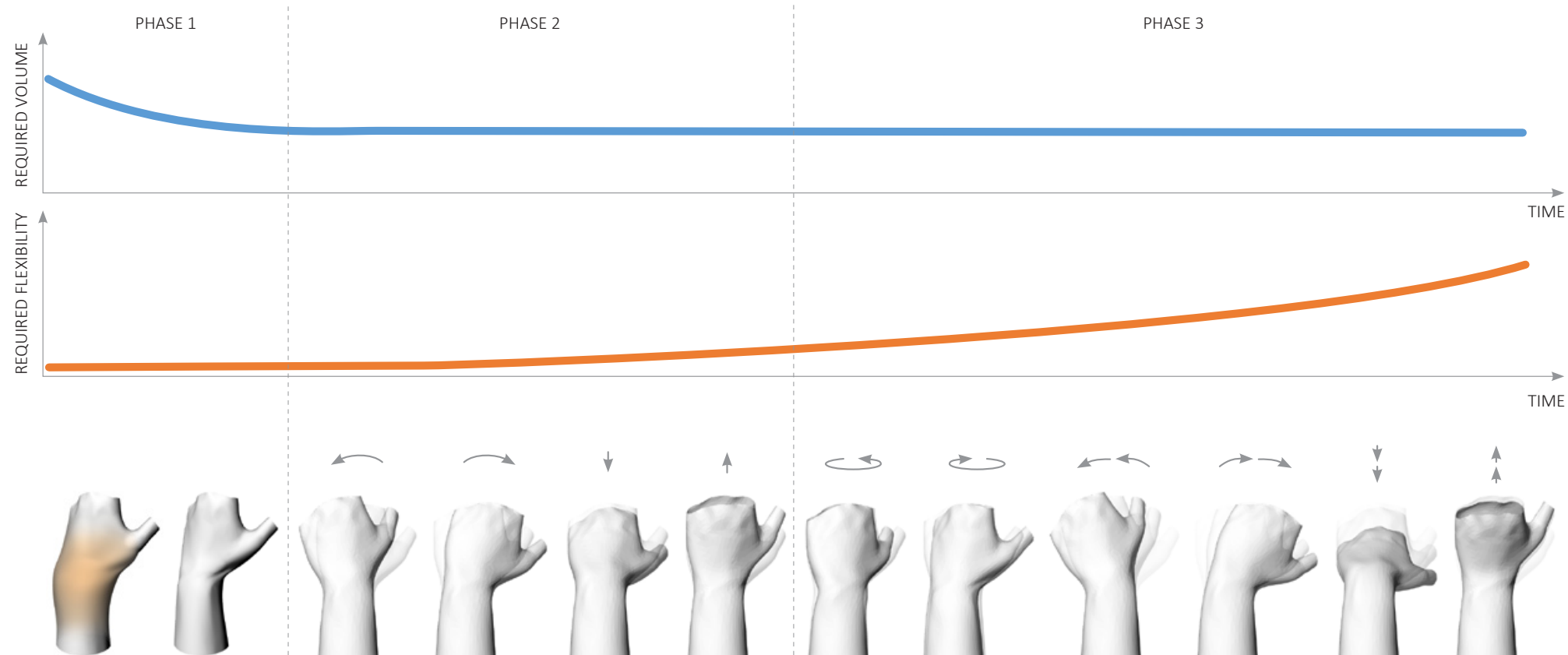


Figure 17. Author, Scenario

4.1 The scenario and concept design

Figure 17 shows the scenario of using the adaptive wrist splint responding to the requirements of a rehabilitation process:

- In the first phase, the splint will provide the swollen wrist with an extra inner volume for appropriate immobilisation and then adapt to the wrist's normal size when swelling decreases;
- In the second phase, the splint will provide appropriate flexibility in certain areas for light exercises in accordance with a prescribed physiotherapy regime;
- In the third phase, the splint will provide more flexibility in certain areas for advanced exercises again, in accordance with a prescribed physiotherapy regime.

Based on my research, I selected inner volume and flexibility to be the two key factors to determine the performance of the adaptive splint. Through the whole healing process, the required inner volume decreases in the first several days or a couple of weeks, and the required flexibility increases over a longer time when the wrist is healed enough for controlled movements. 4D printing

techniques makes it possible to build an adaptive splint to meet the requirements of different phases by integrating the responsive performances into the splint. The responsive performances include shape-shifting and the decrease of stiffness.

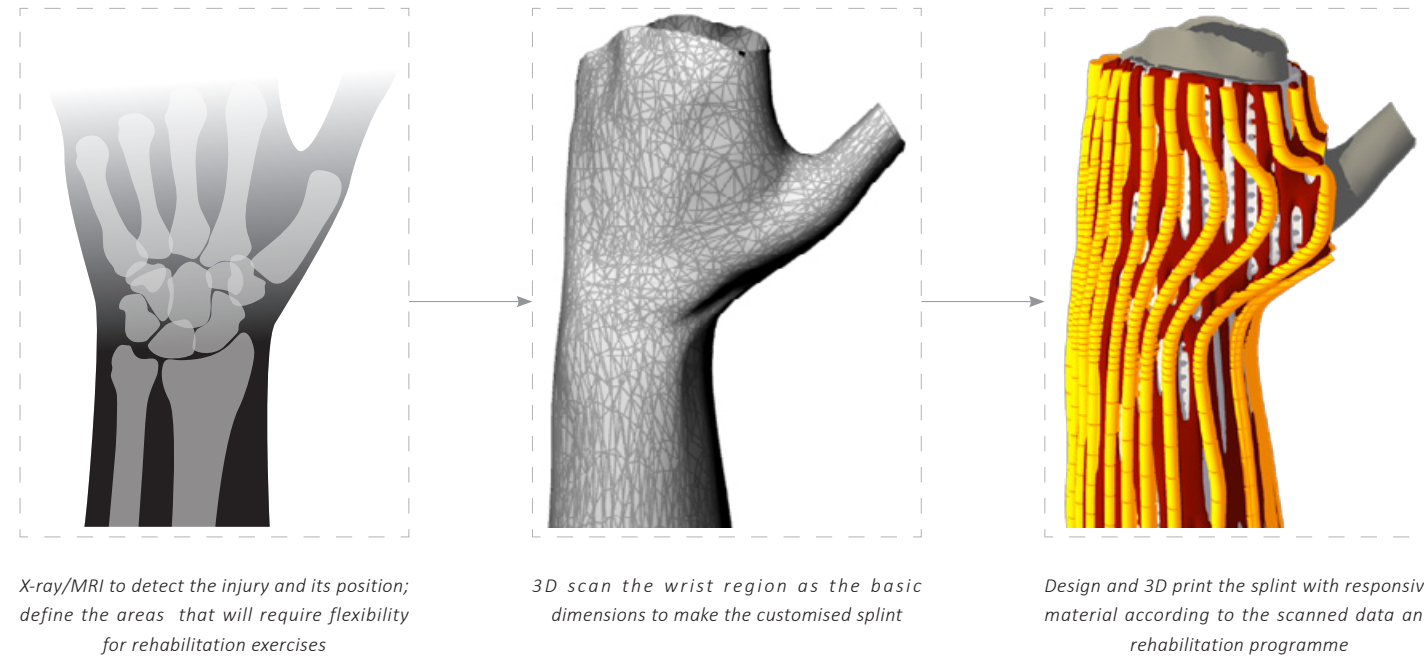


Figure 18. Author, Customised manufacture procedure

As is shown in Figure 18, I designed the procedure of building the customised adaptive splint, which includes three steps. The first step is to examine the injury and plan the rehabilitation programme, including defining the time frame and the areas that will require flexibility for exercises. The second step is to 3D scan the swollen wrist for basic dimensions and 3D scan the opposite wrist to establish the likely normal dimensions of the unswollen wrist, to make the customised splint. The last step is to design and 4D print the splint according to the scan data and the rehabilitation programme prescribed by the therapist.

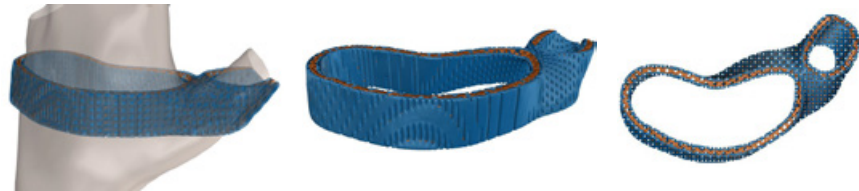


Figure 19. Author, Design inspired by the skeleton-muscle structure of a squid

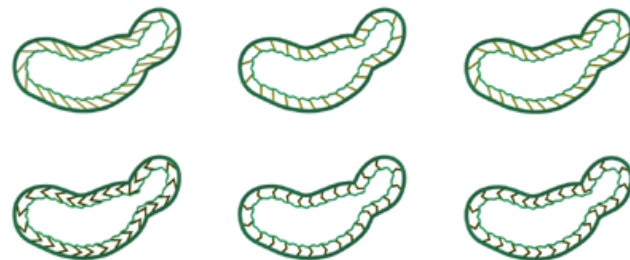


Figure 20. Author, Flat models based on the cross-section of the splint

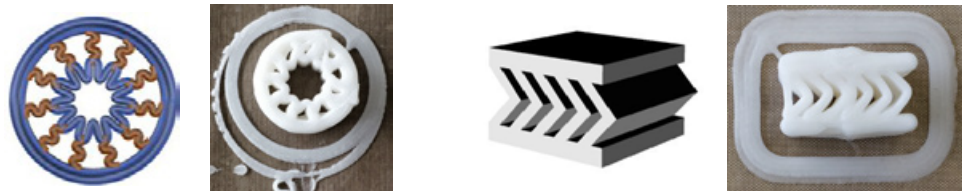


Figure 21. Author, Abstract models and photos of test printing

4.2 Design development with the new materials for responsive performance

4.2.1 Design of the geometric structures

The geometric structure of the adaptive splint was first inspired by the skeleton-muscle structure of a squid's mantle. A squid's mantle is a key part of its body, the shape-shifting of which results in the change its inner volume and consequently enables the locomotion of the squid. According to my research, the shape-shifting behaviour is based on the multi-layered structure composed of muscle fibers aligned in different ways. I was inspired to design a similar structure for the splint to realise the change of its inner volume (Figure 19).

The major difference is that the behaviour of a squid's mantle is an active activity, while the performance of the splint needs to be activated by external forces or conditions. Generally, materials expand when they are heated, and many materials swell when they are hydrated. So heat and water can both be used as the stimulus to activate the shape-shifting. As is shown in Figure 22, expansion and swelling can be used to create shape-

shifting by combining two layers with the same structure made of two different materials, or combining two layers with different structures made of the same material. So I developed a design including three layers with the potential to behave differently when triggered by heat or water. These three layers either perform using different structures or perform through different material formulations.

The above design ideas were developed before I started my internship at the UoW. At that time I received the information that the maximum height of paste-printing was about 15mm and the height decreased after curing. Thus I decided to build some short segments (flat models) based on the design of the full splint to test the performance of the structure (Figure 20). To avoid consuming a large amount of experimental material, I then simplified the contour of the segments and developed some abstract models with only the key features kept. These abstract models were printed during my internship (Figure 21).

After I did my internship, I acquired more information about the properties of the new materials. As is mentioned in the previous chapter, I found the effect of hydro swelling of a single material amplified by the multi-layered structure was not good enough to realise the change of inner volume for the adaptive splint. After

several rounds of discussion with Dr John McDonald-Wharry, I decided to make use of the shape memory property of the rigid material for the change of inner volume.

I designed a corrugated structure based on the scan of my left wrist and cut it to the printable height. In Plan 1.0 (Figure 23), I set the average height of segments at about 30mm according to previous printing experience. Dr John McDonald-Wharry successfully printed the first segment with the height of 32mm, but it collapsed soon after printing. Therefore I reduced the height of all the models.

After that, according to Dr John McDonald-Wharry's observation and suggestion, I made the corrugation square to gain more ability of shape-shifting (Figure 27).

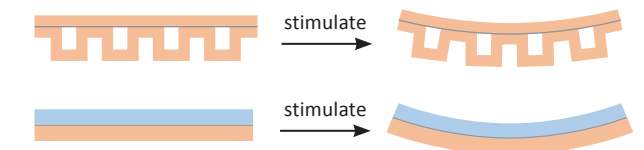


Figure 22. Author, Shape-shifting created by using the expansion or swelling of material

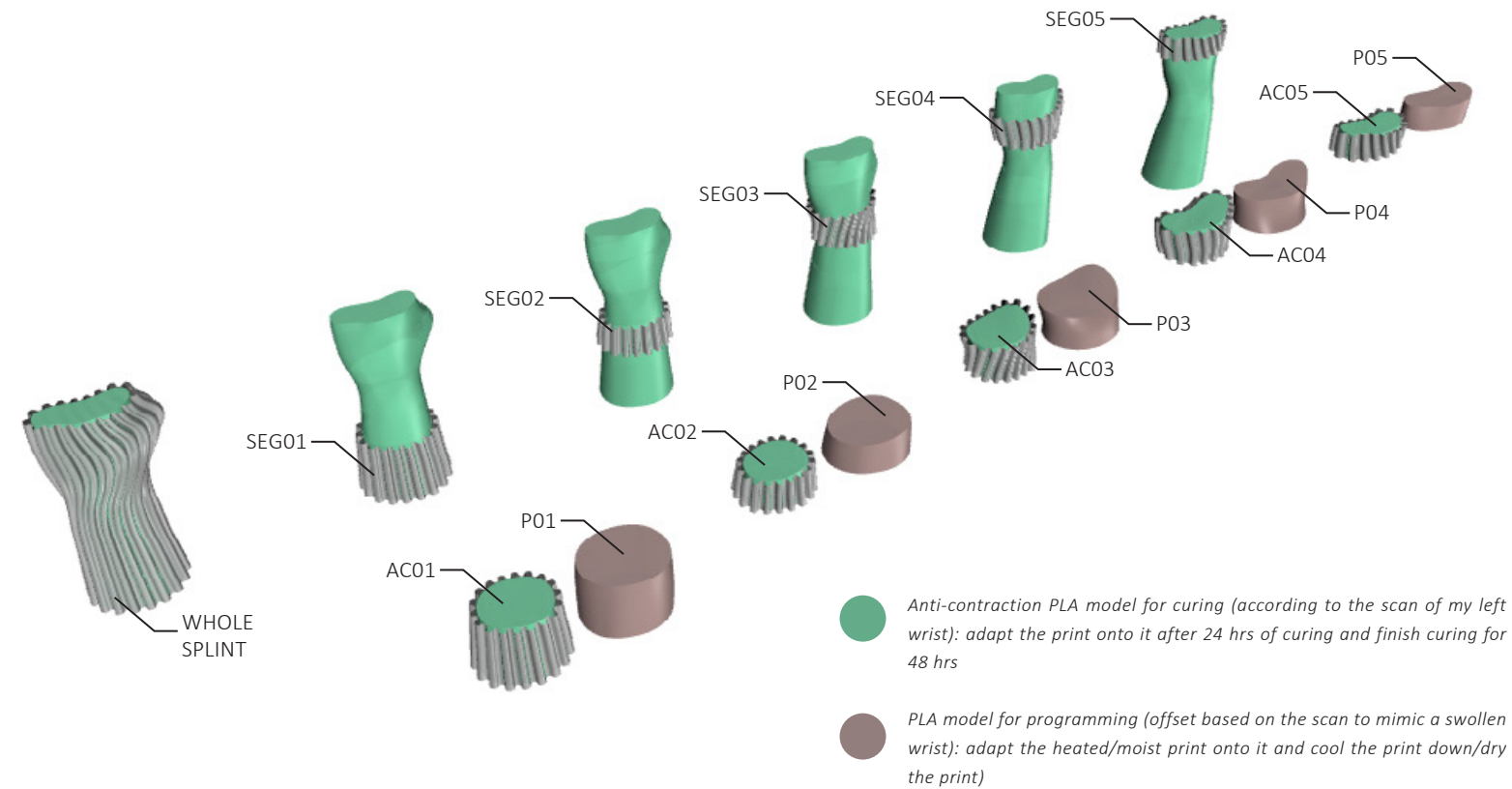


Figure 23. Author, Plan 1.0

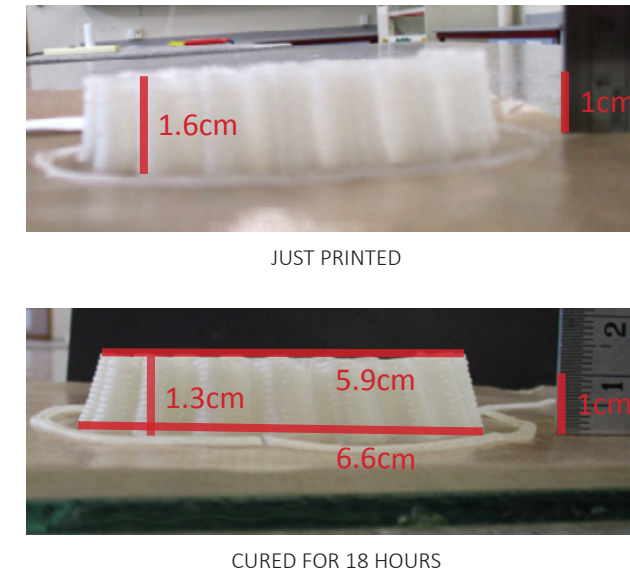


Figure 24. Author, Shrinkage in the vertical direction

Based on the photos taken by Dr John McDonald-Wharry

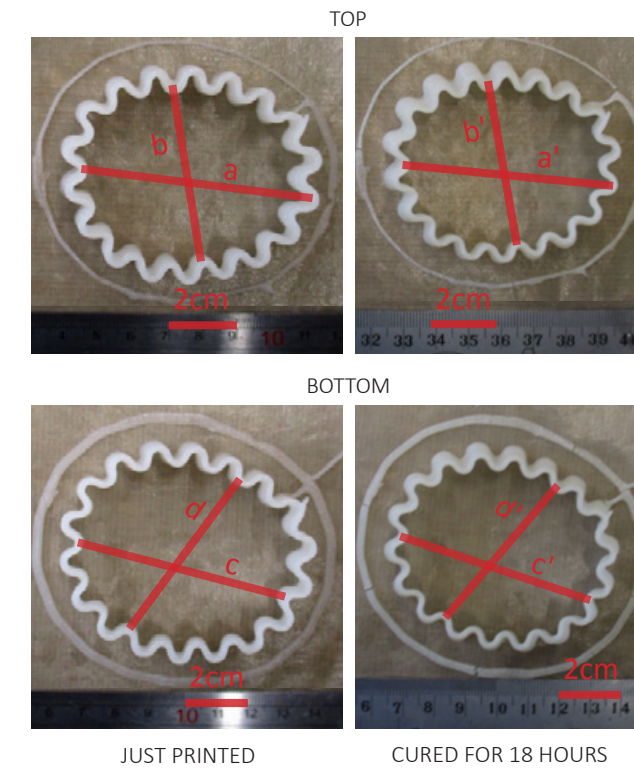


Figure 25. Author, Shrinkage in the horizontal direction

Based on the photos taken by Dr John McDonald-Wharry

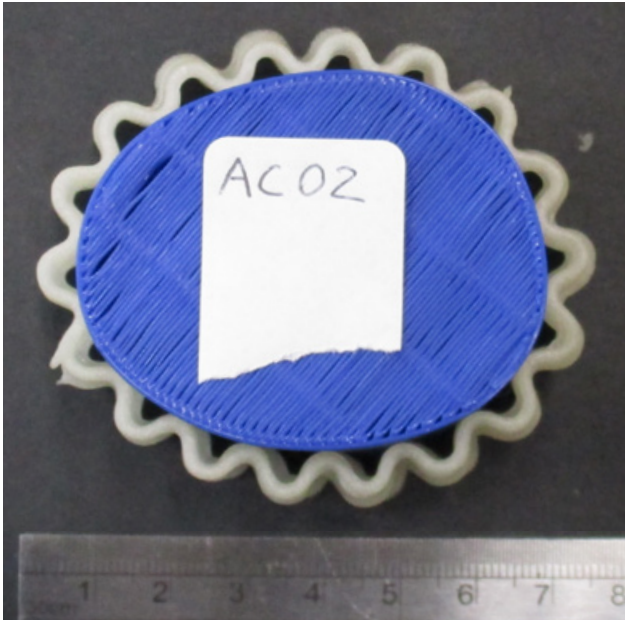
As is shown in Figure 24, after cured for 18 hours, the prototypes shrank by about 19% in the Z direction, compared to just after printing. The shrinkage in the horizontal direction was different in different layers. The top layer shrank 11% more than the bottom layer.

Measurements were taken in the horizontal direction as well, as is shown in Figure 25:

$a = 6.8 \text{ cm}$, $b = 5.2 \text{ cm}$, $c = 6.9 \text{ cm}$, $d = 5.9 \text{ cm}$

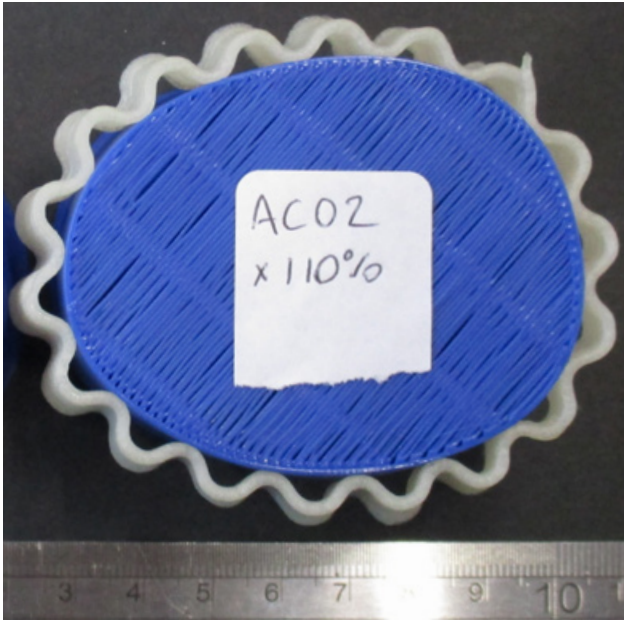
$a' = 6.5 \text{ cm}$, $b' = 5.1 \text{ cm}$, $c' = 6.5 \text{ cm}$, $d' = 5.6 \text{ cm}$

According to the calculation, the average shrinkage along the horizontal directions is 4%.



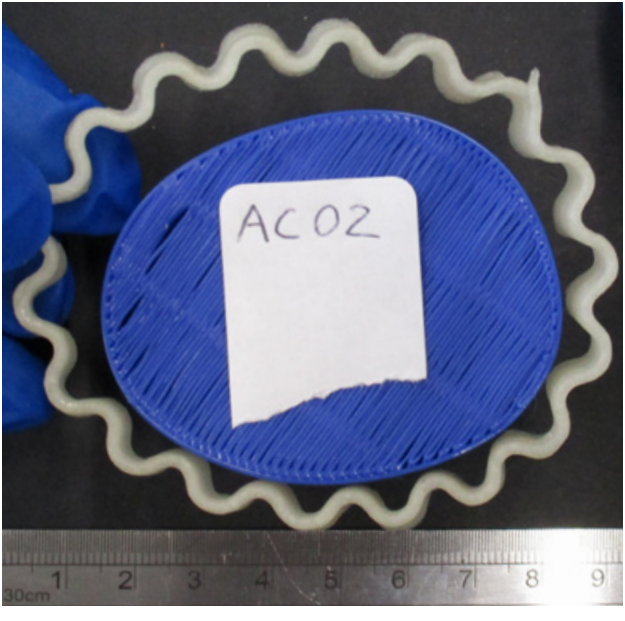
THE PROTOTYPE AT ITS PERMANENT SHAPE

The prototype was cured around the mould for normal-sized wrist



PROGRAMMING

After cured to its permanent shape, the prototype was softened and deformed around a larger mould to gain a temporary shape



TEMPORARY SHAPE (FOR A SWOLLEN WRIST)

Compared with the normal-sized wrist, the inner volume of the temporary shape is larger

Figure 26. Dr John McDonald-Wharry, Programming of the prototype

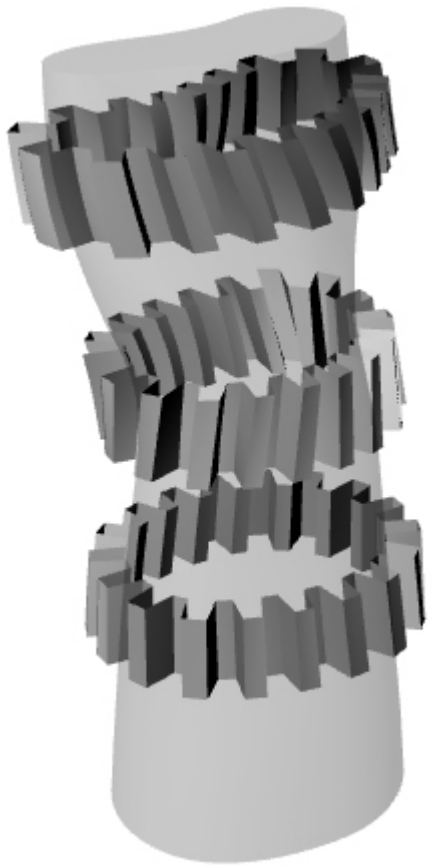


Figure 27. Author, Plan 1.1

After that, according to Dr John McDonald-Wharry's suggestion based on his observation of the prototypes' shape-shifting behaviour, I made the corrugation square to gain more ability of shape-shifting (Figure 27).

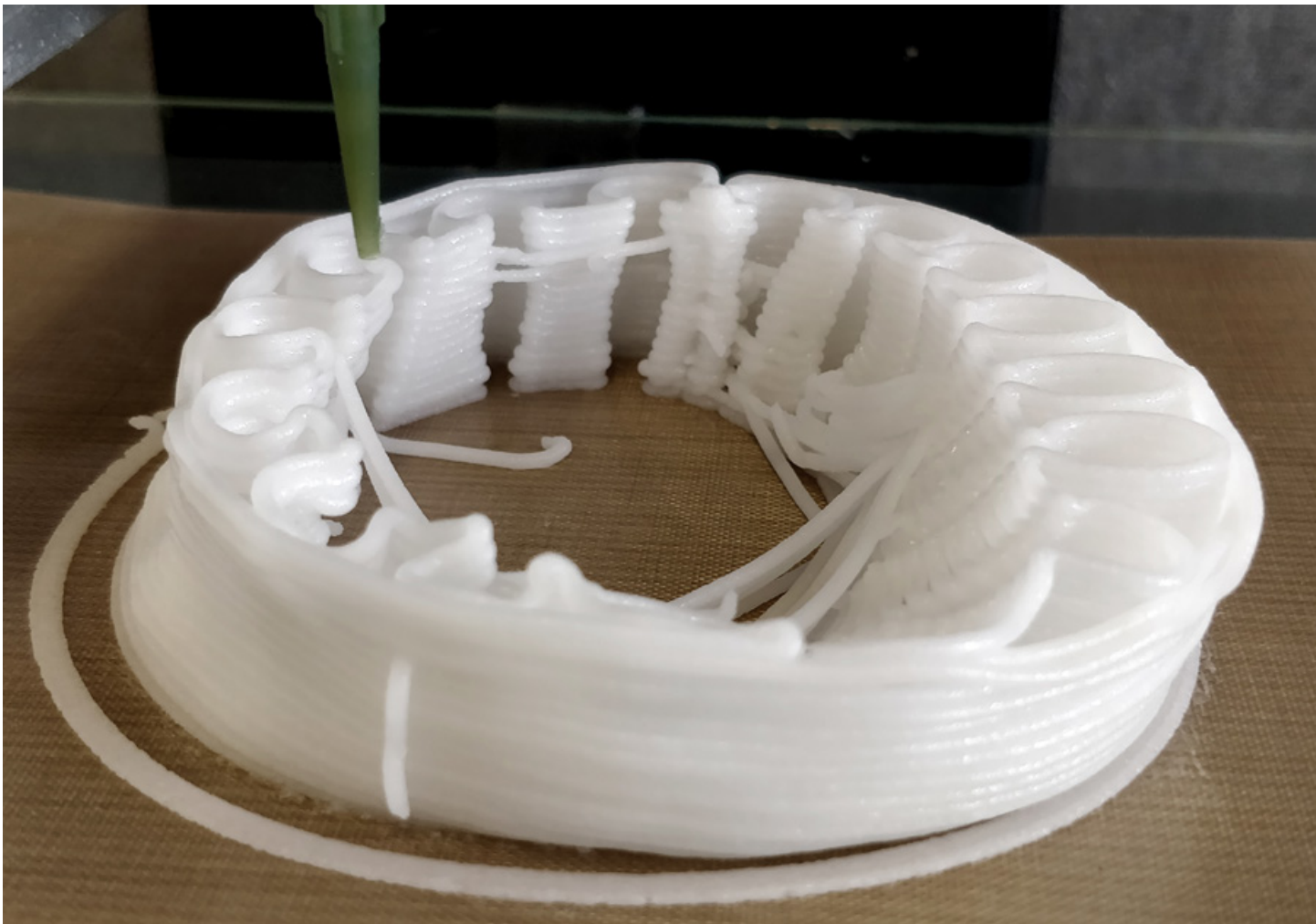


Figure 28. Author, Paste-printing an early design of the splint using the vase mode

4.2.2 Design of the printing paths

The initial models designed for paste-printing are a collection of three-layered walls inspired by a squid’s multi-layered mantle. Anyone of these walls has simple inner and outer layers (which are both continuous lines) and a middle layer with a certain pattern. Compared to the solid inner and outer layers, the middle layer has a loose alignment of material and thus a pattern of voids. As the alignment of muscle fibers in a squid’s mantle can determine the way of its shape-shifting, I expected to compare the walls with different-patterned middle layer to observe different degrees of shape-shifting. So the plan was to start from building linear walls and then adapt them to a circular shape to check the change of the inner volume led by their shape-shifting. The change of inner volume will be a key function of the adaptive splint.

When I started my internship in the UoW, I found that I needed to improve the quality and capability of paste-printing by adjusting the printing paths produced from my design to enable correct printing of relatively complex structures, such as the multi-layered walls mentioned above.

The first problem I tried to tackle was the extra deposit of material. The Hyrel 3D programme of our syringe printer embeds

the functional components of Slic3r to convert stl models to printing paths. Besides printing paths, along which the nozzle of the printer is commanded to extrude material for building the model, there are extra travelling paths for completing the printing process. Extra travelling paths appear when the printer is commanded to print a model including separate parts or a group of G-Codes including separate printing paths. That is to say, the printer is commanded to deposit separate material strands, and consequently the nozzle needs to travel from one deposition area to the next to continue printing. Ideally, the printer can control the instant extrusion of material according to the inputted G-Codes. As long as the G-Codes commands the printer to stop extruding while travelling to the next target deposit position, there will not be any material extruded along the extra travelling paths. But the fluidity of the material we used caused a different result. The inertia of the paste prevented the nozzle from stopping extruding. The leak of the paste between the separate parts of the useful print is difficult to remove after printing because all the extrusions are as vulnerable as piles of whipped cream on a cake. More importantly, the unexpected extrusions are usually woven into the useful parts, which means it is not possible to pick them out even when the prints become solid after curing. The leak of paste largely decreases the quality of prints.

Slic3r provides a spiral vase mode, which automatically attempts to convert the perimeter of a model to a continuous printing path. The vase mode especially benefits the printing of a model in the shape of an open container. Such a model will be easily converted into a continuous spiral printing path, excluding extra travelling paths. In other words, the vase mode can largely improve printing quality, but it typically suits models without infill. Any inner structure will normally be converted to printing paths without avoiding producing extra travelling paths (Figure 28). That is to say, the vase mode can only increase the quality of prints for a narrow range of inputted models, in terms of geometric structure. I decided to look into the potential of using the mode because it provides a great chance to enhance the quality of the prints by omitting the deposit of unexpected material brought about by the leak of paste.

Theoretically, as long as the inner structure of a model could be recognised by Slic3r as a part of the perimeter, the whole model would be printed without an unexpected deposit of material. As is shown in Figure 29, when I cut a tiny gap on a circular perimeter and connected these two ends with the inner structure, I could make the inner structure as an extended part of the original perimeter. Besides, because a material strand had a certain thickness, the gap on the perimeter could be filled in the print as

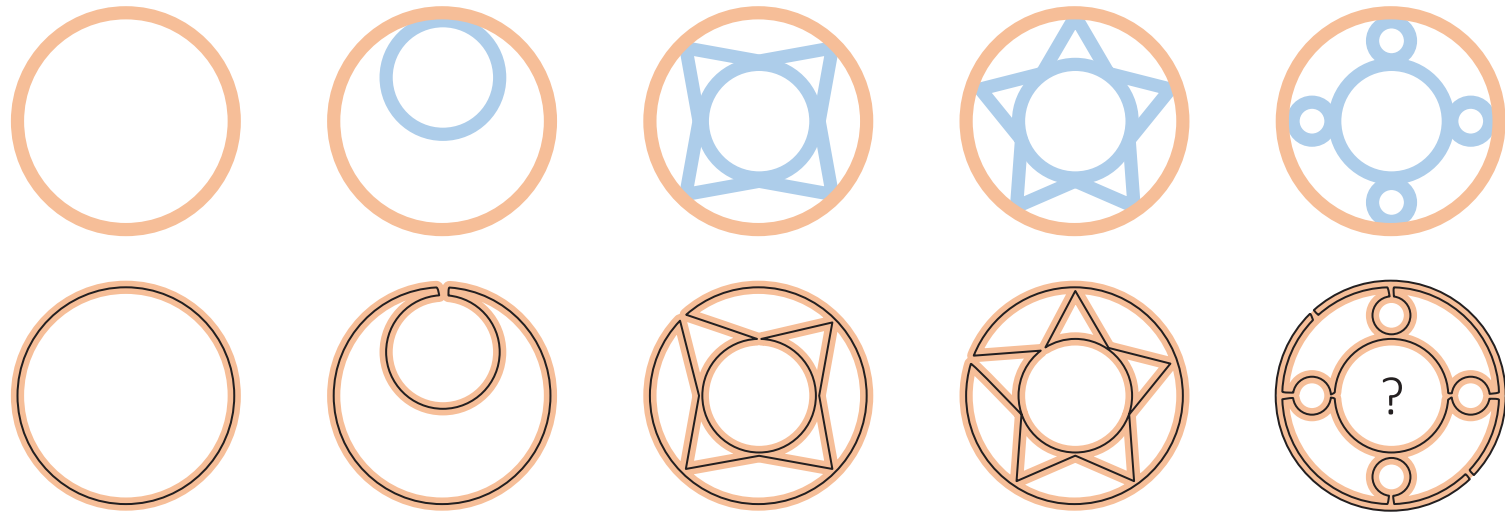


Figure 29. Author, Study on the geometric structures that can be printed without unexpected extrusion by using the vase mode

a real closed perimeter when the material on two sides of the gap was deposited close enough. So I redesigned my multi-layered structures as the 3D models that can be recognised by Slic3r as hollow shapes with irregular perimeters.

After practicing on this strategy, I found it was feasible in realising some designs without any big changes, but some designs could not be realised unless some key features, such as main dimensions and shapes, were changed. Besides, this strategy was not very effective, because I did not have full control of the calculation which the vase mode automatically employed to convert a stl model to printing paths. The stl models were designed based on my understanding of the vase mode and my prediction of the outcome, but the actual outcomes still included some unexpected extrusion when the inputted models were relatively complex, which are shown as red lines in Figure 32.

Therefore I started to consider how to have better control of the printing paths for my designs. The most direct way to fully control printing paths is to control the values of coordinates in G-Codes. These coordinates determine the positions of the points that the printing paths will run through, and the order of these coordinates in G-Codes determines how the printing paths will run through these points. That is to say, printing paths can be produced

without using any CAD programmes. I used Windows Pad as the coding programme to write the codes of a rectangular lattice model (Figure 30). The programme of the Hyrel 3D syringe printer allows editing the generated G-Codes (Figure 32). Theoretically, one could write the values of coordinates to improve printing paths to define the whole form of the printed object, but this would be an inefficient way to produce printing code for any shape with any degree of complexity.

Considering it is not practical to design printing paths for relative complex models, such as curvy multi-layered structures, with only coding

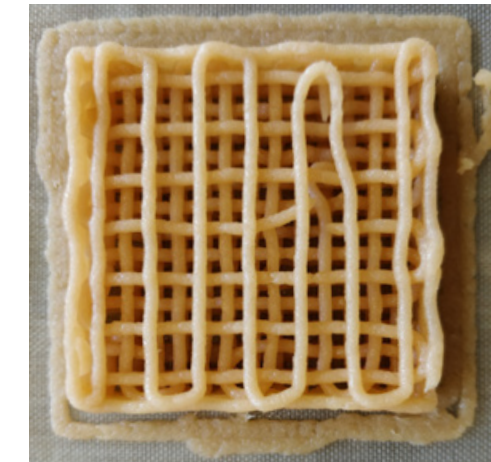


Figure 30. Author, Rectangular lattice model based on G-Codes

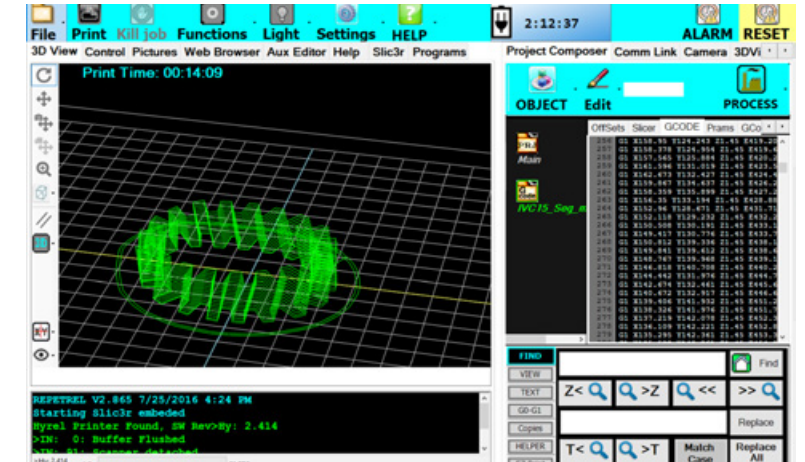


Figure 31. Dr John McDonald-Wharry, Screen shot of interface of Hyrel 3D with the G-Code editing window opened

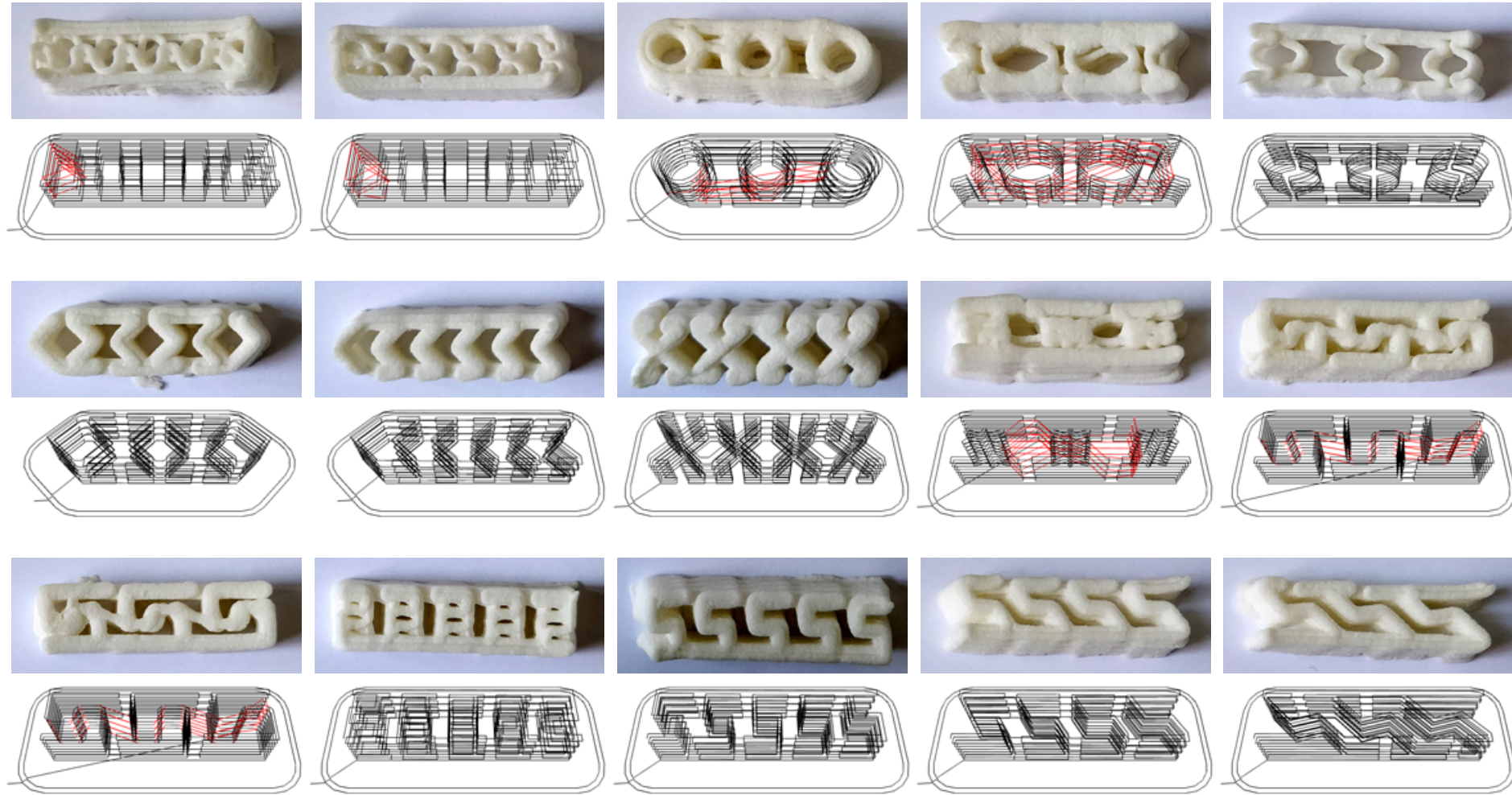


Figure 32. Author, Study on the capability of the vase mode

Selecting the vase mode can automatically convert the perimeter of a model to a continuous printing path, but the automatically calculated outcomes are not good enough for relatively complex structures.

programmes, a better approach needs to be developed. Instead of working on the spatial positions (coordinates) of all points along a printing path, as I coded for the rectangular lattice model, working on the geometric shape of the path is a much more efficient way. So I decided I would still use Rhino to design the geometric structures and use Slic3r to automatically convert them to G-Codes. To improve the way of modifying the printing paths presented by these codes, I looked for a way to view and edit the paths in a CAD programme as usual curves. After research, I found RhinoSlic3r, which enables Rhino to read G-Codes as editable geometric shapes composed of printing paths. This key finding enabled me to develop a new approach to designing printing paths (Figure 33): designing 3D models with Rhino, using Slic3r at the vase mode to automatically convert the models to printing paths (G-Codes) with the least amount of unexpected extrusion, importing the G-Codes with RhinoSlic3r as printing paths to review and optimise the geometric structure of these paths with Rhino before printing. Meanwhile, after several rounds of tests, I obtained the experience in adjusting the parameters of the vase mode to largely avoid extra travelling paths for a specific model. As is mentioned in the previous chapter, Dr John McDonald-Wharry and I conducted tests on the multi-layered structures. We found that the effect of hydro swelling of a single material could be amplified by the multi-layered structure to the necessary extent for the adaptive splint.

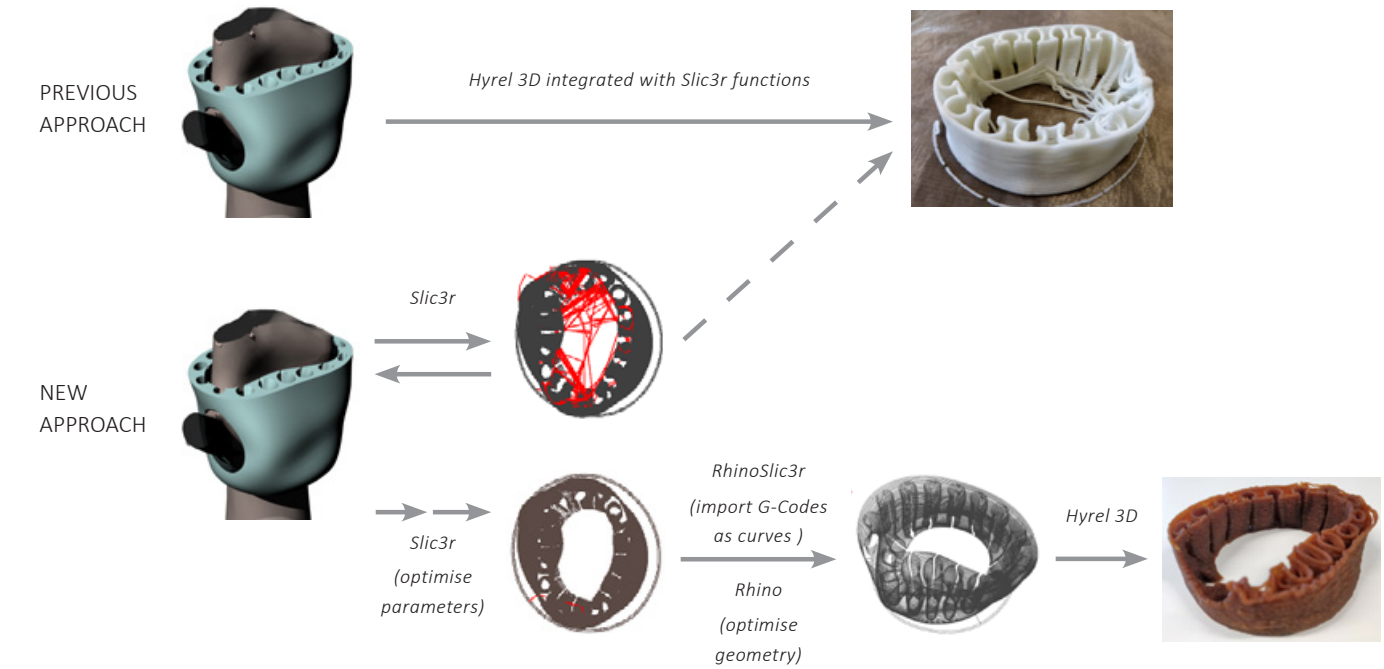


Figure 33. Author, New approach for single-material printing

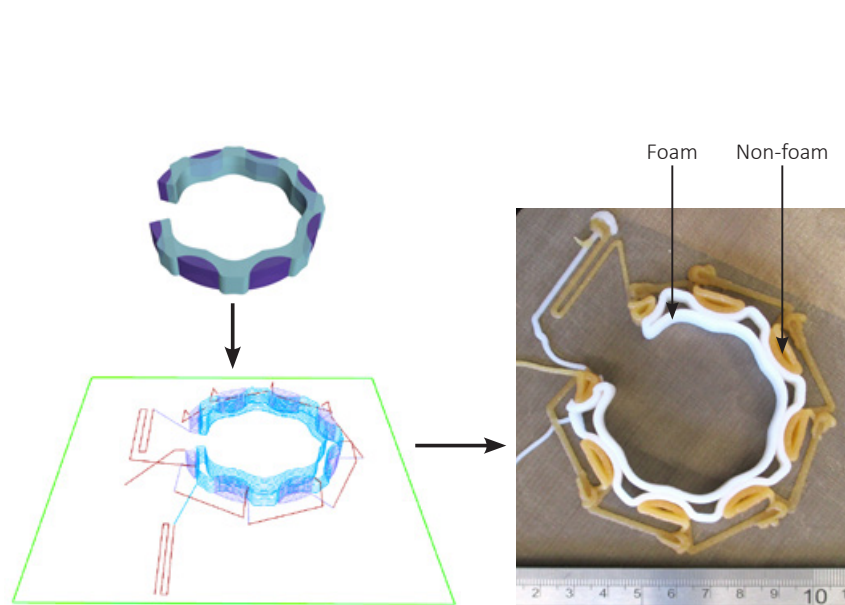


Figure 34. Author, Dual-material printing

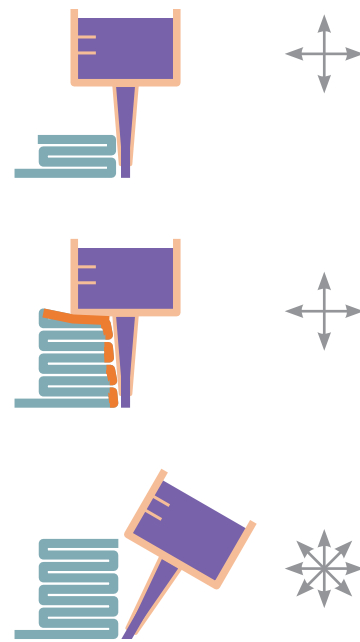


Figure 35. Author, Damage due to the limited printing directions

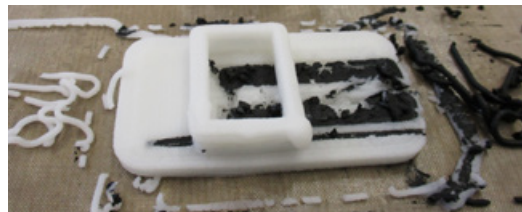


Figure 36. Dr John McDonald-Wharry, A previous dual-material printed model

According to the feedback from Dr John McDonald-Wharry on the feasible properties of the new materials, I decided to use multiple materials for the adaptive splint: the soft material for comfort as the inner layer, the rigid material for shape-shifting and target reinforcement as the outer layers. So I started to design the printing paths for dual-material printing with the new approach I developed previously during designing with single-material printing. The key problem to tackle in dual-material printing was also caused by unexpected extrusion. A typical process of dual-printing includes many times of stopping and restarting extrusion. The two syringes filled with two printing materials. The two nozzles of the syringes travel together. When the required material is extruded on a target position through one nozzle, the other

nozzle stops extruding. As is explained in Chapter 3, we could not achieve an instant stop of extrusion because of the leak of paste. Many times of stopping and restarting extrusion will damage the print, as is shown in Figure 36. In this case, I decided to create a new process for dual-printing. As my internship already ended at this stage, and the only paste-printer appropriate I found for my project was in the UoW, Dr John McDonald-Wharry conducted the following paste-printing for my project.

In the new process, only one syringe will travel on the printing platform at a time. As is shown in Figure 34, I divided the printing paths of two materials into two continuous strands and made the change of materials happen away from the target printing area. When the printing of the first material was completed and the nozzle left the target printing area, the printing process was manually paused to replace the syringe containing the first material with the syringe containing the second material. The second syringe was loaded in the same slot, so when the printing process was continued, the printer started to extrude the second material along the rest part of the printing path. Besides, I designed skirts for each material to stabilise the condition of extrusion before printing the target model.

After several rounds of minor modification on the distance between the two strands based on Dr John McDonald-Wharry's

observation in printing, I achieved a dual-material printed model with relatively good quality. From this round of printing, we can tell that this process benefits the quality of prints, but the problem is that the maximum height of prints was low. Because two materials need to be extruded close to each other to build a solid connection between them, but the physical structure of the printer and the way the nozzle travels prevent the nozzle from getting close to the vulnerable deposited material without damaging the printed work (print head collision) (Figure 35). If a five axis (or more) robotic arm was used to carry the syringe diagonal movement could be achieved, thus making dual-printing a possibility.

Since it is not feasible to print a high model with two materials firmly connected using our current material and printer, a full height dual-material splint cannot be vertically (the length of the splint along Z direction) printed by using this process. For this reason, I decided to consider laying down the splint to find out if the printability could be improved.

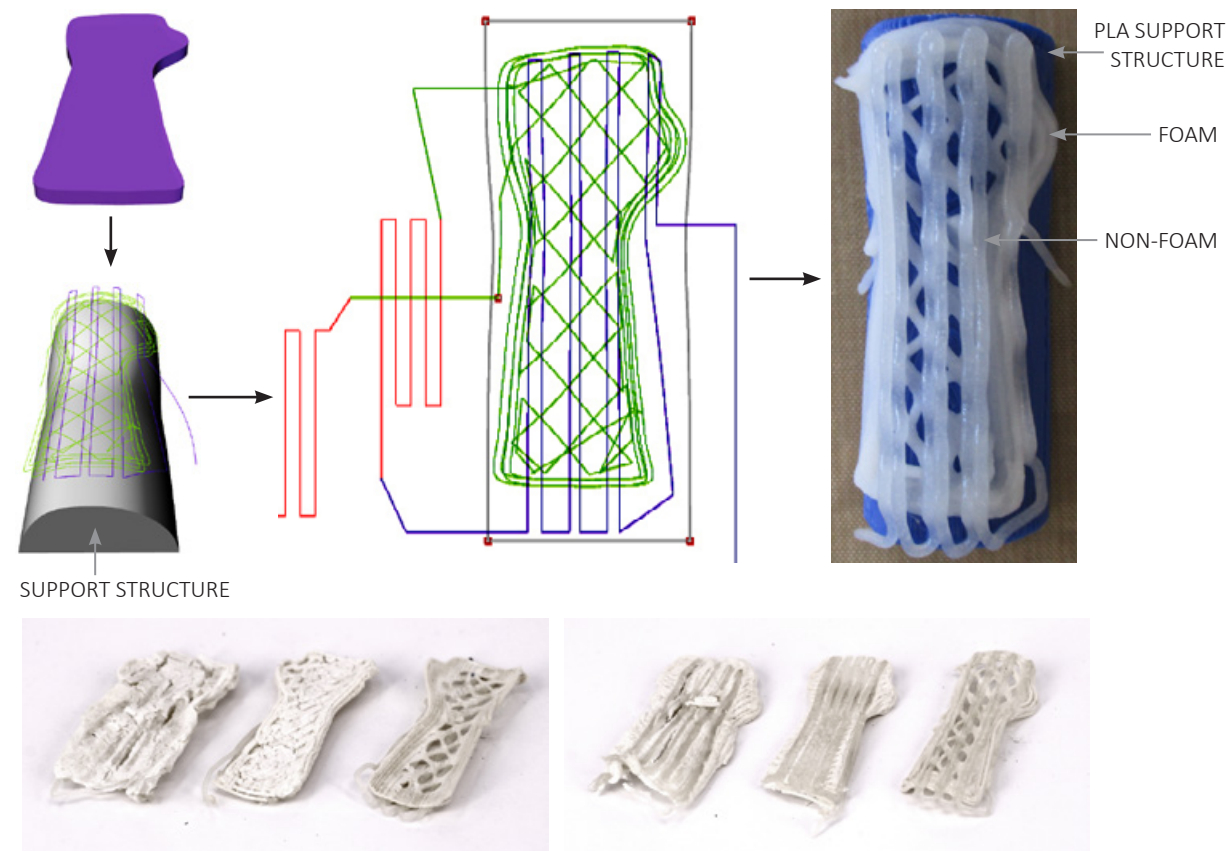


Figure 37. Author, Dual-material printing on a 3D printed curvy mould and the photos of three attempts

To realise this, I developed the G-Codes to paste-print on a 3D printed curvy support structure adapted from the scanned data of my wrist (Figure 37). If this worked, the full splint could be built by combining two multi-layered models. However, I had to make major changes in the main dimensions and main features to enable the printing. As is explained in the previous chapter, firstly, the capability of printing does not support printing a multi-layered model with a relatively complex structure on each layer. Secondly, a large density of voids, in terms of surface area, is necessary to allow the vapourised water to leave the print during curing. It is a critical requirement for avoiding blistering water damaging the models. Considering the relatively low accuracy of the printing, it is not feasible to print a large number of small holes on a surface, leaving the only possibility to realise the large density of voids: designing a relatively small number of large holes on the surface. This requirement seriously limits the design freedom. Thirdly, the shrinkage during curing changes the dimensions of the model, and currently I have only a rough value on the degree of shrinkage based on my measurements. The shrinkage does not only affect the dimensions of a model, but it also weakens the connection between two materials. In conclusion, current paste-printing cannot be used to print the expected multi-layered model.

So for the final prototypes printed with the new material, I designed the corrugated segments, as is mentioned in the previous section. I then converted the segments to single-material printing paths (Figure 38).

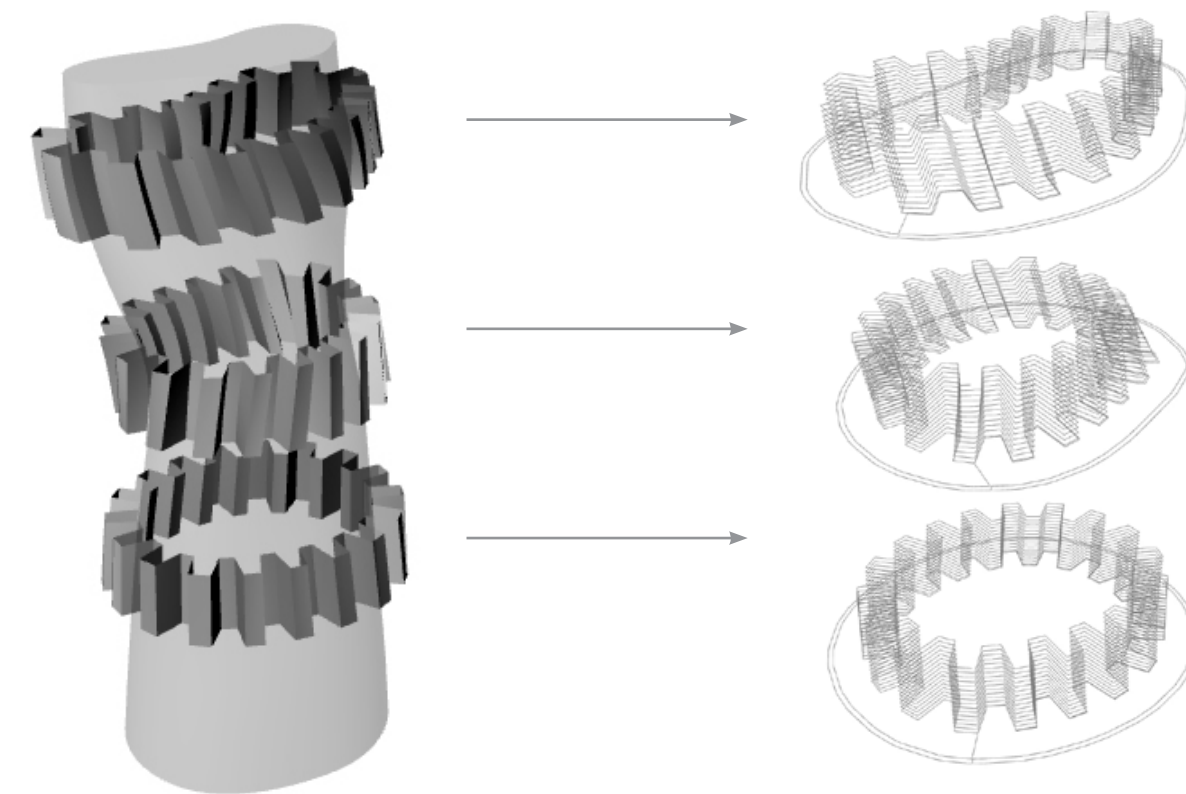


Figure 38. Author, Geometric structures to printing paths

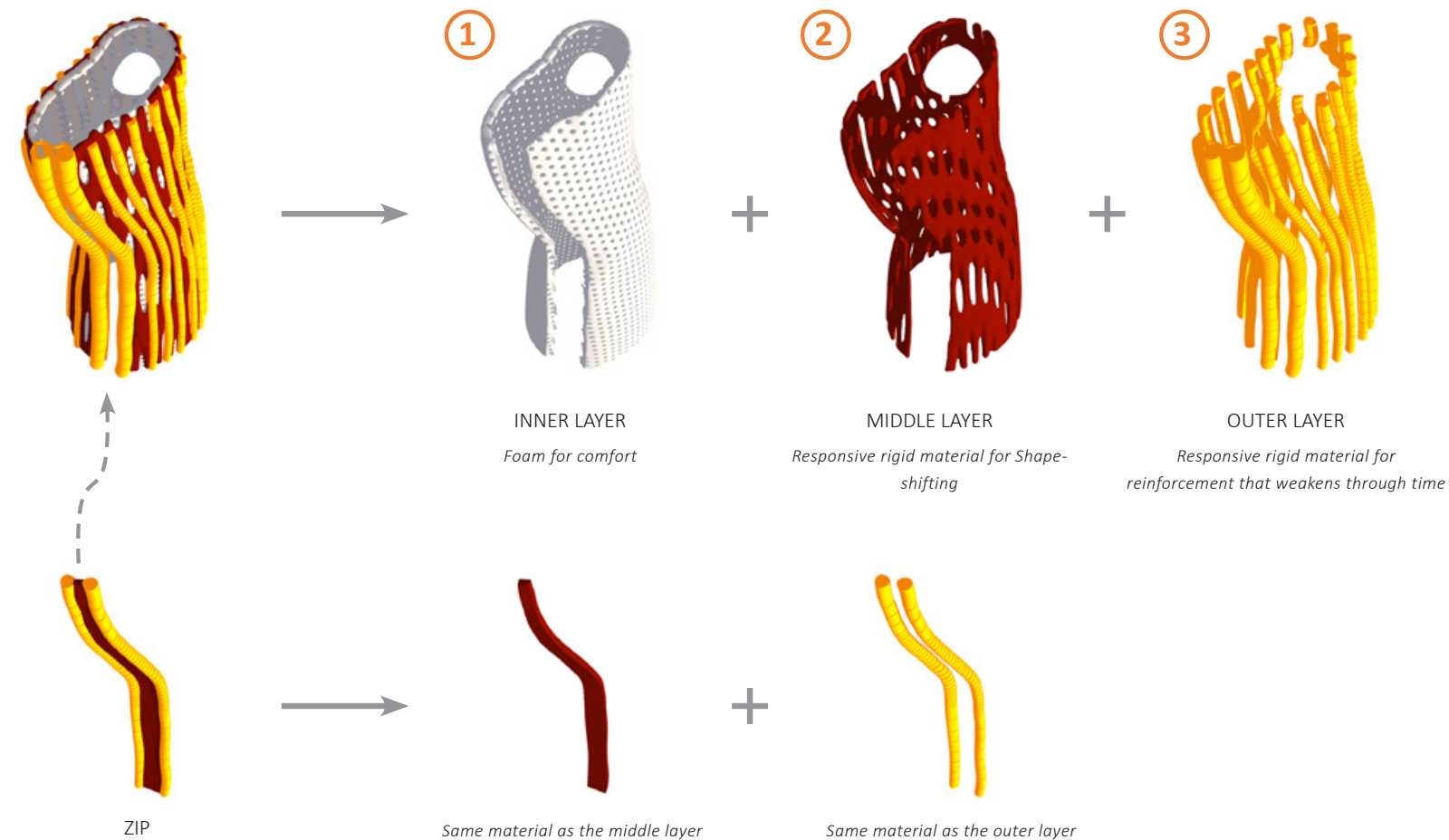


Figure 39. Author, Multi-layered structure made with different materials

4.3 Design development for full functions based on the scenario

As is mentioned earlier in this chapter, I designed the multi-layered structure to incorporate the materials with different properties to fulfil the changing requirements of a wrist's rehabilitation (Figure 39).

I developed the design for full functions based on my scenario. Foam is used to build the inner layer as a comfort pad. The rigid material with SME is used to build the middle layer to provide changeable inner volume for the splint to adapt to the healing wrist when swelling decreases. Meanwhile, the material also has a water plasticisation effect, which enables the immobilisation provided by the middle layer to decrease when the wrist is healed enough to do exercises. The water plasticisation effect is also used on the outer layer to provide the reinforcement that is weakened over time. A zip was designed to close the splint after put it on a wrist.

Based on the application of the materials, I developed geometric structures to ensure their performances. I decided that the voids

in the foam layer should provide good ventilation, but large voids should be avoided to prevent bumpy surface. The middle layer could have larger voids as long as it is strong enough to immobilise the healing wrist when the material is not stimulated.

On the outer layer, the decrease of stiffness provided by the material is not enough to support prescribed exercises. The stiffness should not only weaken over time, but it is also expected to vary in different areas on the splint at one time (Figure 40). In the areas where the splint should be the most flexible to allow movements, the outer layer should provide the least reinforcement. The requirement of multi-flexibility soon reminded me of the function realised by the CVs on a locust wing. According to my research, the diverse diameters of the CVs (Figure 6, p. 24) enable them to reinforce the wing with various levels of stiffness in different areas.

Therefore, I studied the possible ways to define flexibility by controlling geometry (Figure 41). The degree of bendability in a small area can be determined by controlling the spacing between the units or the size of the units within this area. For my project, I employed various-sized units to achieve multiple-flexibility in different areas for target movements. Combining the geometric design with the water plasticisation effect of the material, the splint will be more and more flexible in all areas over time to allow heavier exercises.

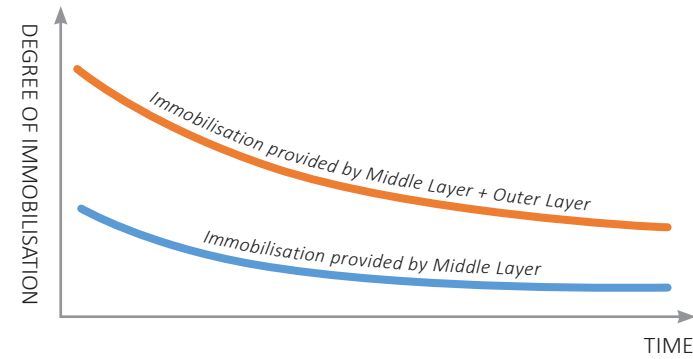


Figure 40. Author, Degree of immobilisation provided by the splint over time

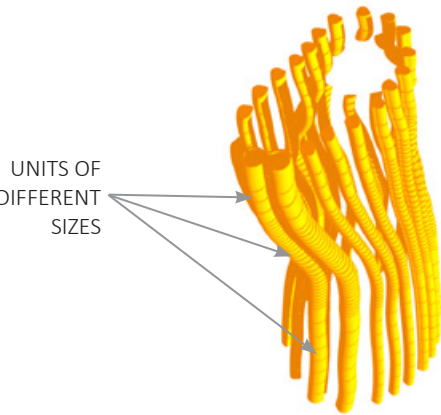
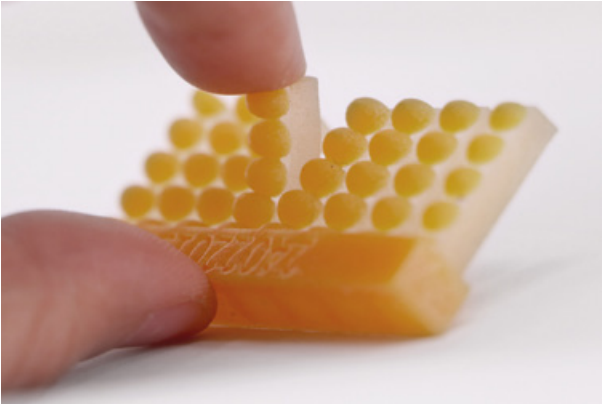
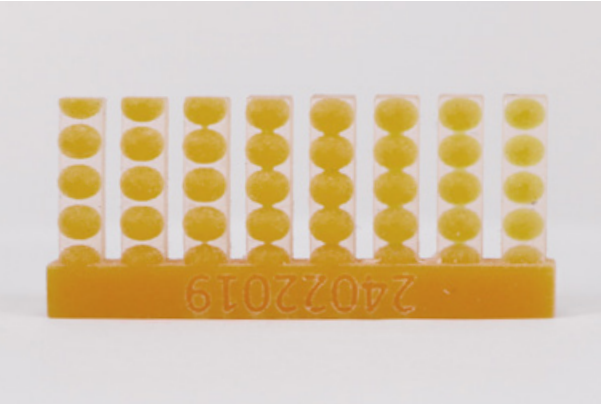
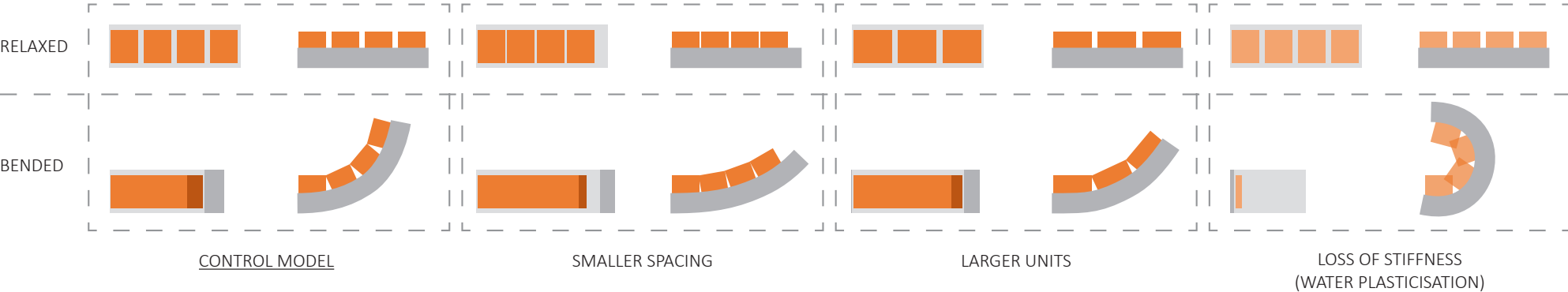


Figure 41. Author, Geometry studies and the design application on the outer layer of the splint

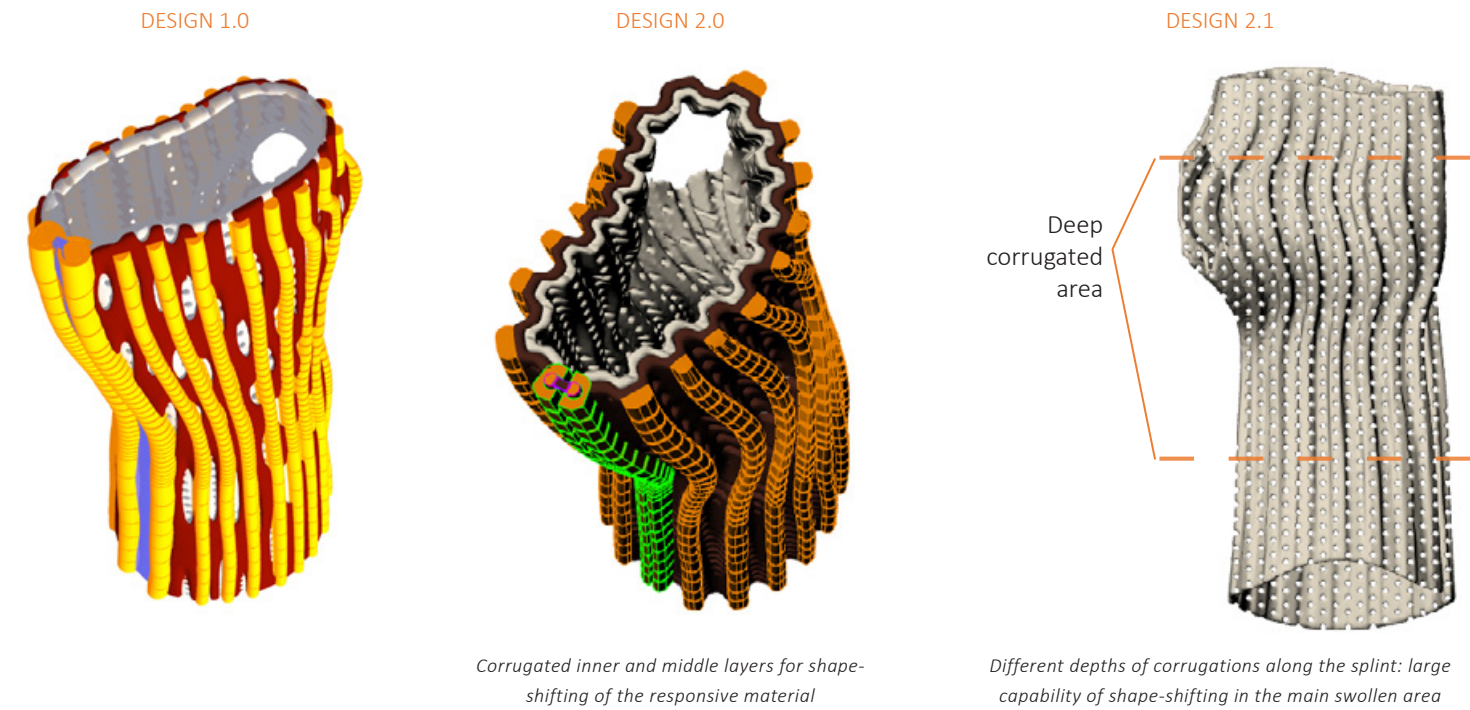


Figure 42. Author, Design development

As is shown in Figure 42, I developed my design by embedding the corrugated structure, which is developed for the new material to effectively deliver shape-shifting. The inner lay inherits the corrugated structure for the capability of following the middle layer's change of shape. After that, I explored the way to control the design more precisely by differentiating the degree of corrugation for different areas. Deepest corrugation is used to acquire the largest shape-shifting in the main swollen area.



Figure 43. Author, Further design development

I then explored the relationship between the directions of cuts on the outer layer, which determines the direction of spacing between the reinforcing units, and the movements the splint supports.



Figure 44. Author, Prototypes printed on a J750 printer

In order to make the outer layer more effectively block the unexpected movements, I redesigned the shape of the reinforcing units (Figure 45). A gap between two units allow movements until these two units touch and block further movements. The wider a gap is, the more freedom of movements is allowed.

By applying different colours on the middle layer and the outer layer, I expect the splint to provide visual signification for the user to see the target extent of a move which is recommended by the therapist. For example, at an early stage, the therapist might prescribe the patient to do light bends until the colour of the middle layer is half concealed. Then when the wrist is healed enough for advanced exercises, the therapist might ask the patient to do bends until the colour of the middle layer is completely concealed.

To build the multi-layered structure with relatively high accuracy and full colour to check my design, I used J750 printer to make several rounds of the prototypes for further optimisation of design (Figure 44).

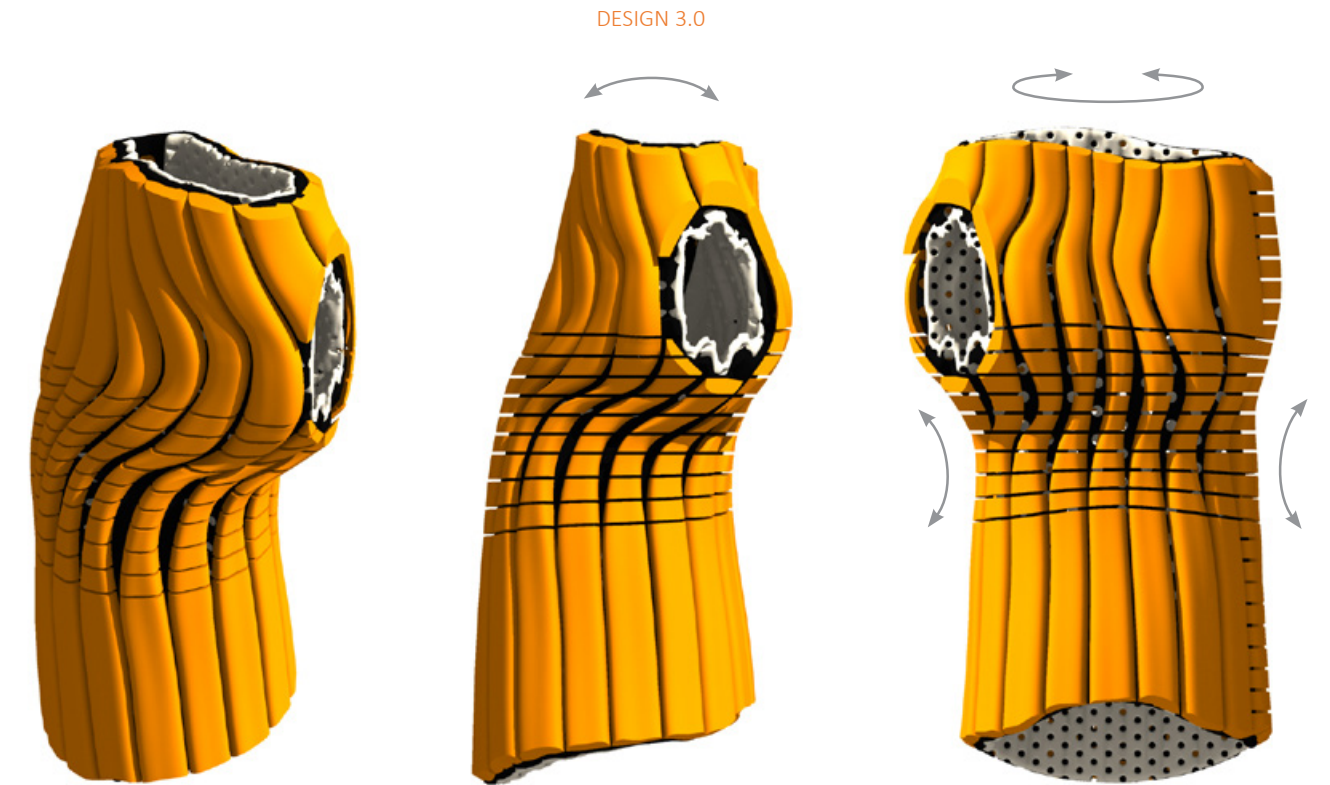


Figure 45. Author, Development of the outer layer to precisely allow certain movements

5 Results and Reflection



Figure 46. Author, Final prototypes printed with the new materials programmed on the two moulds

5.1 Final prototypes printed with the new materials for responsive performance

Due to the limitations of current experimental materials and the associated printing technology, SME behaviour example segments were printed (Figure 46). The prototypes were printed with Formulation QX3. I selected three typical positions along the wrist and build a segment around the wrist at each position to firstly represent the morphology of the splint at those positions and secondly, but more importantly, to demonstrate the splint’s capability of shape-shifting at those positions to fulfil the requirements of a rehabilitation process at an early stage.

I improved the 3D CAD models of the segments based on the previous rounds of prototypes, considering the printability of the material and the degree of shrinkage during curing. The height of the segments was increased by 19% according to the previous calculation to offset the shrinkage in the vertical direction, but the horizontal shrinkage was kept. Based on the observation of the tolerance of the prints compared to the digital models, Dr John

McDonald-Wharry suggested that we make use of the natural shrinkage in the horizontal direction to tightly fit the segments onto the normal-sized mould. I then converted the models to G-Codes and optimised the G-Codes using the new approach I developed for single-material printing. Dr John McDonald-Wharry printed the G-Codes and cured the prototypes at the UoW.

An improvement in the printing process was that the models were printed onto the PTFE-coated fibreglass sheets covered by thin PE sheets instead of being printed directly onto the PTFE-coated fibreglass sheets. According to Dr John McDonald-Wharry’s tests, the PE sheets can effectively reduce the uneven shrinkage along the vertical direction.

Two identical sets of prototypes were fit onto two different moulds: one set onto the normal-sized wrist mould (according to the scan of my wrist), and the second set onto the swollen wrist mould (the surface of which was offset by 2.7mm based on the normal-sized wrist, and consequently the area of its cross-sections was increased by 20% on average). Both of the moulds were printed with high-temperature PLA provided by MADE to resist the deformation caused by heat.

The first set of segments were a little small to be adapted onto the

normal-sized mould. Therefore I heated them in an oven at 100 degrees centigrade for several minutes to soften them slightly, and then they easily fit onto the normal-sized mould.

The second set of segments were heated in the oven at 100 degrees centigrade for 20 minutes to achieve thorough heating for the material to be flexible enough to adapt onto the second mould. By stretching the heated segments over the swollen wrist mould, I deformed the segments for them to achieve a larger inner volume. The segments were kept at the deformed status for about five minutes to let the material thoroughly cool down, so the shape was locked as the temporary shape. This is the programming process. During the programming process, I observed that the segments had a strong tendency to return to their cured shape when they were at a high temperature. This tendency decreased when the temperature of the segments decreased.



Figure 47. Author, SME stimulated by heat

5.2 Experiments for responsive performance on the final prototypes printed with the new materials

The identical sets of the segments on the two different moulds demonstrate the programmability of the new material. I then heated the programmed segments, which were at their temporary shapes, to stimulate their shape-shifting (Figure 47). The responsive performance is based on the SME of the material. When I heated the segments with a hair dryer, the segments returned to the permanent shapes that they had been cured into at the UoW.

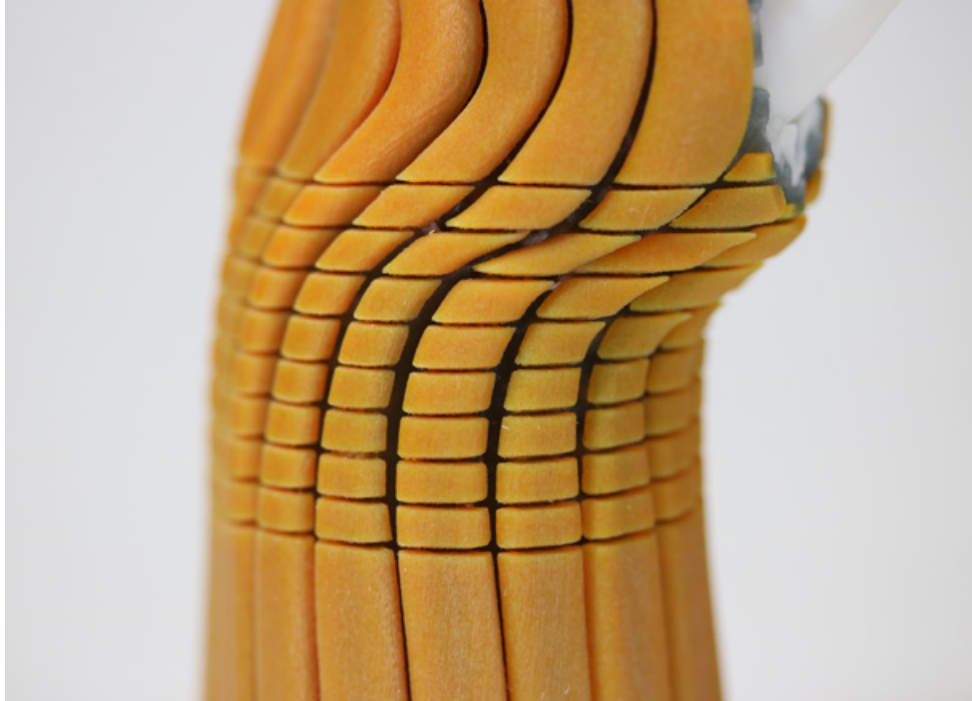


Figure 48. Author, 1:2 Scaled prototype

5.3 Final prototypes for the functions determined by geometric structures incorporating the multi-flexibility of the materials

The final prototypes (Figure 48) were built to display the functions of the adaptive splint that can be realised by combining the multi-layered structures with the materials at different levels of stiffness. The prototypes were made to show the performances of the splint at the consolidation stage of a rehabilitation process.

The two prototypes both have a soft inner layer that mimics a foam pad for comfort and a collection of rigid reinforcing units on the outer layer. The difference between the two prototypes is that the middle layers have different levels of stiffness because they are expected to demonstrate two different states of the splint. The first prototype has a relatively flexible middle layer, which mimics the state of the splint when it allows exercises. More specifically, the flexible middle layer mimics a middle layer made of the responsive material when the material is stimulated (heated or partially water plasticised) to allow prescribed movements. The

second prototype has a rigid middle layer, which mimics the state of the splint when it does not allow exercises. In other words, the rigid middle layer mimics that same middle layer of the first prototype when the responsive material is not stimulated.

In addition to multi-flexibility in the two prototypes, multiple colours were used to build the three-layered structure. The different colours of the middle layer and the outer layer enable the splint to provide a visual sign for the user to see the target extent of a movement which is recommended by the therapist.

Furthermore, to display how the splint supports the target movements and blocks the unexpected movements, a model was made based on the scan data to mimic a bendable wrist inside the splint.

A few colour and pattern combinations are shown by the renders in Figure 49.



Figure 49. Author, Renders showing other possible colour and pattern combinations

5.4 Reflection

Upon examining the outcomes of the project, I have found several problems that need to be tackled before the splint can be applied for practical use.

Firstly, the dry working temperature for the shape-shifting of the current experimental responsive material is likely too high to be safe for human skin. Therefore, new materials are under development. The target working temperature is below 45 degrees centigrade, which is stated by the New Zealand Building Codes as the maximum water temperature at hand-basins, baths and showers in places such as childcare centres, schools and old people's homes (Econation, n.d.).

Secondly, the stiffness of the material affects the strength of the zip structure. In the final prototypes, the zip structure (Figure 50) was not included. This is because according to previous rounds of prototypes, the zip area became the weakest area during dynamic movements and broke quickly. This largely shortened the duration of the splint (Figure 51). This split in the zip area could be caused by the insufficient thickness of the material, especially in the small

scale prototype, and it could also be caused by the low strength of the material. More research needs to be done to refine the structure and the target level of stiffness for the zip components. Another structure to close the splint is to use clips along the edge (Figure 52).

Thirdly, the corrugated structure of the foam layer might affect the comfort of wearing the splint. Though the foam pad is soft, the corrugation has reduced the contact area and made the support from the splint onto the wrist distributed less evenly.



Figure 51. Author, Split of the zip in a previous 1:3.3 scaled prototype

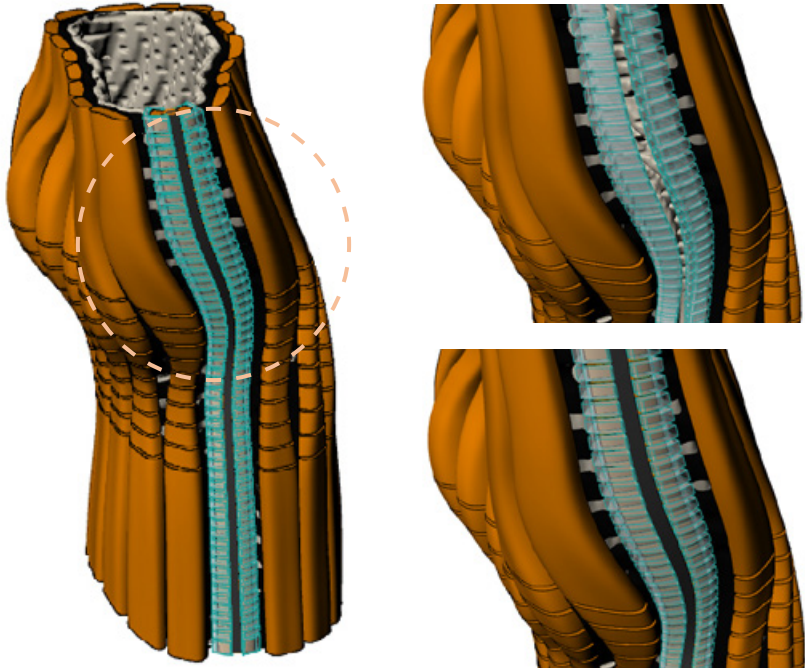


Figure 50. Author, Zip

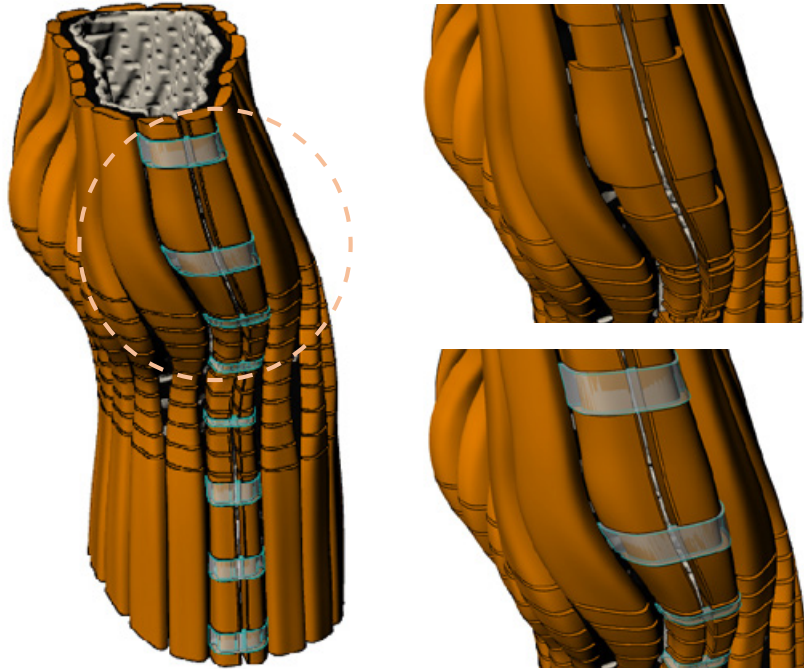


Figure 52. Author, Clips

6 Discussion

My project was done to explore the design opportunities of 4D printing with bio-based polymers for manufacturing adaptive wearable devices. I set two aims to guide my research process. Aim 1 is to explore literature and precedents for a 3D printed self-actuating wearable device, exemplified by a wrist splint. To fulfil this aim, I applied RFD by doing literature review and studying relevant precedents on 4D printing, the rehabilitation process of an injury and biomimicry theory. I also looked into relevant biological structures as the inspiration of geometric design. Aim 2 is to design and build an adaptive splint, and discuss the potential capability of 4D printing in building a wearable device. To fulfil this aim, I explored the properties of the new materials and developed an adaptive splint based on the potential responsive performances (the decrease of stiffness over time triggered by water and the SME triggered by heat) in combination with the requirements of rehabilitation.

Tibbits, McKnelly, Olguin, Dikovsky, and Hirsch's (2014) metaphor of current printing technology as "a Materials Science chamber" best describes the opportunity and challenge I have encountered in this project.

On the one hand, the responsive property and the biocompatibility of the new materials offer me the opportunity to embed

revolutionary new functions into 3D printed structures. Previous precedents in 4D printing combining with responsive bio-based materials are mostly used to build medical products such as implants. By developing the adaptive splint for progressive rehabilitation, my project has shown that with the new materials and 4D printing technology, we can incorporate multiple layers of responsive materials with different geometric structures to build a wearable device which fulfils diverse requirements of a human body at different stages. In addition to wearable devices for rehabilitation and healthcare, the design concept can also be used to design high performance sports guards.

On the other hand, the ongoing development of the new materials has barriers to overcome before the materials can be applied to build a structure for practical use. The first barrier to overcome is to increase the printability of the new materials to a satisfactory level. I have developed new techniques and approaches to improve the quality of paste-printing. The new techniques and approaches broaden the range of structures that can be built by using the vase mode and consequently realising continuous paste-printing with the minimum leak of material. The new techniques and approaches also allow paste-printing with multiple syringes of (different) materials without damaging the models.

However currently, the printability of the new materials is still lower than commercial printing materials. I believe the two most effective ways are: to solidify a strand of material quickly after it is deposited on the target position (Figure 52), or to deposit a support material as the basis for the fluid paste to be printed on (Figure 53). The method of solidifying material depends on the property of the material. For example, for UV curable materials, UV can be applied to realise cross-linking between the ingredients and thus solidify the material (Ligon, Liska, Stampfl, Gurr, & Mülhaupt, 2017). However, the formulations will need re-engineering to be compatible with UV curing, and the printer equipped with UV lamps will likely require extra safety features to be installed. Another group in our material development team has already developed a tool to solidify extrusion during printing. It is possible that this tool can be adapted to solidify our materials during printing. Besides, our material development team has started to develop the support material that can be separated from the model after curing.

The second barrier to overcome is to decrease the trigger temperature of the responsive materials to a safe level for human skin. The ideal temperature might be in a narrow target range from 40 to 45 degrees centigrade, which is below the maximum safe water temperature from taps for children and old people

according to the New Zealand Building Codes. According to the information provided by Dr John McDonald-Wharry, the small gap between the target temperature and the room temperature (around 23 degrees centigrade) can cause the material to shape-shift at room temperature if the material takes up too much water in humid weather. More research needs to be done to realise the safe working temperature and control humidity sensitivity.

Last but not least, when I tried to respond to the opportunity and challenge of the project, I maintained a collaborative relationship with the material scientists, especially Dr John McDonald-Wharry, throughout my research. During the process, I learned how to cooperate with professionals in other fields. Firstly, direct communication using words in combination with images can largely avoid misunderstanding and thus increase the efficiency of discussion. In this project, Dr John McDonald-Wharry and I mainly used email to communicate, and I found that different perspectives (of a scientist and a designer) of viewing one subject could sometimes lead to very different opinions on, for example, the hierarchy of problems to be solved and the way to solve problems. For this reason, though aiming at the same target, different starting points could lead to misunderstanding without clear communication and thus ineffective cooperation. In this case, it is very important that one does not take one's own idea

for granted, but to clearly explain it, for example by stating the premiss behind the idea and the expectation to realise with the idea. Besides, images are very helpful in communicating one's idea on the subjects of shapes, forms and 3D positions. Secondly, keeping an open mind is important for the practitioners in a project to mutually benefit the project. For example, Dr John McDonald-Wharry's observation and understanding of the new materials enabled him to provide me useful advice on improving the design of the printing paths, which helped me to increase the quality of the prints in a short time. I provided Dr John McDonald-Wharry with ideas on increasing the printability of the new materials based on my knowledge on the design and coding programmes, which improved the printing techniques and process associated with the new materials for further research. The project shows how the collaborative relationship between a material scientist and an industrial designer could benefit the development of a designed product.

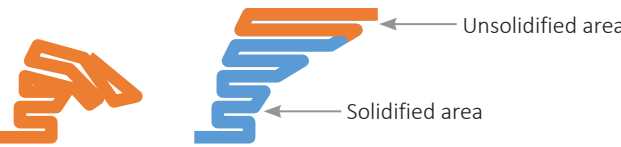


Figure 53. Author, Solidify the extrusion during printing to increase the printability



Figure 54. Author, Use support material to increase the printability

7 Conclusion

This project was initiated by the development of bio-based and bio-derived materials which have provided a means of initiating change and transforming 3D printing to 4D printing. By designing the customised adaptive splint for progressive rehabilitation, I explored the possibility of engaging 4D printing in building a wearable device.

The design process of this project differentiated itself from my previous projects by involving the accessibility to the new materials and also a large amount of background research on various fields such as 4D printing, therapy and biomimicry. These enabled my design to be inspired by not only the biological structures perpetuated through the long-term evolution but also the most advanced technology to respond to the unfulfilled human needs in real life.

The design of the adaptive splint challenges the properties of the new materials and the associated printing processes. More research and development need to be done to improve printability and control responsive performance before the materials can be used to build products for practical use. Besides, more clinical knowledge and experience need to be taken into consideration. Collaboration with a therapist will be essential to specifically refine the functions of the project before it can be applied in real life.

However, the project has shown the possibility of incorporating multiple layers of responsive materials and different geometries to build a wearable device which fulfils diverse human requirements at different stages.

List of Figures

Figure 1. Author. (2019). Research process

Figure 2. Author. (2019). Functions and goals of devices for various phases of the wound-healing process

Figure 3. Author. (2019). Biomimicry approaches applied in the precedents according to Zari’s way of division

Figure 4. Author. (2019). Typical skeleton-muscle structures of animals and the mechanics behind movements

Figure 5. Author. (2019). Comparison between the new experimental materials and some typical natural materials

Figure 6. Author. (2019). Two types of vein forms on a locust wing

Figure 7. Author. (2019). Exploration of new experimental materials

Figure 8. Author. (2019). Study on the printability of the new materials

Figure 9. Author. (2019). Shape-shifting

Figure 10. Author. (2019). Decrease of stiffness

Figure 11. Author. (2019). First round of research on hydro swelling

Figure 12. Author. (2019). Second round of research on hydro swelling

Figure 13. Author. (2019). Shrinkage, collapse, blistering caused by water and cracks

Figure 14. Author. (2019). Summary of design possibilities based on one material and request on the specifications of the material

Figure 15. Author. (2019). Summary of design possibilities based on dual material and request on the specifications of the materials

Figure 16. Author. (2019). Determined responsive performances of the new materials potentially available for the project and the specific application in the structure

Figure 17. Author. (2019). Scenario

Figure 18. Author. (2019). Customised manufacture procedure

Figure 19. Author. (2019). Design inspired by the skeleton-muscle structure of a squid

Figure 20. Author. (2019). Flat models based on the cross-section of the splint

Figure 21. Author. (2019). Abstract models and photos of test printing

Figure 22. Author. (2019). Shape-shifting created by using the expansion or swelling of material

Figure 23. Author. (2019). Plan 1.0

Figure 24. Author. (2019). Shrinkage in the vertical direction

Figure 25. Author. (2019). Shrinkage in the horizontal direction

Figure 26. McDonald-Wharry, J. (2019). Programming of the prototype

Figure 27. Author. (2019). Plan 1.1

Figure 28. Author. (2019). Paste-printing an early design of the splint using the vase mode

Figure 29. Author. (2019). Study on the geometric structures that can be printed without unexpected extrusion by using the vase mode

Figure 30. Author. (2019). Rectangular lattice model based on G-Codes

Figure 31. McDonald-Wharry, J. (2019). Screen shot of interface of Hyrel 3D with the G-Code editing window opened

Figure 32. Author. (2019). Study on the capability of the vase mode

Figure 33. Author. (2019). New approach for single-material printing

Figure 34. Author. (2019). Dual-material printing

Figure 35. Author. (2019). Damage due to the limited printing directions

Figure 36. McDonald-Wharry, J. (2018). A previous dual-material printed model

Figure 37. Author. (2019). Dual-material printing on a 3D printed curvy mould and the photos of three attempts

Figure 38. Author. (2019). Geometric structures to printing paths

Figure 39. Author. (2019). Multi-layered structure made with different materials

Figure 40. Author. (2019). Degree of immobilisation provided by the splint over time

Figure 41. Author. (2019). Geometry studies and the design application on the outer layer of the splint

Figure 42. Author. (2019). Design development

Figure 43. Author. (2019). Further design development

Figure 44. Author. (2019). Prototypes printed on a J750 printer

Figure 45. Author. (2019). Development of the outer layer to precisely allow certain movements

Figure 46. Author. (2019). Final prototypes printed with the new materials programmed on the two moulds

Figure 47. Author. (2019). SME stimulated by heat

Figure 48. Author. (2019). 1:2 Scale pending images of full size (1:1) prints

Figure 49. Author. (2019). Renders showing other possible colour and pattern combinations

Figure 50. Author. (2019). Zip

Figure 51. Author. (2019). Split of the zip in a previous 1:3.3 scaled prototype

Figure 52. Author. (2019). Clips

Figure 53. Author. (2019). Solidify the extrusion during printing to increase the printability

Figure 54. Author. (2019). Use support material to increase the printability

References

Benyus, J. M. (1997). *Biomimicry: Innovation inspired by nature / Janine M. Benyus*. (1st ed..). New York: Morrow.

Cyr, L. M., & Ross, R. G. (1998). How controlled stress affects healing tissues. *Journal of Hand Therapy*, 11(2), 125–130. [https://doi.org/10.1016/S0894-1130\(98\)80009-4](https://doi.org/10.1016/S0894-1130(98)80009-4)

Ding, Z., Yuan, C., Peng, X., Wang, T., Qi, H. J., & Dunn, M. L. (2017). Direct 4D printing via active composite materials. *Science Advances*, 3(4), e1602890 (1–6). <https://doi.org/10.1126/sciadv.1602890>

Dirks, J.-H., & Taylor, D. (2012). Veins Improve Fracture Toughness of Insect Wings. *PLoS One; San Francisco*, 7(8). <http://dx.doi.org/10.1371/journal.pone.0043411>

Econation. (n.d.). Hot water cylinder temperature. Retrieved from <https://econation.co.nz/hot-water-temperature/>

Frankel, L., & Racine, M. (n.d.). *The Complex Field of Research: For Design, through Design, and about Design*. 12.

Hanington, B., & Martin, B. (2012). *Universal Methods of Design: 100 Ways to Research Complex Problems, Develop Innovative Ideas, and Design Effective Solutions*. Retrieved from <http://ebookcentral.proquest.com/lib/vuw/detail.action?docID=3399583>

Hendrikson, W. J., Rouwkema, J., Clementi, F., van Blitterswijk, C. A., Farè, S., & Moroni, L. (2017). Towards 4D printed scaffolds for tissue engineering: Exploiting 3D shape memory polymers to deliver time-controlled stimulus on cultured cells. *Biofabrication*, 9(3), 031001. <https://doi.org/10.1088/1758-5090/aa8114>

Kennedy, E. B. (2017). Biomimicry: Design by Analogy to Biology. *Research-Technology Management*, 60(6), 51–56. <https://doi.org/10.1080/08956308.2017.1373052>

Kellert, S. (2011).Dimensions, Elements, and Attributes of Biophilic Design. In Kellert, S. Heerwagen, J., & Mador, M. (Ed.). *Biophilic Design*. John Wiley & Sons Inc.

Kellert, S. & Heerwagen, J. (2011).Preface. In Kellert, S. Heerwagen, J., & Mador, M. (Ed.). *Biophilic Design*. John Wiley & Sons Inc.

Kier, W. M. (2012). The diversity of hydrostatic skeletons. *Journal of Experimental Biology*, 215(8), 1247–1257. <https://doi.org/10.1242/jeb.056549>

Kokkinis, D., Schaffner, M., & Studart, A. R. (2015). Multimaterial magnetically assisted 3D printing of composite materials. *Nature Communications*, 6(1). <https://doi.org/10.1038/ncomms9643>

Kuksenok, O., & Balazs, A. C. (2015). Stimuli-responsive behavior of composites integrating thermo-responsive gels with photo-responsive fibers. *Materials Horizons*, 3(1), 53–62. <https://doi.org/10.1039/C5MH00212E>

Lewis, J. A., Smay, J. E., Stuecker, J., & Cesarano, J. (2006). Direct Ink Writing of Three-Dimensional Ceramic Structures. *Journal of the American Ceramic Society*, 89(12), 3599–3609. <https://doi.org/10.1111/j.1551-2916.2006.01382.x>

Ligon, S. C., Liska, R., Stampfl, J., Gurr, M., & Mülhaupt, R. (2017). Polymers for 3D Printing and Customized Additive Manufacturing. *Chemical Reviews*, 117(15), 10212–10290. <https://doi.org/10.1021/acs.chemrev.7b00074>

Mao, Y., Ding, Z., Yuan, C., Ai, S., Isakov, M., Wu, J., ... Qi, H. J. (2016). 3D Printed Reversible Shape Changing Components with Stimuli Responsive Materials. *Scientific Reports*, 6, 24761(1–13). <https://doi.org/10.1038/srep24761>

Miao, S., Castro, N., Nowicki, M., Xia, L., Cui, H., Zhou, X., ... Zhang, L. G. (2017). 4D printing of polymeric materials for tissue and organ regeneration. *Materials Today*, 20(10), 577–591. <https://doi.org/10.1016/j.mattd.2017.06.005>

Momeni, F., M.Mehdi Hassani.N, S., Liu, X., & Ni, J. (2017). A review of 4D printing. *Materials & Design*, 122, 42–79. <https://doi.org/10.1016/j.matdes.2017.02.068>

Momeni, F., M.Mehdi Hassani.N, S., Liu, X., & Ni, J. (2017). A review of 4D printing. *Materials & Design*, 122, 42–79. <https://doi.org/10.1016/j.matdes.2017.02.068>

Pitts, D., Willoughby, J. , & Morgan, R. (2013). Clinical Reasoning and Problem Solving to Prevent Pitfalls in Hand Injuries. In Cooper, C. (Ed.). *Fundamentals of Hand Therapy: Clinical Reasoning and Treatment Guidelines for Common Diagnoses of the Upper Extremity*. Elsevier Health Sciences.

Rasavong, C., MPT, COMT, & MBA. (2015). Brief Review of Maitland Joint Mobilization Grades. Retrieved 14 July 2019, from <http://www.cyberpt.com/maitlandjointmobilizationgradereview.asp>

Raviv, D., Zhao, W., McNelly, C., Papadopoulou, A., Kadambi, A., Shi, B., ... Tibbits, S. (2014). Active Printed Materials for Complex Self-Evolving Deformations. *Scientific Reports*, 4, 7422 (1–6). <https://doi.org/10.1038/srep07422>

Swann, C. (2002). Action Research and the Practice of Design. *Design Issues*, 18(1), 49–61. <https://doi.org/10.1162/07479360252756287>

Sydney Gladman, A., Matsumoto, E. A., Nuzzo, R. G., Mahadevan, L., & Lewis, J. A. (2016). Biomimetic 4D printing. *Nature Materials; London*, 15(4), 413–418. <http://dx.doi.org/10.1038/nmat4544>

Tavsan, F., & Sonmez, E. (2015). Biomimicry in Furniture Design. *Procedia - Social and Behavioral Sciences*, 197, 2285–2292. <https://doi.org/10.1016/j.sbspro.2015.07.255>

Themes, U. F. O. (2016). Clinical Reasoning and Problem Solving to Prevent Pitfalls in Hand Injuries. Retrieved 28 May 2019, from Musculoskeletal Key website: <https://musculoskeletalkey.com/clinical-reasoning-and-problem-solving-to-prevent-pitfalls-in-hand-injuries/>

Themes, U. F. O. (2016). Concepts of Joint Mobilization. Retrieved 18 June 2019, from Musculoskeletal Key website: <https://musculoskeletalkey.com/concepts-of-joint-mobilization/>

Tibbits, S. (2014). 4D Printing: Multi-Material Shape Change. *Architectural Design*, 84(1), 116–121. <https://doi.org/10.1002/ad.1710>

Tibbits, S., McNelly, C., Olguin, C., Dikovsky, D., & Hirsch, S. (2014). 4D Printing and Universal Transformation. *ACADIA 14: Design Agency [Proceedings of the 34th Annual Conference of the Association for Computer Aided Design in Architecture (ACADIA) ISBN 9781926724478]Los Angeles 23-25 October, 2014)*, 539-548. Retrieved from http://papers.cumincad.org/cgi-bin/works/Show?acadia14_539

Vogel, S. (2003). *Comparative biomechanics: Life’s physical world / Steven Vogel*. Princeton, NJ: Princeton University Press.

Volstad, N. L., & Boks, C. (2012). On the use of Biomimicry as a Useful Tool for the Industrial Designer. *Sustainable Development*, 20(3), 189–199. <https://doi.org/10.1002/sd.1535>

Zarek, M., Mansour, N., Shapira, S., & Cohn, D. (2017). 4D Printing of Shape Memory-Based Personalized Endoluminal Medical Devices. *Macromolecular Rapid Communications*, 38(2), 1600628 (1–6). <https://doi.org/10.1002/marc.201600628>

Zari, M. P. (2007, November). *Biomimetic approaches to architectural design for increased sustainability*. Paper presented at the meeting of SB07 New Zealand Conference, Auckland, New Zealand. Retrieved from https://www.branz.co.nz/cms_show_download.php?id=5dbe91c43fc173275e1bf6bdd988b587bc5cd4b5

Appendix

Study on paste-printing

Date: 19/11/2019															
No.	Model dim (mm)	Core	Nozzle (colour) diameter (mm)	Slicer	Printing speed; Traveling speed (mm/s)	Material flow rate multiplier	Infill (%)	Layer height (mm)	Overlap between perimeter and infill (%)	Printing time (min)	Material (ml)	Strands in all (including loops at ends)	Effective strands	Including effective cube (Sat x 5st)	
1	60x60x10	Preset rectilinear pattern	Olive/1.524	K_trial	10; 20	2.5	40	1.15	20	20.00	16.4	19x19	17x17	3x3=9	
2	20x20x11.1	02__s155i155dg90	Olive/1.524	P_trial	10; 20	2.5	100	1.15	20	5.00	3.7	/	/	/	
3	20x20x11.1	02__s155i155dg90	Olive/1.524	P_trial layer height changed	10; 20	2.5	100	1.20	20	5.00	3.7	/	/	/	
4	20x20x11.1	02__s155_Xi155dg120	Olive/1.524	P_trial	10; 20	2.5	100	1.20	20	5.00	3.8	/	/	/	
5	20x20x11.1	02__s155_Xi155dg120	Green/0.84	P_trial layer height changed	10; 20	2.5	100	0.60	20	9.00	3.8	/	/	/	
6	40x20x11.1	02__s155i155dg90	Olive/1.524	P_trial layer height changed	10; 20	2.5	100	1.20	20	8.00	7.5	/	/	/	
7	82x7x10	Preset rectilinear pattern	Olive/1.524	K_trial	10; 20	2.5	40	1.20	20	?	?	27x6	25x4	5x0.8=none	
8	7x65x10	Preset rectilinear pattern	Olive/1.524	K_trial	10; 20	2.5	40	1.20	20	?	?	8x22	6x20	1x4=4	
9	28x28x13.1	02__s250i155dg90_2800x2800x1310	Olive/1.524	P_trial	10; 20	2.5	100	1.20	20	10.00	7.4	/	/	/	

Date: 21/11/2019															
No.	Model dim (mm)	Core	Nozzle (colour) diameter (mm)	Slicer	Printing speed; Traveling speed (mm/s)	Material flow rate multiplier	Infill (%)	Layer height (mm)	Overlap between perimeter and infill (%)	Printing time (min)	Material (ml)	Strand in all (including loops at ends)	Effective strand	Including effective cube (?)	Curing time
1	65x20x10	Preset rectilinear pattern	Olive/1.524	K_trial	10; 20	2.5	40	1.15	20	9.00	6.8	6x22	4x20	?	12:30 -
2	d31, h10	03_cir_s250i155_d31mmh10mm	Olive/1.524	P_trial	10; 20	2.5	100	1.20	20	7.00	4.6	/	/	/	12:30 -

Date: 26/11/2019

No.	Model dim (mm)	Core	Physical Nozzle Setting in Sli3er	Slicer	Printing speed; Traveling speed (mm/s)	Material flow rate multiplier	Infill (%)	Layer height (mm)	Overlap between perimeter and infill (%)	Extrusion width (mm)	Printing time (min)	Material (ml)	Strand in all (including loops at ends)	Effective strand	Including effective cube (?)	Curing time
1	65x82x10	Preset rectilinear pattern	Olive/1.524 1.524	K_trial overlapping changed	10; 20	2.5	40	1.15	100	1.45	30	24.8	22x27	20x25	?	/
2	65x82x10	Preset rectilinear pattern	Olive/1.524 1.524	K_trial layer height and extrusion width changed	10; 20	2.5	40	1.20	100	1.20	34	22.5	28x34	26x32	?	/
3	62.5x82x10	Preset rectilinear pattern	Olive/1.524 1.524	same as above	10; 20	2.5	40	1.20	100	1.20	?	?	26x34	24x32	?	/
4	63.5x78x10	Preset rectilinear pattern	Olive/1.524 1.524	same as above	10; 20	2.5	40	1.20	100	1.20	31	21	27x33	25x31	?	/
5	63.5x63.5x10	Preset rectilinear pattern	Olive/1.524 1.524	same as above	10; 20	2.5	40	1.20	100	1.20	26	17.4	27x27	25x25	?	/
6	63.5x63.5x10	Preset rectilinear pattern	Olive/1.524 1.20	same as above	10; 20	2.5	40	1.20	100	1.20	26	17.4	27x27	25x25	?	12:15 -
7	63.5x63.5x10	Preset rectilinear pattern	Olive/1.524 1.20	same as above	10; 20	2.5	40	1.20	100	1.20	26	17.4	27x27	25x25	?	12:15 -
8	63.5x63.5x10	Preset rectilinear pattern	Olive/1.524 1.20	same as above	10; 20	2.5	40	1.20	100	1.20	26	17.4	27x27	25x25	?	15:30 -
9	63.5x63.5x10	Preset rectilinear pattern	Olive/1.524 1.20	same as above	10; 20	2.5	40	1.20	100	1.20	26	17.4	27x27	25x25	?	15:30 -

10	63.5x63.5x10	Preset rectilinear pattern	Olive/1.524 1.20	same as above	10; 20	2.5	40	1.20	100	1.20	26	17.4	27x27	25x25	?	16:30 -
11	63.5x63.5x10	Preset rectilinear pattern	Olive/1.524 1.20	same as above	10; 20	2.5	40	1.20	100	1.20	26	17.4	27x27	25x25	?	16:30 -
12	20.5x17.8x9.5	AuxeticCube205x178x95_01A_M2.gcode	Olive/1.524 1.20	same as above	10; 20	2.5	40	1.20	100	1.20	n.a.	n.a.	/	/	/	17:20 -

Date: 04/12/2019

No.	Model dim (mm)	Core	Physical Nozzle Setting in Sli3er	Slicer	Printing speed; Traveling speed (mm/s)	Material flow rate multiplier	Infill (%)	Layer height (mm)	Overlap between perimeter and infill (%)	Extrusion width (mm)	Printing time (min)	Material (ml)	Strand in all (including loops at ends)	Effective strand	Including effective cube (?)	Curing time
1	39x39x4.5	AuxeticCube390x390x45_03_M2.gcode	Olive/1.524 1.20	K_trial	10; 20	2.5	40	1.20, 1.20	100	1.20	3	n.a.	/	/	/	14:20 -
2	39x39x4.5	AuxeticCube390x390x45_03_M3.gcode	Olive/1.524 1.20	K_trial	10; 20	2.5	40	1.20, 1.20	100	1.20	3	n.a.	/	/	/	14:20 -
3	39x39x4.5	AuxeticCube390x390x45_03_M4_F300_20'6.gcode	Olive/1.524 1.20	K_trial	10; 20	2.5	40	1.20, 1.20	100	1.20	3	n.a.	/	/	/	14:20 -
4	39x39x6	AuxeticCube390x390x60_03_M6_F600_Ly0_Z1'15_Ly1_Z2'15.gcode	Olive/1.524 1.20	K_trial	10; 20	2.5	40	1.20, 1.20	100	1.20	3	n.a.	/	/	/	14:20 -
5	42x42x7	AuxeticCube420x420x70_03_M7_F600_Ly0_Z1'15_Ly1_Z2'15.gcode	Olive/1.524 1.20	K_trial	10; 20	2.5	40	1.20, 1.20	100	1.20	3	n.a.	/	/	/	14:20 -
6	42x42x7	AuxeticCube420x420x70_03_M7_F600_Ly0_Z1'15_Ly1_Z2'15.gcode	Olive/1.524 1.20	K_trial	10; 20	2.5	40	1.20, 1.20	100	1.20	3	n.a.	/	/	/	14:20 -
7	42x42x7	AuxeticCube420x420x70_03_M8_F600_Ly0_Z1'15_Ly1_Z2'15_Ex0'05.gcode	Olive/1.524 1.20	K_trial	10; 20	2.5	40	1.20, 1.20	100	1.20	3	n.a.	/	/	/	14:20 -
8	42x42x7	AuxeticCube420x420x70_03_M9_F600_Ly0_Z1'15_Ly1_Z2'15_Ex0'7.gcode	Olive/1.524 1.20	K_trial	10; 20	2.5	40	1.20, 1.20	100	1.20	3	n.a.	/	/	/	14:20 -
9	42x42x7	AuxeticCube420x420x70_03_M10_F600_Ly0_Z1'15_Ly1_Z2'15_Ex0'8.gcode	Olive/1.524 1.20	K_trial	10; 20	2.5	40	1.20, 1.20	100	1.20	3	n.a.	/	/	/	14:20 -
10	42x42x7	AuxeticCube420x420x70_03_M11_F600_Ly0_Z1'15_Ly1_Z2'15_Ex1'0.gcode	Olive/1.524 1.20	K_trial	10; 20	2.5	40	1.20, 1.20	100	1.20	3	n.a.	/	/	/	14:20 -
11	232x100	Sandglass232x100_03_M4_Ex1'0.gcode	Olive/1.524 1.20	K_trial	10; 20	2.5	40	1.20, 1.20	100	1.20	/		/	/	/	/
12	?	Splint_03_M5_Ex1'2.gcode	Olive/1.524 1.20	K_trial	10; 20	2.5	40	1.20, 1.20	100	1.20	/		/	/	/	/
13	?	Vase cone	Olive/1.524 1.20	Vase mode	5; 30	3.5	0	1.15, 1.15	0	1.20	?	?	/	/	/	?
14	scaled?	Vase_hexo01.stl	Olive/1.524 1.20	Vase mode	5; 30	3.5	0	1.15, 1.15	0	1.20	14	4.8	/	/	/	?
15	scaled?	Vase_hexo03.stl	Olive/1.524 1.20	Vase mode	5; 30	3.5	0	1.15, 1.15	0	1.20	7	2?	/	/	/	?
16	scaled?	Vase_hexo03.stl	Olive/1.524 1.20	Vase mode	5; 30	3.5	0	1.15, 1.15	0	1.20	30	10.5	/	/	/	?
17	scaled?	Vase_hexo03.stl	Olive/1.524 1.20	Vase mode	8; 30	3.5	0	1.15, 1.15	0	1.20	18	10.5	/	/	/	?
18	scaled?	Vase_hexo03.stl	Olive/1.524 1.20	Vase mode	10; 20	3.5	0	1.15, 1.15	0	1.20	15	10.5	/	/	/	?

Best printed data of its series

Failed to print

Data made by John

Settings not used(?) when Gcode is imported to print

Date: 07/12/2019																
No.	Model dim (mm)	Core	Physical Nozzle Setting in Sli3er	Slicer	Printing speed: Travelling speed (mm/s)	Matelial flow rate multipler	Infill (%)	Layer height (mm)	Overlap between perimeter and infill (%)	Extrusion width (mm)	Printing time (min)	Material (ml)	Strand in all (including loops at ends)	Effective strand	Including effective cube (?)	Curing time
1	60x4	bracelet_a01.stl	Olive/1.524 1.20	Vase mode	10; 20	3.5	0	1.15, 1.15	0	1.20	?	?	/	/	/	?
2	60x4	bracelet_a01.stl	Olive/1.524 1.20	Vase mode	10; 20	2.5	0	1.15, 1.15	0	1.20	?	?	/	/	/	?
3	60x20	bracelet_b01.stl	Olive/1.524 1.20	Vase mode	10; 20	2.5	0	1.15, 1.15	0	1.20	10	7.5	/	/	/	?
4	40x12x10	demonstrator 400x120x10_a01.stl	Olive/1.524 1.20	Vase mode	10; 20	2.5	0	1.15, 1.15	0	1.20	4	?	/	/	/	?
5	40x12x9.2	demonstrator 400x120x9'2_a02.stl	Olive/1.524 1.20	Vase mode	10; 20	2.5	0	1.15, 1.15	0	1.20	4	2.6	/	/	/	?
6	40x12x9.2	demonstrator 400x120x9'2_a02.stl	Olive/1.524 1.20	Vase mode	10; 20	2.0	0	1.15, 1.25	0	1.20	4	2.6	/	/	/	?
7	40x12x9.2	demonstrator 400x120x9'2_a02.stl	Olive/1.524 1.20	Vase mode	15; 20	2.0	0	1.15, 1.25	0	1.20	?	2.6	/	/	/	?
8	40x12x9.2	demonstrator 400x120x9'2_a02.stl	Olive/1.524 1.20	Vase mode	20; 20	2.0	0	1.15, 1.25	0	1.20	2	2.6	/	/	/	?
9	40x12x9.2	demonstrator 400x120x9'2_a02.stl	Olive/1.524 1.20	Vase mode	15; 20	2.5	0	1.15, 1.25	0	1.20	3	2.6	/	/	/	?
10	40x12x9.2	demonstrator 400x120x9'2_a02.stl	Olive/1.524 1.20	Vase mode	15; 20	2.0	0	1.15, 1.25	0	1.20	4	2.6	/	/	/	?
11	40x12x9.2	demonstrator 400x120x9'2_a02.stl	Olive/1.524 1.20	Vase mode	15; 20	1.5	0	1.15, 1.25	0	1.20	?	2.6	/	/	/	?
12	40x12x9.2	demonstrator 400x120x9'2_a02.stl	Olive/1.524 1.20	Vase mode	15; 20	2.2	0	1.15, 1.35	0	1.20	3	2.6	/	/	/	?

Date: 10/12/2019																
No.	Model dim (mm)	Core	Physical Nozzle Setting in Sli3er	Slicer	Printing speed: Travelling speed (mm/s)	Matelial flow rate multipler	Infill (%)	Layer height (mm)	Overlap between perimeter and infill (%)	Extrusion width (mm)	Printing time (min)	Material (ml)	Strand in all (including loops at ends)	Effective strand	Including effective cube (?)	Curing time
1	?	dmst_etc 06_pttrn_a01.stl	Olive/1.524 1.20	P_trial ?	15; 20	2.2	100	1.15, 1.45	?	?	≈3	≈3	/	/	/	14:03 -
2	?	dmst_etc 06_pttrn_b01.stl	Olive/1.524 1.20	P_trial ?	15; 20	2.2	100	1.15, 1.45	?	?	≈3	≈3	/	/	/	14:03 -
3	?	dmst_etc 06_pttrn_b01.stl	Olive/1.524 1.20	P_trial ?	15; 20	2.2	100	1.15, 1.45	?	?	≈3	≈3	/	/	/	14:03 -
4	?	dmst_etc 06_pttrn_c01.stl	Olive/1.524 1.20	P_trial ?	15; 20	2.2	100	1.15, 1.45	?	?	≈3	≈3	/	/	/	14:03 -
5	?	dmst_etc 06_pttrn_d01.stl	Olive/1.524 1.20	P_trial ?	15; 20	2.2	100	1.15, 1.45	?	?	≈3	≈3	/	/	/	14:03 -
6	?	dmst_etc 06_pttrn_e01.stl	Olive/1.524 1.20	P_trial ?	15; 20	2.2	100	1.15, 1.45	?	?	≈3	≈3	/	/	/	14:03 -
7	?	dmst_etc 06_pttrn_f01.stl	Olive/1.524 1.20	P_trial ?	15; 20	2.2	100	1.15, 1.45	?	?	≈3	≈3	/	/	/	14:03 -
8	?	dmst_etc 06_pttrn_g01.stl	Olive/1.524 1.20	P_trial ?	15; 20	2.2	100	1.15, 1.45	?	?	≈3	≈3	/	/	/	14:03 -
9	?	dmst_etc 06_pttrn_h01.stl	Olive/1.524 1.20	P_trial ?	15; 20	2.2	100	1.15, 1.45	?	?	≈3	≈3	/	/	/	14:03 -
10	?	dmst_etc 06_pttrn_i01.stl	Olive/1.524 1.20	P_trial ?	15; 20	2.2	100	1.15, 1.45	?	?	≈3	2.5	/	/	/	14:03 -

11	?	dmst_etc 06_pttrn_i01.stl	Olive/1.524 1.20	P_trial ?	15; 20	2.2	100	1.15, 1.45	?	?	≈3	≈3	/	/	/	14:03 -
12	?	dmst_etc 06_pttrn_i01.stl	Olive/1.524 1.20	P_trial ?	15; 20	2.2	100	1.15, 1.45	?	?	≈3	≈3	/	/	/	14:03 -
13	?	dmst_etc 06_pttrn_k01.stl	Olive/1.524 1.20	P_trial ?	15; 20	2.2	100	1.15, 1.45	?	?	≈3	≈3	/	/	/	17:09 -
14	?	dmst_etc 06_pttrn_i01.stl	Olive/1.524 1.20	P_trial ?	15; 20	2.2	100	1.15, 1.45	?	?	≈3	2.8	/	/	/	17:09 -
15	?	dmst_etc 06_pttrn_m01.stl	Olive/1.524 1.20	P_trial ?	15; 20	2.2	100	1.15, 1.45	?	?	≈3	3.2	/	/	/	17:09 -
16	?	dmst_etc 06_pttrn_n01.stl	Olive/1.524 1.20	P_trial ?	15; 20	2.2	100	1.15, 1.45	?	?	≈3	3.2	/	/	/	17:09 -
17	?	dmst_etc 06_pttrn_o01_0mm.stl	Olive/1.524 1.20	P_trial ?	15; 20	2.2	100	1.15, 1.45	?	?	/	/	/	/	/	17:09 -
18	?	dmst_etc 06_pttrn_o01_ovlp2mm.stl	Olive/1.524 1.20	P_trial ?	15; 20	2.2	100	1.15, 1.45	?	?	2.5	2.6	/	/	/	17:09 -
19	?	dmst_etc 06_pttrn_o01_ovlp4mm.stl	Olive/1.524 1.20	P_trial ?	15; 20	2.2	100	1.15, 1.45	?	?	2.5	2.7	/	/	/	17:09 -
20	?	dmst_etc 06_pttrn_o01_ovlp-3mm.stl	Olive/1.524 1.20	P_trial ?	15; 20	2.2	100	1.15, 1.45	?	?	2.5	2.5	/	/	/	17:09 -
21	?	dmst_etc 06_pttrn_o01_ovlp-1mm.stl	Olive/1.524 1.20	P_trial ?	15; 20	2.2	100	1.15, 1.45	?	?	2.5	2.6	/	/	/	17:09 -
22	Z x Z	dmst_etc 06_pttrn_k01.stl	Olive/1.524 1.20	P_trial ?	15; 20	2.2	100	1.15, 1.45	?	?	≈5	5.1	/	/	/	17:09 -

Failed to print:
Canceled
Unexpected travelling
Key features of print didn't follow design

Date: 11/12/2019																
No.	Model dim (mm)	Core	Physical Nozzle Setting in Sli3er	Slicer	Printing speed: Travelling speed (mm/s)	Matelial flow rate multipler	Infill (%)	Layer height (mm)	Overlap between perimeter and infill (%)	Extrusion width (mm)	Printing time (min)	Material (ml)	Strand in all (including loops at ends)	Effective strand	Including effective cube (?)	Curing time
1	Z x Z	dmst_etc 06_pttrn_k01.stl	Olive/1.524 1.20	Vase mode	15; 20	2.2	0	1.15, 1.45	0	?	≈4	?	/	/	/	?
2	?	dmst_etc 07_brc01_H506-sector67'5.stl	Olive/1.524 1.20	Vase mode	15; 20	2.2	0	1.15, 1.45	0	?	≈14	14.5	/	/	/	?
3	?	dmst_etc 07_brc01_H506-sector67'5.stl	Olive/1.524 1.20	Vase mode	15; 20	2.5	0	1.15, 1.45	0	?	≈14	14.5 (actually 30ml)	/	/	/	?
4	?	dmst_etc 07_brc01_H506.stl	Olive/1.524 1.20	Vase mode	15; 20	2.5	0	1.15, 1.45	0	?	60	30	/	/	/	?
5	?	de2018splintV2	Olive/1.524 1.20	Vase mode	15; 20	2.5	0	1.15, 1.45	0	?	40	44	/	/	/	?
6	?	de2018splintV3	Olive/1.524 1.20	Vase mode	15; 20	2.5	0	1.15, 1.45	0	?	40	44	/	/	/	?
7	?	de2018splintV3	Olive/1.524 1.20	Vase mode	15; 20	2.5	0	1.15, 1.30	0	?	41	44.5	/	/	/	?
8	?	de2018splintV3	Olive/1.524 1.20	Vase mode	15; 20	2.5	0	1.15, 1.30	0	?	41	44.5	/	/	/	?
9	?	demonstrator for furniture folding test	Olive/1.524 1.20	?	?	2.0	?	?	?	?	?	?	/	/	/	?

Data made by John

No.	Model dim (mm)	Core	Physical Nozzle Setting in Sli3er	Slicer	Printing speed; Traveling speed (mm/s)	Mateial flow rate multipler	Infill (%)	Layer height (mm)	Overlap between perimeter and infill (%)	Extrusion width (mm)	Printing time (min)	Material (ml)	Strand in all (including loops at ends)	Effective strand	Including effective cube (?)	Curing time
1	?	dmst_etc 08_brc01_H506.stl	Olive/1.524 1.20	Vase mode	15; 20	2.2	0	1.15, 1.45	0	1.30	65	7.06	/	/	/	?
2	Z x 3	Vase_hexo01.stl (fell down at 6cm high)	Olive/1.524 1.20	Vase mode	15; 20	2.5	0	1.15, 1.45	0	1.30	6.5	7	/	/	/	?
3	Z x 3	Vase_hexo02.stl (fell down at 6cm high)	Olive/1.524 1.20	Vase mode	15; 20	2.5	0	1.15, 1.45	0	1.30	6.1	?	/	/	/	?
4	?	Vase_hexo02.stl + preset Honey comb (fell down at 5cm high)	Olive/1.524 1.20	K_trial	15; 20	2.5	15	1.15, 1.25	0	1.30	15	8.5	/	/	/	?
5	Z x 3	Vase_hexo02.stl + preset Rectilinear	Olive/1.524 1.20	K_trial	10; 20	2.5	15	1.15, 1.25	0	1.30	?	?	/	/	/	?
6	?	Vase_hexo02.stl + 2x perimeters	Olive/1.524 1.20	K_trial	10; 20	2.5	0	1.15, 1.25	0	1.30	13	13.3	/	/	/	?
7	?	hexagon_cone_trial01.stl	Olive/1.524 1.20	Vase mode	15; 20	2.5	0	1.15, 1.45	0	1.30	4	4	/	/	/	?
8	?	hexagon_cone_trial01.stl	Olive/1.524 1.20	Vase mode	10; 20	3.0	0	1.15, 1.25	0	1.30	?	?	/	/	/	?
9	?	dmst_etc 08_brc02_ovlp+_H506.stl	Olive/1.524 1.20	Vase mode	10; 20	3.0	?	1.15, 1.25	?	1.30	93	71	/	/	/	?
10	?	dmst_etc 08_brc02_ovlp+_H506.stl	Olive/1.524 1.20	Vase mode	20; 20	2.2	?	1.15, 1.45	?	1.30	51	71	/	/	/	?

fell down
Canceled
printed well and stopped midway

Date: 13/12/2019																
No.	Model dim (mm)	Core	Physical Nozzle Setting in Sli3er	Slicer	Printing speed; Traveling speed (mm/s)	Mateial flow rate multipler	Infill (%)	Layer height (mm)	Overlap between perimeter and infill (%)	Extrusion width (mm)	Printing time (min)	Material (ml)	Strand in all (including loops at ends)	Effective strand	Including effective cube (?)	Curing time
1	?	dmst_etc 08_brc_D60H6'9_01_outer gapslarger_pttrn8.stl	Olive/1.524 1.20	Vase mode	20; 20	2.2	0	1.2, 1.45	0	1.30	4	6.2	/	/	/	?
2	?	dmst_etc 08_brc_D60H6'9_02_outer gapslarger_ovlp_pttrn8.stl	Olive/1.524 1.20	Vase mode	20; 20	2.2	0	1.25, 1.45	0	1.30	3.8	5.6	/	/	/	?
3	?	dmst_etc 08_brc_D60H6'9_03_inner gapslarger_pttrn8.stl	Olive/1.524 1.20	Vase mode	20; 20	2.2	0	1.25, 1.45	0	1.30	n.a.	n.a.	/	/	/	?
4	?	dmst_etc 08_brc_D60H6'9_04_inner gapslarger_ovlp_pttrn8.stl	Olive/1.524 1.20	Vase mode	20; 20	2.2	0	1.25, 1.45	0	1.30	3.8	5.8	/	/	/	?
5	Z x 2	dmst_etc 08_brc_D60H6'9_02_outer gapslarger_ovlp_pttrn8.stl	Olive/1.524 1.20	Vase mode	20; 20	2.2	0	1.25, 1.45	0	1.30	7.7	11.4	/	/	/	?

6	Z x 2	dmst_etc 08_brc_D60H6'9_04_inner gapslarger_ovlp_pttrn8.stl	Olive/1.524 1.20	Vase mode	20; 20	2.2	0	1.25, 1.45	0	1.30	n.a.	n.a.	/	/	/	?
7	?	dmst_etc 08_brc_D60H6'9_03_inner gapslarger_pttrn8.stl	Olive/1.524 1.20	Vase mode	20; 20	2.2	0	1.25, 1.45	0	1.30	3.7	5.6	/	/	/	?
8	Z x 2	dmst_etc 08_brc_D60H6'9_04_inner gapslarger_ovlp_pttrn8.stl	Olive/1.524 1.20	Vase mode	20; 20	2.2	0	1.25, 1.45	0	1.30	7.7	11.7	/	/	/	?
9	?	dmst_etc 08_brc_D60H6'9_03C_inner gapslarger_pttrn8.stl	Olive/1.524 1.20	Vase mode	20; 20	2.2	0	1.25, 1.45	?	1.30	6	9.1	/	/	/	?
10	?	dmst_etc 08_brc_D60H6'9_05_outer ergapslarger_pttrn_n_8.stl	Olive/1.524 1.20	Vase mode	20; 20	2.2	0	1.25, 1.45	?	1.30	3.4	5.2	/	/	/	?
11	?	dmst_etc 08_brc_D60H6'9_06_inner ergapslarger_pttrn_n_8.stl	Olive/1.524 1.20	Vase mode	20; 20	2.2	0	1.25, 1.45	?	1.30	?	?	/	/	/	?
12	?	dmst_etc 08_brc_D60H6'9_07_outer ergapslarger_pttrn_e_8.stl	Olive/1.524 1.20	Vase mode	20; 20	2.2	0	1.25, 1.45	?	1.30	4.8	?	/	/	/	?

failed to generate Gcode
Gcode generated from unchanged data

Date: 14/12/2019																
No.	Model dim (mm)	Core	Physical Nozzle Setting in Sli3er	Slicer	Printing speed; Traveling speed (mm/s)	Mateial flow rate multipler	Infill (%)	Layer height (mm)	Overlap between perimeter and infill (%)	Extrusion width (mm)	Printing time (min)	Material (ml)	Strand in all (including loops at ends)	Effective strand	Including effective cube (?)	Curing time
1	?	MDL05_splint_to_print_H80_withGap_andChamfer.stl	Olive/1.524 1.20	Vase mode	15; 15	3.2	0	1.2, 1.45	0	1.30	69.7	71.1	/	/	/	12:02 -
2	?	MDL05_splint_to_print_H80_withGap_andChamfer.stl	Olive/1.524 1.20	Vase mode	15; 15	4.0	0	1.25, 1.45	0	1.30	69.7	71.1	/	/	/	12:02 -
3	?	MDL05_splint_to_print_H73_withGap_andChamfer_MMfixed.stl	Olive/1.524 1.20	Vase mode	15; 15	4.0	0	1.25, 1.45	0	1.30	62.5	64.1	/	/	/	15:45 -
4	scaled 0.5	bishop01_0'4.stl + preset hexagon infill	Olive/1.524 1.20	?	15; 15	4.0	?	1.15, 1.40	?	?	?	?	/	/	/	?
5	scaled 0.5	bishop01_0'4.stl	Olive/1.524 1.20	Vase mode	15; 15	4.0	0	1.15, 1.40	0	?	?	?	/	/	/	?
6	scaled 1	bishop01_0'4.stl	Olive/1.524 1.20	Vase mode	15; 15	4.0	0	1.15, 1.40	0	?	?	?	/	/	/	?

printed well and stopped midway

4D Printing with Bio-based Polymers for Adaptive Wearable Devices

YEJUN FU